People's Democratic Republic of Algeria Ministry of Higher Education and Scientific Research

University Echahid Hamma Lakhdar El Oued

Faculty of Exact Sciences

Department of Physics

Lecture Notes on

Quantum Optics and Lasers

Mosbah Difallah

E-mail : mosbah-difallah@univ-eloued.dz

Contents

List of Figures

List of Tables

Chapter 1

Quantum Optics

Q What is quantum optics?

A It is the quantum theory of light with the concept of the *photon* as an elementary excitation of the electromagnetic field.

- A nonrelativistic version of quantum electrodynamics.
- The first quantum optics paper by Roy J. Glauber (1925-2018, Nobel Prize 2005) in 1963 [R. J. Glauber, The quantum theory of optical coherence, *Phys. Rev.* **130**, 2529 (1963)].
- It describes the interaction of the quantized electromagnetic field with atoms, molecules, and macroscopic dielectrics.
- Today also covers a large portion of atomic physics. It is more than light (see Fig. (1.1)).
- We study quantum-mechanical description of light, which enables us to study effects that have *no* classical analogue. These include squeezing and photon antibunching, which we will analyze in more detail in this chapter.

1.1 Field quantization in free space

- For the quantum theory of light the quantization of the electromagnetic field is needed.

Q What is the (canonical) quantization procedure?

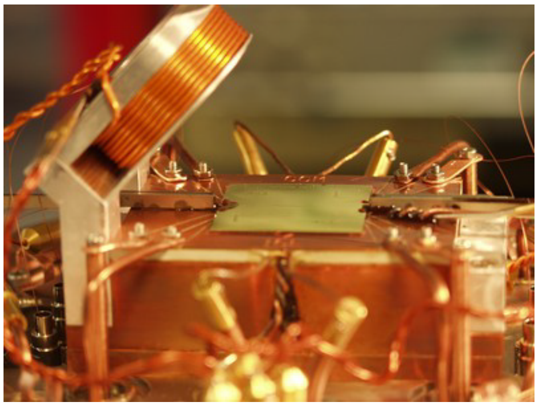

(a) Cooling and trapping of neutral atoms.

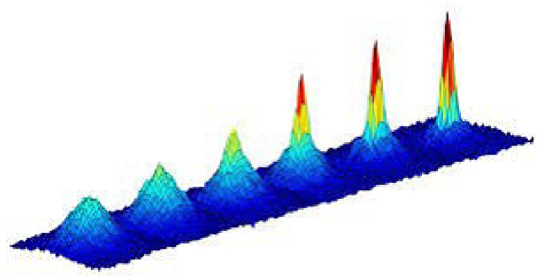

(b) Bose-Einstein condensates (Nobel Prize 2001: Eric A. Cornell, Wolfgang Ketterle, Carl E. Wieman).

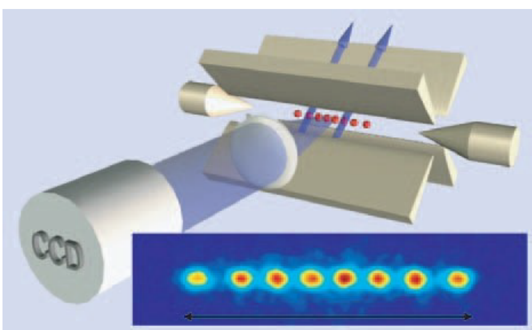

(c) Manipulation of individual quantum systems (Nobel Prize 2012: Serge Haroche, David J. Wineland).

(d) Dispersion forces (Casimir and van der Waals forces).

Fig. 1.1: Recent developments of quantum optics.

A

1. Promote complex number quantities such as position x and momentum p to HILBERT-space operators.
2. Postulate (equal-time) commutation relations, i.e. replace POISSON brackets by $\mathrm{i}\hbar$ times the commutator: $\{\cdot,\cdot\} = \mathrm{i}\hbar[\cdot,\cdot]$.

- There are two ways to field quantization:

  1. *Quantum field theoretic approach*: start straightaway from canonical variables of MAXWELL theory, postulate field commutator and hope for the best.
  2. *Pedestrian approach*: perform mode expansion of electromagnetic field, quantize each individual mode separately, construct field commutator from mode expansion.

- MAXWELL's equations in free space without sources reads

$$
\begin{aligned}
\nabla \cdot \mathbf{D}(\mathbf{r},t) &= 0, && (1.1)\\
\nabla \cdot \mathbf{B}(\mathbf{r},t) &= 0, && (1.2)\\
\nabla \times \mathbf{E}(\mathbf{r},t) &= -\dot{\mathbf{B}}(\mathbf{r},t), && (1.3)\\
\nabla \times \mathbf{H}(\mathbf{r},t) &= \dot{\mathbf{D}}(\mathbf{r},t), && (1.4)
\end{aligned}
$$

  where $\mathbf{B}(\mathbf{r},t)$ represents the magnetic induction field, $\mathbf{E}(\mathbf{r},t)$ is the electric field, $\mathbf{D}(\mathbf{r},t)$ denotes the electric displacement field, $\mathbf{H}(\mathbf{r},t)$ is the magnetic field.

- Moreover, we can write the constitutive equations as

$$
\begin{aligned}
\mathbf{D}(\mathbf{r},t) &= \varepsilon_0 \mathbf{E}(\mathbf{r},t) && (1.5)\\
\mathbf{H}(\mathbf{r},t) &= \frac{1}{\mu_0}\mathbf{B}(\mathbf{r},t), && (1.6)
\end{aligned}
$$

  where ε_0 and μ_0 represent the permittivity and the permeability of the vacuum, respectively.

- The two equations (1.2) and (1.3) exactly solved by introduction of potentials

$$
\mathbf{B}(\mathbf{r},t) = \nabla \times \mathbf{A}(\mathbf{r},t), \qquad \mathbf{E}(\mathbf{r},t) = -\nabla\phi(\mathbf{r},t) - \dot{\mathbf{A}}(\mathbf{r},t), \tag{1.7}
$$

  with the scalar potential $\phi(\mathbf{r},t)$ and the vector potential $\mathbf{A}(\mathbf{r},t)$. But for the rest of two equations (1.1) and (1.4)

$$
\nabla \cdot \mathbf{D}(\mathbf{r},t) = 0 \;\Rightarrow\; \boxed{-\varepsilon_0\left[\Delta\phi(\mathbf{r},t) + \nabla\cdot\dot{\mathbf{A}}(\mathbf{r},t)\right] = 0,} \tag{1.8}
$$

and

$$\nabla \times \mathbf{H}(\mathbf{r},t) = \dot{\mathbf{D}}(\mathbf{r},t) \quad \Rightarrow \quad \boxed{\nabla \times \nabla \times \mathbf{A}(\mathbf{r},t) + \frac{1}{c^2}\ddot{\mathbf{A}}(\mathbf{r},t) = -\frac{1}{c^2}\nabla\dot{\phi}(\mathbf{r},t).} \tag{1.9}$$

yields two coupled partial differential equations for potentials. ☹

- But: potentials are not uniquely defined due to gauge freedom

$$\mathbf{A}(\mathbf{r},t) \ \mapsto \ \mathbf{A}(\mathbf{r},t) + \nabla g(\mathbf{r},t), \qquad \phi(\mathbf{r},t) \ \mapsto \ \phi(\mathbf{r},t) - \dot{g}(\mathbf{r},t), \tag{1.10}$$

which gives identical electromagnetic fields for arbitrary gauge function. Hence choose $g(\mathbf{r},t)$ such that

$$\boxed{\nabla \cdot \mathbf{A}(\mathbf{r},t) = 0} \tag{1.11}$$

known as COULOMB gauge (transverse vector potential). Therefore

$$\Delta\phi(\mathbf{r},t) = 0 \Rightarrow \phi(\mathbf{r},t) = 0 \tag{1.12}$$

using boundary conditions at infinity for the scalar potential, and the vector identity

$$\nabla \times \nabla \times \mathbf{A} = \nabla(\nabla \cdot \mathbf{A}) - \Delta\mathbf{A}, \tag{1.13}$$

we obtain the wave equation for vector potential

$$\boxed{\Delta\mathbf{A}(\mathbf{r},t) - \frac{1}{c^2}\frac{\partial^2}{\partial t^2}\mathbf{A}(\mathbf{r},t) = 0.} \tag{1.14}$$

1.1.1 Maxwell's equations in covariant form

- MAXWELL's equations (1.1-1.4), and the wave equation (1.14), can be written in a very compact covariant form. For this purpose, we introduce the following notation: the *contravariant* and *covariant* components of a four-vector a consist of the temporal component a^0 and the spatial three-vector $\mathbf{a}$, which can be combined into

$$a^\mu = (a^0, \mathbf{a}), \qquad a_\mu = (a^0, -\mathbf{a}). \tag{1.15}$$

- The transformation from covariant to contravariant vectors is carried out with the metric tensor $g^{\mu\nu}$ in the form

$$a^\mu = g^{\mu\nu}a_\nu, \qquad a_\mu = g_{\mu\nu}a^\nu \tag{1.16}$$

according to EINSTEIN's summation convention, a summation is carried out over indices that appear twice (one upper and one lower index). In this way, one obtains the invariant $a^2 = a^\mu a_\mu = (a^0)^2 - \mathbf{a}^2$.

- In flat space, the metric tensor takes the diagonal form $g^{\mu\nu} = \mathrm{diag}(1, -1, -1, -1)$. Important examples of four-vectors are:

$$\begin{aligned}
\text{position four-vector:} \quad & x^\mu = (ct, \mathbf{x}), \\
\text{velocity four-vector:} \quad & u^\mu = (\gamma, \gamma\boldsymbol{\beta}), \\
\text{wavevector four-vector:} \quad & k^\mu = \left(\tfrac{\omega}{c}, \mathbf{k}\right), \\
\text{current density four-vector:} \quad & j^\mu = (c\rho, \mathbf{j}), \\
\text{potential four-vector:} \quad & A^\mu = \left(\tfrac{\phi}{c}, \mathbf{A}\right), \\
\text{gradient four-vector:} \quad & \partial_\mu = \partial/\partial x^\mu = (\partial/\partial ct, \nabla).
\end{aligned}$$

The four-velocity here is dimensionless and is expressed in terms of the dimensionless velocity $\boldsymbol{\beta} = \mathbf{v}/c$ and the Lorentz factor $\gamma = (1-\beta^2)^{-1/2}$.

E The field strength tensor is defined as

$$F^{\mu\nu}(x) = \partial^\mu A^\nu(x) - \partial^\nu A^\mu(x). \tag{1.17}$$

Using Eq. (1.7) prove that

$$F^{\mu\nu}(x) = \begin{pmatrix} 0 & -E^1/c & -E^2/c & -E^3/c \\ E^1/c & 0 & B^3 & -B^2 \\ E^2/c & -B^3 & 0 & B^1 \\ E^3/c & B^2 & -B^1 & 0 \end{pmatrix}. \tag{1.18}$$

- The field stress tensor is antisymmetric, i.e., $F^{\mu\nu} = -F^{\nu\mu}$. The Maxwell equations (1.1)–(1.4) now read in covariant notation

$$\partial^\mu F^{\nu\rho}(x) + \partial^\rho F^{\mu\nu}(x) + \partial^\nu F^{\rho\mu}(x) = 0, \tag{1.19}$$

$$\partial_\mu F^{\mu\nu}(x) = 0. \tag{1.20}$$

- The equation (1.19) replaces equations (1.2) and (1.3), whereby it must be noted that none of the indices are contracted. This is the covariant form of a Jacobi identity. Equation (1.20) replaces the other two Maxwell equations (1.1) and (1.4). The first of the two covariant equations (1.19) can be further simplified with the aid of the dual field strength tensor. The dual tensor of an arbitrary second-rank tensor $T^{\mu\nu}$ is defined as

$${}^*T^{\mu\nu} = \frac{1}{2}\epsilon^{\mu\nu\alpha\beta}T_{\alpha\beta}, \tag{1.21}$$

where $\epsilon^{\mu\nu\alpha\beta}$ is the four-dimensional (completely antisymmetric) Levi–Civita pseudotensor ($\epsilon^{1234} = 1$ and cyclic). The dual field strength tensor is thus

$$ {}^{*}F^{\mu\nu}(x) = \begin{pmatrix} 0 & -B^1 & -B^2 & -B^3 \\ B^1 & 0 & E^3/c & -E^2/c \\ B^2 & -E^3/c & 0 & E^1/c \\ B^3 & E^2/c & -E^1/c & 0 \end{pmatrix}, \tag{1.22} $$

and Equation (1.19) is replaced by

$$ \partial_\mu \, {}^{*}F^{\mu\nu}(x) = 0, \tag{1.23} $$

which, apart from the duality transformation, is equivalent to (1.20).

1.1.2 Lagrangian and Hamiltonian

- From classical electrodynamics it is known that Maxwell's equations can be derived from a Lagrangian formalism. The Lagrangian density of the electromagnetic field in this case is given by

$$ \mathcal{L} = \tfrac{1}{2}\left\{ \varepsilon_0 \dot{\mathbf{A}}^2(\mathbf{r},t) - \frac{1}{\mu_0}\left[\nabla \times \mathbf{A}(\mathbf{r},t)\right]^2 \right\} = -\tfrac{1}{4} F_{\mu\nu}F^{\mu\nu}. \tag{1.24} $$

The vector potential here plays the role of the generalized coordinates. The Hamilton principle of least action,

$$ \delta_\perp \int L \mathrm{d}t = 0, \qquad \mathrm{L} = \int \mathrm{d}^3\mathrm{r}\,\mathcal{L}, \tag{1.25} $$

yields the Euler–Lagrange equations

$$ \frac{\mathrm{d}}{\mathrm{dt}} \frac{\delta_\perp L}{\delta_\perp \dot{\mathbf{A}}(\mathbf{r},t)} - \frac{\delta_\perp L}{\delta_\perp \mathbf{A}(\mathbf{r},t)} = 0, \tag{1.26} $$

which is nothing other than the wave equation (1.14) for the vector potential. Since the vector potential is a transverse vector field, the variation may only be carried out over such fields. This is what is meant by the notation $\delta_\perp$.

- The vector potential, as a generalized coordinate, has a corresponding canonical momentum, which is obtained from the Lagrangian density as follows

$$ \mathbf{\Pi}(\mathbf{r},t) = \frac{\delta_\perp L}{\delta_\perp \dot{\mathbf{A}}(\mathbf{r},t)} = \varepsilon_0 \dot{\mathbf{A}}(\mathbf{r},t) = -\varepsilon_0 \mathbf{E}^\perp(\mathbf{r},t). \tag{1.27} $$

The LEGENDRE transformation

$$H = \int \mathrm{d}^3\mathrm{r}\big[\mathbf{\Pi}(\mathbf{r},\mathrm{t})\cdot\dot{\mathbf{A}}(\mathbf{r},\mathrm{t}) - \mathcal{L}\big] \tag{1.28}$$

then yields the classical Hamiltonian function as

$$H = \tfrac{1}{2}\int \mathrm{d}^3 r \left\{\frac{1}{\varepsilon_0}\mathbf{\Pi}^2(\mathbf{r},t) + \frac{1}{\mu_0}\left[\nabla\times\mathbf{A}(\mathbf{r},t)\right]^2\right\},$$

or

$$\boxed{H = \tfrac{1}{2}\int \mathrm{d}^3 r \left\{\varepsilon_0\mathbf{E}^{\perp 2}(\mathbf{r},t) + \frac{1}{\mu_0}\mathbf{B}^2(\mathbf{r},t)\right\}.} \tag{1.29}$$

which, as expected, represents the electromagnetic field energy.

1.1.3 Classical mode expansion

- In order to arrive at a canonical quantization of the electromagnetic field in free space, two approaches can in principle be taken. On the one hand, starting from the knowledge of the canonically conjugate variables $\mathbf{A}(\mathbf{r},t)$ and $\mathbf{\Pi}(\mathbf{r},t)$, a field quantization can be carried out by directly promoting these classical quantities to HILBERT space operators and postulating for them the equal-time canonical commutation relations

$$\left[\mathbf{A}_i(\mathbf{r},t),\mathbf{\Pi}_j(\mathbf{r}',t)\right] = \mathrm{i}\hbar\delta_{ij}\delta^{\perp}(\mathbf{r}-\mathbf{r}'). \tag{1.30}$$

  The alternative, which we shall pursue here, is based on the mode expansion of the classical fields, which then leads to the quantization of an (infinite) set of harmonic oscillators.

- For this reason, let us recall that the fundamental solutions of the wave equation (1.14) are plane waves. Obviously, any arbitrary vector potential can be represented as a superposition of such plane waves with certain expansion coefficients

$$\mathbf{A}(\mathbf{r},t) = \sum_\lambda c_\lambda\mathbf{A}_\lambda(\mathbf{r})u_\lambda(t), \tag{1.31}$$

  where $\mathbf{A}_\lambda(\mathbf{r})$ being a set of spatial mode functions and $u_\lambda(t)$ are the amplitude functions.

- The separation of variables with separation constant ω_λ^2/c^2 yields

$$\Delta\mathbf{A}_\lambda(\mathbf{r}) + \frac{\omega_\lambda^2}{c^2}\mathbf{A}_\lambda(\mathbf{r}) = 0, \tag{1.32}$$

$$\ddot{u}_\lambda(t) + \omega_\lambda^2 u_\lambda(t) = 0. \tag{1.33}$$

- The equation (1.32) is known as HELMHOLTZ equation which is an eigenvalue problem for the hermitian operator $(-\Delta)$. Therefore $\mathbf{A}_\lambda(\mathbf{r})$ is a complete set of orthonormal functions, i.e.,

$$\sum_\lambda |c_\lambda|^2 \mathbf{A}_\lambda(\mathbf{r}) \otimes \mathbf{A}_\lambda^*(\mathbf{r}') = \delta(\mathbf{r}-\mathbf{r}')\mathbb{1} \tag{1.34}$$

$$|c_\lambda|^2 \int \mathrm{d}^3 r \mathbf{A}_\lambda^*(\mathbf{r}) \cdot \mathbf{A}_{\lambda'}(\mathbf{r}) = \delta_{\lambda\lambda'} \tag{1.35}$$

- As an example we choose transverse plane waves $\mathbf{A}_\lambda(\mathbf{r}) \sim \mathbf{e}_\sigma \mathrm{e}^{\mathrm{i}\mathbf{k}\cdot\mathbf{r}}$ where $\lambda \equiv (\mathbf{k}, \sigma)$. Hence

$$\mathbf{A}(\mathbf{r}, t) = \sum_\sigma \int \frac{\mathrm{d}^3 k}{(2\pi)^{3/2}} \mathbf{e}_\sigma \left[u_{\mathbf{k}\sigma} \mathrm{e}^{\mathrm{i}(\mathbf{k}\cdot\mathbf{r}-\omega t)} + u_{\mathbf{k}\sigma}^* \mathrm{e}^{-\mathrm{i}(\mathbf{k}\cdot\mathbf{r}-\omega t)} \right], \tag{1.36}$$

where the coefficients $u_{\mathbf{k}\sigma} = u_{-\mathbf{k}\sigma}^*$ carry a vector index with respect to the wavevector $\mathbf{k}$ and a discrete index σ for the two orthogonal transverse polarization degrees of freedom, with unit vectors satisfying $\mathbf{e}_\sigma \cdot \mathbf{e}_{\sigma'} = \delta_{\sigma\sigma'}$. The expansion (2.144) by construction yields a real vector potential.

- We now insert the mode expansion (2.144) into the Hamiltonian (1.29) and obtain

$$\begin{aligned} H = -\tfrac{1}{2} \sum_{\sigma,\sigma'} \iiint \frac{\mathrm{d}^3 r \mathrm{d}^3 k \mathrm{d}^3 k'}{(2\pi)^3} \Bigg\{ & \left[\varepsilon_0 (\mathbf{e}_\sigma \cdot \mathbf{e}_{\sigma'}) \omega\omega' + \frac{1}{\mu_0} (\mathbf{k} \times \mathbf{e}_\sigma) \cdot (\mathbf{k}' \times \mathbf{e}_{\sigma'}) \right] \\ & \times \left[u_{\mathbf{k}\sigma} \mathrm{e}^{\mathrm{i}(\mathbf{k}\cdot\mathbf{r}-\omega t)} - u_{\mathbf{k}\sigma}^* \mathrm{e}^{-\mathrm{i}(\mathbf{k}\cdot\mathbf{r}-\omega t)} \right] \\ & \times \left[u_{\mathbf{k}'\sigma'} \mathrm{e}^{\mathrm{i}(\mathbf{k}'\cdot\mathbf{r}-\omega' t)} - u_{\mathbf{k}'\sigma'}^* \mathrm{e}^{-\mathrm{i}(\mathbf{k}'\cdot\mathbf{r}-\omega' t)} \right] \Bigg\}. \end{aligned} \tag{1.37}$$

- Using the orthogonality of the polarization unit vectors $\mathbf{e}_\sigma \cdot \mathbf{e}_{\sigma'} = \delta_{\sigma\sigma'}$ as well as the relation $(\mathbf{k} \times \mathbf{e}_\sigma) \cdot (\mathbf{k} \times \mathbf{e}_{\sigma'}) = k^2 (\mathbf{e}_\sigma \cdot \mathbf{e}_{\sigma'}) = k^2 \delta_{\sigma\sigma'}$, integration over $\mathbf{r}$ as $\int \mathrm{d}^3 r \mathrm{e}^{\mathrm{i}(\mathbf{k}-\mathbf{k}')\cdot\mathbf{r}}$ yields $(2\pi)^3 \delta(\mathbf{k}-\mathbf{k}')$ and then integrate over $\mathbf{k}'$ to find

$$\boxed{H = 2\varepsilon_0 \sum_\sigma \int \mathrm{d}^3 k\, \omega^2 |u_{\mathbf{k}\sigma}|^2.} \tag{1.38}$$

- The expansion coefficients $u_{\mathbf{k}\sigma}$ are in general complex functions, which we decompose into their real and imaginary parts

$$u_{\mathbf{k}\sigma} = \frac{1}{2\sqrt{\varepsilon_0}} \left[q_{\mathbf{k}\sigma} + \mathrm{i} \frac{p_{\mathbf{k}\sigma}}{\omega} \right], \qquad u_{\mathbf{k}\sigma}^* = \frac{1}{2\sqrt{\varepsilon_0}} \left[q_{\mathbf{k}\sigma} - \mathrm{i} \frac{p_{\mathbf{k}\sigma}}{\omega} \right], \tag{1.39}$$

with

$$q_{\mathbf{k}\sigma} = \sqrt{\varepsilon_0} \left(u_{\mathbf{k}\sigma} + u_{\mathbf{k}\sigma}^* \right), \qquad p_{\mathbf{k}\sigma} = -\mathrm{i}\omega\sqrt{\varepsilon_0} \left(u_{\mathbf{k}\sigma} - u_{\mathbf{k}\sigma}^* \right). \tag{1.40}$$

- With these definitions, we obtain the classical Hamiltonian as

$$\boxed{H = \frac{1}{2}\sum_{\sigma}\int \mathrm{d}^3k\left(p_{\mathbf{k}\sigma}^2 + \omega^2 q_{\mathbf{k}\sigma}^2\right).} \tag{1.41}$$

The electromagnetic field is composed of infinitely many uncoupled harmonic oscillators with frequencies $\omega = |\mathbf{k}|c$. The interpretation suggested by this result is that the electromagnetic field in free space can be regarded as an ensemble of uncoupled harmonic oscillators, each of which can now be quantized separately.

1.1.4 Creation and annihilation operators

- In Equation (1.41) variables appear that correspond to the position and momentum variables of harmonic oscillators. Each of these oscillators corresponds to an electromagnetic field mode, characterized by a continuous wavevector index and a discrete polarization index. Each of these variables is then canonically quantized by promoting the c-numbers to Hilbert space operators,

$$q_{\mathbf{k}\sigma} \mapsto \hat{q}_{\mathbf{k}\sigma}, \qquad p_{\mathbf{k}\sigma} \mapsto \hat{p}_{\mathbf{k}\sigma},$$

and postulating the equal-time commutation relations

$$\left[\hat{q}_{\mathbf{k}\sigma}, \hat{p}_{\mathbf{k}'\sigma'}\right] := \mathrm{i}\hbar\delta(\mathbf{k}-\mathbf{k}')\delta_{\sigma\sigma'}. \tag{1.42}$$

- As in the usual theory of the quantum-mechanical harmonic oscillator, we introduce, analogous to the complex expansion coefficients $u_{\mathbf{k}\sigma}$, the non-Hermitian operators $\hat{a}_\sigma(\mathbf{k})$ and $\hat{a}_\sigma^\dagger(\mathbf{k})$ as

$$\hat{a}_\sigma(\mathbf{k}) = \sqrt{\frac{\omega}{2\hbar}}\left(\hat{q}_{\mathbf{k}\sigma} + \frac{\mathrm{i}}{\omega}\hat{p}_{\mathbf{k}\sigma}\right), \tag{1.43}$$

$$\hat{a}_\sigma^\dagger(\mathbf{k}) = \sqrt{\frac{\omega}{2\hbar}}\left(\hat{q}_{\mathbf{k}\sigma} - \frac{i}{\omega}\hat{p}_{\mathbf{k}\sigma}\right). \tag{1.44}$$

- From the commutation relations of $\hat{q}_{\mathbf{k}\sigma}$ and $\hat{p}_{\mathbf{k}\sigma}$ it follows that the new operators satisfy

$$\left[\hat{a}_\sigma(\mathbf{k}), \hat{a}_{\sigma'}^\dagger(\mathbf{k}')\right] = \delta(\mathbf{k}-\mathbf{k})\delta_{\sigma\sigma'}. \tag{1.45}$$

- We know from the quantum theory of the harmonic oscillator that the operators $\hat{a}_{\mathbf{k}\sigma}$ and $\hat{a}_{\mathbf{k}\sigma}^\dagger$ annihilate or create quanta of energy $\hbar|\mathbf{k}|c$, respectively. The natural interpretation here is that these quanta represent excitations of the electromagnetic field mode λ. These elementary excitations are called *photons*.

- If we insert these ladder operators into the mode expansion of the vector potential, we obtain

$$\boxed{\hat{\mathbf{A}}(\mathbf{r}) = \sum_\sigma \int \frac{\mathrm{d}^3k}{(2\pi)^{3/2}} \sqrt{\frac{\hbar}{2\varepsilon_0\omega}} \mathbf{e}_\sigma \left[\mathrm{e}^{\mathrm{i}\mathbf{k}\cdot\mathbf{r}} \hat{a}_\sigma(\mathbf{k}) + \mathrm{e}^{-\mathrm{i}\mathbf{k}\cdot\mathbf{r}} \hat{a}_\sigma^\dagger(\mathbf{k}) \right].} \tag{1.46}$$

- The expansion (1.46) refers specifically to the decomposition of the vector potential into plane waves. However, one may also use any complete orthonormal set of functions as the basis of the HELMHOLTZ operator. In general, this relation can be written as

$$\hat{\mathbf{A}}(\mathbf{r}) = \sum_\lambda \left[\mathbf{A}_\lambda(\mathbf{r}) \hat{a}_\lambda + \mathbf{A}_\lambda^*(\mathbf{r}) \hat{a}_\lambda^\dagger \right]. \tag{1.47}$$

  with $\mathbf{A}_\lambda(\mathbf{r})$ as the spatial mode functions from classical optics (e.g. HERMITE-GAUSS modes, LAGUERRE-GAUSS modes etc), written with a mode index λ that is not further specified.

- Inserting into the Hamiltonian function (1.41), we obtain

$$\boxed{\hat{H} = \frac{1}{2} \sum_\lambda \hbar\omega_\lambda \left(\hat{a}_\lambda \hat{a}_\lambda^\dagger + \hat{a}_\lambda^\dagger \hat{a}_\lambda \right) = \sum_\lambda \hbar\omega_\lambda \left(\hat{a}_\lambda^\dagger \hat{a}_\lambda + \frac{1}{2} \right),} \tag{1.48}$$

  where in the last equation we have used the commutation relations (1.45) in the form $[\hat{a}_\lambda, \hat{a}_{\lambda'}^\dagger] = \delta_{\lambda\lambda'}$. The Hamiltonian (1.48) yields HEISENBERG equations of motion for the photonic ladder operators

$$\dot{\hat{a}}_\lambda = \frac{1}{\mathrm{i}\hbar} \left[\hat{a}_\lambda, \hat{H} \right] = -\mathrm{i}\omega_\lambda \hat{a}_\lambda \quad \Rightarrow \quad \hat{a}_\lambda(t) = \mathrm{e}^{-\mathrm{i}\omega_\lambda t} \hat{a}_\lambda, \tag{1.49}$$

$$\dot{\hat{a}}_\lambda^\dagger = \frac{1}{\mathrm{i}\hbar} \left[\hat{a}_\lambda^\dagger, \hat{H} \right] = \mathrm{i}\omega_\lambda \hat{a}_\lambda^\dagger \quad \Rightarrow \quad \hat{a}_\lambda^\dagger(t) = \mathrm{e}^{\mathrm{i}\omega_\lambda t} \hat{a}_\lambda^\dagger. \tag{1.50}$$

- We have here explicitly distinguished between the HEISENBERG picture, in which the operators carry the time dependence, and the SCHRÖDINGER picture, in which the states carry the time dependence and the operators are time-independent. Both pictures coincide at $t = 0$. The amplitude operators appear in the combinations $\mathrm{e}^{\mathrm{i}(\mathbf{k}\cdot\mathbf{r}-\omega t)} \hat{a}_\sigma(\mathbf{k})$ and $\mathrm{e}^{-\mathrm{i}(\mathbf{k}\cdot\mathbf{r}-\omega t)} \hat{a}_\sigma^\dagger(\mathbf{k})$. For this reason, the annihilation operators $\hat{a}_\sigma(\mathbf{k})$ are associated with the positive frequency part of the electromagnetic field, and the creation operators with the negative frequency part. From the classical relation $\mathbf{E}(\mathbf{r}, t) = -\dot{\mathbf{A}}(\mathbf{r}, t)$, it now follows from the HEISENBERG equations of motion, (1.49) and (1.50), that the operator of the electric field is given as

$$\boxed{\hat{\mathbf{E}}(\mathbf{r}) = -\dot{\hat{\mathbf{A}}}(\mathbf{r}) = \mathrm{i} \sum_\lambda \omega_\lambda \left[\mathbf{A}_\lambda(\mathbf{r}) \hat{a}_\lambda - \mathbf{A}_\lambda^*(\mathbf{r}) \hat{a}_\lambda^\dagger \right].} \tag{1.51}$$

- From the Hamiltonian (1.48) one sees that, even in the absence of any photonic excitations, the electromagnetic field possesses a ground-state energy

$$|0\rangle = |0\rangle_{\lambda_1} \otimes |0\rangle_{\lambda_2} \otimes \cdots \otimes |0\rangle_{\lambda_N} \tag{1.52}$$

$$\langle 0|\hat{H}|0\rangle = \frac{1}{2}\sum_{\lambda} \hbar\omega_\lambda = \frac{\hbar c}{2}\sum_{\sigma}\int \frac{\mathrm{d}^3k}{(2\pi)^{3/2}}|\mathbf{k}| \longrightarrow +\infty. \tag{1.53}$$

  Each harmonic oscillator contributes $\hbar\omega_\lambda/2$ to vacuum energy. This is, of course, infinitely large because there are infinitely many modes, hence vacuum energy is $+\infty$. This is an effect that is solely due to the quantization of the field, since it originates from the non-vanishing commutator of the ladder operators. Does that matter? Is the infinite energy a constant or is there a physical effect associated with it?

- In summary, the quantized electromagnetic field consists of infinitely many uncoupled harmonic oscillators associated with each mode $\longrightarrow$ Hamiltonian is a sum of Hamiltonians for each mode. Photons are elementary excitations of a (monochromatic) mode or narrow-band collection of these modes (pulse). The ladder operators create/destroy photons.

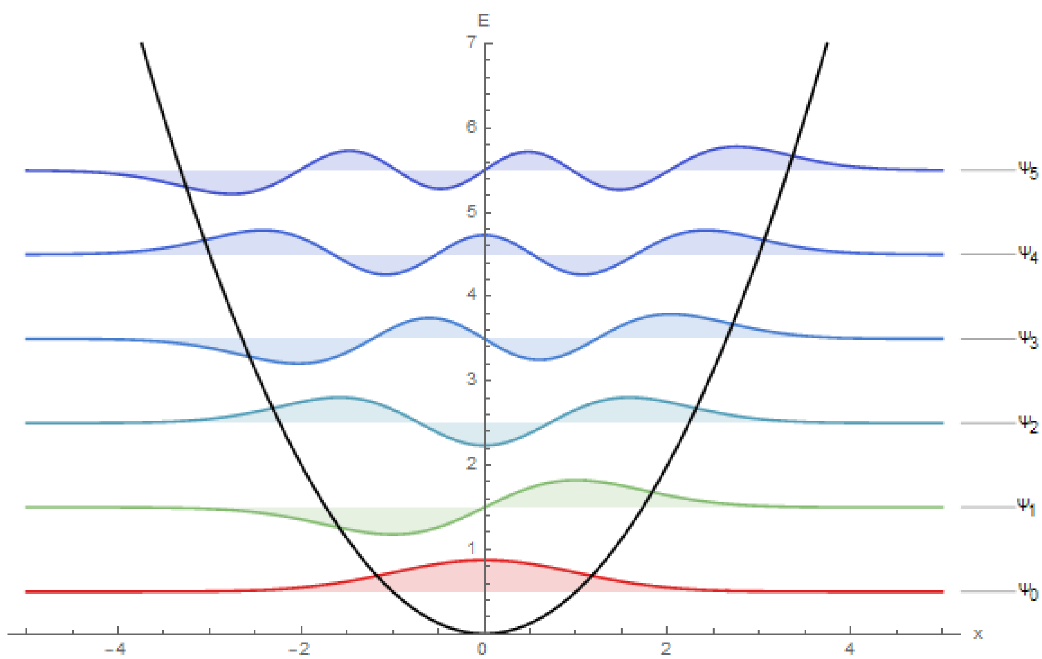

1.2 Quantum states of light

- In the quantization of the electromagnetic field operators, we have seen that the quantized electromagnetic field is a collection of uncoupled harmonic oscillators, each of which is described by a Hamiltonian

$$\hat{H}_\lambda = \hbar\omega_\lambda \left(\hat{n}_\lambda + \tfrac{1}{2}\right). \tag{1.54}$$

  It is therefore possible, when introducing the possible quantum states, to focus on a single mode and, if necessary, extend this to a multimode system. From now on, we will therefore no longer explicitly carry the mode index λ.

- What is the quantum state of a photon? $\longrightarrow$ eigenvalue problem for Hamiltonian.

1.2.1 Fock states

- First look at single-mode monochromatic field described by Hamiltonian

$$\hat{H} = \hbar\omega\left(\hat{a}^\dagger\hat{a} + 1/2\right)$$

  is solved by considering the eigenvalue problem $\hat{a}^\dagger\hat{a}$. Both problems are equivalent, since

$$[\hat{H}, \hat{a}^\dagger\hat{a}] = 0.$$

- Define number operator as $\hat{a}^\dagger\hat{a} = \hat{n}$ fulfilling the eigenvalue equation

$$\hat{n}|\psi_n\rangle = n|\psi_n\rangle, \tag{1.55}$$

  where n is the eigenvalue of $\hat{n}$ and $|\psi_n\rangle$ is the corresponding eigenstate.

- Since the number operator $\hat{n}$ is Hermitian, its eigenvalues are real, and its eigenvectors $|\psi_n\rangle$ form a complete set of orthogonal states. From

$$\begin{aligned}\langle\psi_n|\hat{n}|\psi_n\rangle &= \langle\psi_n|\hat{a}^\dagger\hat{a}|\psi_n\rangle = n\langle\psi_n|\psi_n\rangle \\ &= ||\hat{a}|\psi_n\rangle||^2 \geq 0,\end{aligned} \tag{1.56}$$

  it follows that n must be a nonnegative number, since both $|\psi_n\rangle$ and $\hat{a}|\psi_n\rangle$ are Hilbert space vectors with nonnegative norm.

- Applying the commutation relation $[\hat{a}, \hat{a}^\dagger] = 1$ gives

$$[\hat{a}, \hat{n}] = [\hat{a}, \hat{a}^\dagger \hat{a}] = \hat{a},$$

and thus

$$\hat{n}(\hat{a}|\psi_n\rangle) = (\hat{a}\hat{n} - [\hat{a}, \hat{n}])|\psi_n\rangle = (n-1)(\hat{a}|\psi_n\rangle). \tag{1.57}$$

This means that $\hat{a}|\psi_n\rangle$ is an eigenvector of the number operator with eigenvalue $n-1$, which we denote by $|\psi_{n-1}\rangle$.

- Since all eigenvalues must be nonnegative, there must exist a state $|\psi_0\rangle$ such that

$$\hat{a}|\psi_0\rangle = 0.$$

This state is called the *ground state*. It contains *no* excitations and cannot be annihilated further. Similarly, one finds

$$\hat{n}(\hat{a}^\dagger|\psi_n\rangle) = (n+1)(\hat{a}^\dagger|\psi_n\rangle). \tag{1.58}$$

- From equations (1.57) and (1.58), it follows that $\hat{a}$ and $\hat{a}^\dagger$ indeed decrease or increase the number of excitations of the electromagnetic field mode.

- Starting from the ground state $|\psi_0\rangle$, all other states can now be generated by successive application of the creation operator $\hat{a}^\dagger$,

$$|\psi_n\rangle = (\hat{a}^\dagger)^n|\psi_0\rangle.$$

If we normalize these states as $|n\rangle = |\psi_n\rangle / \sqrt{\langle\psi_n|\psi_n\rangle}$, we obtain the **Fock states** or **photon-number states**. We assume that the ground state $|0\rangle = |\psi_0\rangle$ is already normalized. The n-th Fock state is then given by

$$|n\rangle = c_n(\hat{a}^\dagger)^n|0\rangle, \tag{1.59}$$

where the normalization constant c_n still needs to be determined.

- This is obtained from the condition

$$\langle n|n\rangle = |c_n|^2\langle 0|\hat{a}^n(\hat{a}^\dagger)^n|0\rangle = 1, \tag{1.60}$$

by calculating

$$\begin{aligned}
\langle 0|\hat{a}^n(\hat{a}^\dagger)^n|0\rangle &= \langle 0|\hat{a}^{n-1}\big(\hat{a}\hat{a}^\dagger\big)(\hat{a}^\dagger)^{n-1}|0\rangle \\
&= \langle 0|\hat{a}^{n-1}(\hat{a}^\dagger\hat{a}+1)(\hat{a}^\dagger)^{n-1}|0\rangle \\
&= \langle 0|\hat{a}^{n-1}\hat{n}(\hat{a}^\dagger)^{n-1}|0\rangle + \langle 0|\hat{a}^{n-1}(\hat{a}^\dagger)^{n-1}|0\rangle.
\end{aligned}$$

- Applying the commutation rule

$$[\hat{n}, (\hat{a}^\dagger)^k] = k(\hat{a}^\dagger)^k,$$

one obtains the result

$$\langle 0|\hat{a}^n(\hat{a}^\dagger)^n|0\rangle = n\langle 0|\hat{a}^{n-1}(\hat{a}^\dagger)^{n-1}|0\rangle = n(n-1)\langle 0|\hat{a}^{n-2}(\hat{a}^\dagger)^{n-2}|0\rangle = \cdots = n!\langle 0|0\rangle. \tag{1.61}$$

It immediately follows from (1.60) that

$$c_n = 1/\sqrt{n!}. \tag{1.62}$$

- In summary, we therefore find the normalized Fock states

$$|n\rangle = \frac{1}{\sqrt{n!}}(\hat{a}^\dagger)^n|0\rangle. \tag{1.63}$$

The action of the ladder operators is

$$\hat{a}^\dagger|n\rangle = \sqrt{n+1}\,|n+1\rangle, \tag{1.64}$$
$$\hat{a}|n\rangle = \sqrt{n}\,|n-1\rangle. \tag{1.65}$$

- Since the eigenvectors of the number operator are mutually orthogonal, we have

$$\langle m|n\rangle = \delta_{mn}. \tag{1.66}$$

and they form a complete set of orthonormal vectors. Thus, with the identity operator

$$\sum_{n=0}^{\infty}|n\rangle\langle n| = \mathbb{1}, \tag{1.67}$$

any arbitrary state can be expanded in terms of the Fock basis.

1.2.1.1 Photon statistics of Fock states

- We will now consider some properties of Fock states with respect to their photon statistics. A single mode in a Fock state $|n\rangle$ contains exactly n quanta of excitation energy $\hbar\omega$. Thus, the state describes a photon number state with exactly n quanta. The mean energy in such a mode is

$$\langle n|\hat{H}|n\rangle = \hbar\omega\left(n+\tfrac{1}{2}\right), \tag{1.68}$$

so that we can indeed identify an energy $\hbar\omega$ with each photon. Note that even in the absence of photons, the ground state energy is

$$\langle 0|\hat{H}|0\rangle = \hbar\omega/2 > 0.$$

- The fluctuations of an observable $\hat{O}$ are expressed by its variance $\langle(\Delta\hat{O})^2\rangle$, where $\Delta\hat{O} = \hat{O} - \langle\hat{O}\rangle$. For the photon-number variance in a FOCK state we obtain

$$\langle n|(\Delta\hat{n})^2|n\rangle = \langle n|\hat{n}^2|n\rangle - \langle n|\hat{n}|n\rangle^2 = 0. \tag{1.69}$$

This is of course to be expected, since the photon number in a FOCK state is well-defined and thus no energy fluctuations can occur.

- Things become more interesting if one considers the mean electric field. From equation (1.46) and the relation $\hat{\mathbf{E}}(\mathbf{r}) = -\dot{\mathbf{A}}(\mathbf{r})$ it follows for a single-mode field

$$\hat{\mathbf{E}}(\mathbf{r}) = \hat{\mathbf{E}}^{(+)}(\mathbf{r}) + \hat{\mathbf{E}}^{(-)}(\mathbf{r}) = \mathrm{i}\omega\left[\mathbf{A}(\mathbf{r})\hat{a} - \mathbf{A}^*(\mathbf{r})\hat{a}^\dagger\right], \tag{1.70}$$

where $\mathbf{A}(\mathbf{r})$ is again the spatial mode function, and $\hat{\mathbf{E}}^{(+)}(\mathbf{r})$ and $\hat{\mathbf{E}}^{(-)}(\mathbf{r})$ represent the positive and negative frequency parts of the electric field, respectively. This leads to the expectation value

$$\langle n|\hat{\mathbf{E}}(\mathbf{r})|n\rangle = 0. \tag{1.71}$$

- This is obviously an unusual result, since classically one would expect that a state with n photons should contain an electric field. However, if one considers the intensity of the field $\hat{I}(\mathbf{r}) = \hat{\mathbf{E}}^{(-)}(\mathbf{r}) \cdot \hat{\mathbf{E}}^{(+)}(\mathbf{r})$, one obtains

$$\langle n|\hat{I}(\mathbf{r})|n\rangle = \omega^2|\mathbf{A}(\mathbf{r})|^2 n, \tag{6.45}$$

which, as expected, grows with the photon number.

- The fluctuations of the k-th component of the electric field are

$$\langle n|\left[\Delta\hat{E}_k(\mathbf{r})\right]^2|n\rangle = \omega^2|A_k(\mathbf{r})|^2(2n+1), \tag{1.72}$$

and these also increase with photon number. In the absence of all photons, however, residual field fluctuations remain

$$\langle 0|\left[\Delta\hat{E}_k(\mathbf{r})\right]^2|0\rangle = \omega^2|A_k(\mathbf{r})|^2. \tag{1.73}$$

This means that the finite ground-state energy can be interpreted as the energy of the vacuum fluctuations. All these unusual properties make the FOCK states highly nonclassical states. We shall postpone the precise definition of nonclassicality until later.

1.2.1.2 Multi-mode states

- The monochromatic, single-mode light represents very strong (often unphysical) approximation.

- Generalize to multi-mode light fields labelled by $\lambda = 1 \dots n$, the HILBERT space is tensor product space $H = H_1 \otimes H_2 \otimes \dots \otimes H_n$ where eigenstates of Hamiltonian are tensor products of single-mode eigenstates $|\{n_\lambda\}\rangle = \otimes_\lambda |n_\lambda\rangle$, hence

$$\hat{H}\,|\{n_\lambda\}\rangle = \sum_\lambda \hbar\omega \left(n_\lambda + \tfrac{1}{2}\right) |\{n_\lambda\}\rangle\,. \tag{1.74}$$

The total number of photons $\hat{N} = \sum_\lambda \hat{n}_\lambda$ commutes with the Hamiltonian $[\hat{N}, \hat{H}] = 0$. Therefore

$$\hat{N}\,|\{n_\lambda\}\rangle = \left(\sum_\lambda n_\lambda\right) |\{n_\lambda\}\rangle\,. \tag{1.75}$$

- But: different possibilities of distributing N photons across M modes.

- **Example**: two-mode states $|n_1, n_2\rangle \equiv |n_1\rangle \otimes |n_2\rangle$

$$N = 0 : \{|0,0\rangle\}$$

$$N = 1 : \{|1,0\rangle, |0,1\rangle\}$$
$$N = 2 : \{|2,0\rangle, |1,1\rangle, |0,2\rangle\}$$

- The properties of multi-mode FOCK states are

$$\langle\{n_\lambda\}|(\Delta\hat{N})^2|\{n_\lambda\}\rangle = 0,$$

and

$$\langle\{n_\lambda\}|\hat{E}(\mathbf{r})|\{n_\lambda\}\rangle = 0.$$

1.2.1.3 Polarization states

- The electromagnetic field has two orthogonal transverse polarizations, hence we use multi-mode description even for monochromatic light.

- Possible choices of bases are
  - H/V (horizontal/vertical),

- D/A (diagonal/anti-diagonal), and
- R/L (right/left circular)

with ladder operators (for single frequency) $\hat{a}_H, \hat{a}_V$.

- Fock states can be expressed as

$$|1_H\rangle = \hat{a}_H^\dagger |0_H\rangle, \ldots$$

$$|1_V\rangle = \hat{a}_V^\dagger |0_V\rangle, \ldots$$

- **Notation**: sometimes found in the literature

$$|1_H\rangle \equiv |H\rangle, \quad |1_V\rangle \equiv |V\rangle$$

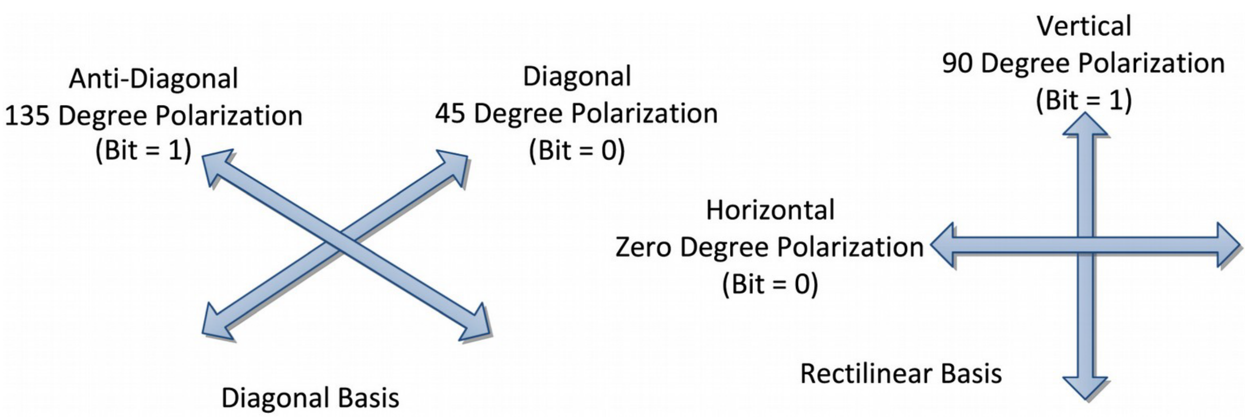

1.2.1.4 Density operator

- **Pure states**: quantum system prepared in state $|\psi\rangle$ $\rightarrow$ full knowledge that the state is indeed $|\psi\rangle$, but the measurement of an observable $\hat{O}$ still subject to quantum mechanical indeterminism

$$\langle\hat{O}\rangle = \langle\psi|\hat{O}|\psi\rangle \equiv \mathrm{Tr}\left[\,|\psi\rangle\langle\psi|\hat{O}\,\right] \tag{1.76}$$

- **Mixed state**: statistical uncertainty about preparation of a quantum system in states $\{|\psi_i\rangle\}$ with probabilities $p_i \geq 0, \sum_i p_i = 1$:

$$\langle \hat{O} \rangle = \sum_i p_i \mathrm{Tr}\left[|\psi_i\rangle\langle\psi_i|\hat{O}\right] = \mathrm{Tr}\big[\underbrace{\sum_i p_i |\psi_i\rangle\langle\psi_i|}_{\hat{\rho}}\hat{O}\big] \tag{1.77}$$

where the statistical (density) operator

$$\boxed{\hat{\rho} = \sum_i p_i \,|\psi_i\rangle\langle\psi_i|} \tag{1.78}$$

reflects classical statistical uncertainty about which states have been prepared.

- **Example**: single-photon source with probability p_1 to generate a photon in a given mode, and probability $p_0 = 1 - p_1$ of producing no photon at all:

$$\hat{\rho} = p_1|1\rangle\langle 1| + (1-p_1)|0\rangle\langle 0|$$

.

- The measure for mixedness of $\hat{\rho}$ is stated as

$$\boxed{\langle \hat{\rho} \rangle = \mathrm{Tr}\big[\hat{\rho}^2\big] \leq 1.} \tag{1.79}$$

- **Example**: for pure state

$$\hat{\rho} = |\psi\rangle\langle\psi| \Rightarrow \hat{\rho}^2 = |\psi\rangle\langle\psi|\psi\rangle\langle\psi| = |\psi\rangle\langle\psi| = \hat{\rho}$$

$$\Rightarrow \mathrm{Tr}\,\hat{\rho}^2 = \mathrm{Tr}\hat{\rho} = 1$$

- **Example**: for mixed state

$$\hat{\rho} = p_1|1\rangle\langle 1| + (1-p_1)|0\rangle\langle 0| \Rightarrow \hat{\rho}^2 = p_1^2|1\rangle\langle 1| + (1-p_1)^2|0\rangle\langle 0|$$

$$\Rightarrow \mathrm{Tr}\,\hat{\rho}^2 = p_1^2 + (1-p_1)^2 < 1$$

- **Example**: for maximally mixed state

$$\hat{\rho} = \frac{1}{n}\sum_{i=1}^{n} |\psi_i\rangle\langle\psi_i| \Rightarrow \mathrm{Tr}\hat{\rho}^2 = \frac{1}{n},$$

this reflects total lack of knowledge as to which state has been prepared.

- The properties of the density operator are

  1. $\hat{\rho} = \hat{\rho}^\dagger$,
  2. $\mathrm{Tr}\hat{\rho} = 1$,
  3. $\hat{\rho} \geq 0$.

- From the SCHRÖDINGER equation for state vector $|\psi\rangle$ and its hermitian adjoint

$$\mathrm{i}\hbar\frac{\mathrm{d}}{\mathrm{d}t}|\psi(t)\rangle = \hat{H}|\psi(t)\rangle,$$

$$-\mathrm{i}\hbar\frac{\mathrm{d}}{\mathrm{d}t}\langle\psi(t)| = \langle\psi(t)|\hat{H},$$

we obtain the VON NEUMANN equation for density operator $\hat{\rho} = |\psi\rangle\langle\psi|$

$$\mathrm{i}\hbar\frac{\mathrm{d}\hat{\rho}}{\mathrm{d}t} = \mathrm{i}\hbar\frac{\mathrm{d}}{\mathrm{d}t}\Big(|\psi\rangle\langle\psi|\Big) = \mathrm{i}\hbar\left(\frac{\mathrm{d}|\psi\rangle}{\mathrm{d}t}\langle\psi| + |\psi\rangle\frac{\mathrm{d}\langle\psi|}{\mathrm{d}t}\right)$$

$$\frac{\mathrm{d}\hat{\rho}}{\mathrm{d}t} = \hat{H}|\psi\rangle\langle\psi| - |\psi\rangle\langle\psi|\hat{H},$$

or

$$\boxed{\frac{\mathrm{d}\hat{\rho}}{\mathrm{d}t} = \frac{1}{\mathrm{i}\hbar}[\hat{H}, \hat{\rho}],} \tag{1.80}$$

which is analogue to the HEISENBERG equation of motion for an observable $\hat{O}$

$$\boxed{\frac{\mathrm{d}\hat{O}}{\mathrm{d}t} = \frac{1}{\mathrm{i}\hbar}[\hat{O}, \hat{H}].} \tag{1.81}$$

- Beside the minus sign difference between (1.80) and (1.81), the quantum state or statistical operator is expressed in SCHRÖDINGER picture, whereas the operator $\hat{O}$ in HEISENBERG picture.

- The density operator encodes the state of the quantum system, and its time evolution follows directly from the VON NEUMANN equation (1.80).

1.2.1.5 Multi-mode quantum systems and single-mode observables

- Assume a quantum system consisting of two (interacting subsystems) A, B with Hamiltonian
$$\hat{H} = \hat{H}_A + \hat{H}_B + \hat{H}_{AB}.$$

- $|\psi_i^A\rangle, |\psi_i^B\rangle$ form a complete set of basis states of subsystems A, B of Hamiltonians $\hat{H}_A, \hat{H}_B$, respectively, and $|\psi_i^A, \psi_i^B\rangle$ for the total system of Hamiltonian $\hat{H}$.

- But: the expectation value of observable $\hat{O}_A$ associated with subsystem A is
$$\langle \hat{O}_A \rangle = \mathrm{Tr}\left[\hat{\rho}_A \hat{O}_A\right].$$

- The *partial trace* over subsystem B reads
$$\hat{\rho}_A = \mathrm{Tr}_B \hat{\rho} = \sum_i \langle \psi_i^B | \hat{\rho} | \psi_i^B \rangle.$$

- The partial trace reflects complete lack of knowledge about the state of a subsystem, e.g. environment.

- Even if state of total system is pure, partial trace generically results in mixed states, except when $|\psi_i^{AB}\rangle = |\psi_i^A\rangle|\psi_i^B\rangle$.

- **Example**: equal superposition of pure states
$$|\psi^{AB}\rangle = \frac{1}{\sqrt{d}} \sum_{i=1}^{d} |\psi_i^A, \psi_i^B\rangle$$
yields
$$\hat{\rho}_A = \mathrm{Tr}_B\, |\psi^{AB}\rangle\langle\psi^{AB}| = \frac{1}{d} \sum_{i=1}^{d} |\psi_i^A\rangle\langle\psi_i^A|$$
$$\hat{\rho}_B = \mathrm{Tr}_A\, |\psi^{AB}\rangle\langle\psi^{AB}| = \frac{1}{d} \sum_{i=1}^{d} |\psi_i^B\rangle\langle\psi_i^B|,$$
which are maximally mixed states.

- Entanglement means the quantum correlations between subsystems.

- **Example**: polarization state of two photons:

$$|\psi^{AB}\rangle = \frac{1}{\sqrt{2}}\left(|H^A, H^B\rangle + |V^A, V^B\rangle\right),$$

i.e. the detection of photon A in H polarization *predetermines* outcome of subsequent measurement of polarization of photon B $\rightarrow$ this state is *entangled*.

- But: the state

$$|\psi^{AB}\rangle = \frac{1}{2}\left(|H^A\rangle + |V^A\rangle\right)\left(|H^B\rangle + |V^B\rangle\right)$$

is *separable*, i.e. the measurement outcome of A does not influence outcome in B.

- **Definition**: A quantum state is separable if and only if it can be written in the form

$$\hat{\rho} = \sum_i p_i \hat{\rho}_i^A \otimes \hat{\rho}_i^B,$$

otherwise, it is entangled.

1.2.2 Coherent states

- The preparation of the quantized electromagnetic field in a Fock state has the unusual effect that the expectation value of the electric field vanishes. We therefore look for other quantum states whose statistics resemble those of classical light. In particular, we look for states $|\alpha\rangle$ for which the expectation value of the electric field has the classical value

$$\langle\alpha|\hat{\mathbf{E}}(\mathbf{r})|\alpha\rangle = \mathrm{i}\omega\left[\mathbf{A}(\mathbf{r})\alpha - \mathbf{A}^*(\mathbf{r})\alpha^*\right], \tag{1.82}$$

where the ladder operators $\hat{a}$ and $\hat{a}^\dagger$ are replaced by the complex numbers α and α^*, respectively. Such states are called *coherent states*.

- These states can be constructed as follows. From quantum theory, we know that any given complete set of orthonormal functions can be transformed into another such set by a unitary transformation. Here, we consider the unitary operator

$$\hat{U} = \hat{D}(\alpha) = \mathrm{e}^{\alpha\hat{a}^\dagger - \alpha^*\hat{a}}, \tag{1.83}$$

where α is a complex number. This operator, known as *displacement operator*, can be written in different operator orderings. The Baker-Campbell-Hausdorff formula for two operators $\hat{A}$ and $\hat{B}$, with $[\hat{A},[\hat{A},\hat{B}]] = [\hat{B},[\hat{A},\hat{B}]] = 0$, can be written as

$$e^{\hat{A}+\hat{B}} = e^{\hat{A}}e^{\hat{B}}e^{-\frac{1}{2}[\hat{A},\hat{B}]}. \tag{1.84}$$

- Applied to the displacement operator (1.83) with $\hat{A} = \alpha\hat{a}^\dagger$ and $\hat{B} = -\alpha^*\hat{a}$, this yields the normal- and anti-normal-ordered forms of the displacement operator as

$$\begin{aligned} \hat{D}(\alpha) &= e^{\alpha\hat{a}^\dagger}e^{-\alpha^*\hat{a}}e^{-|\alpha|^2/2}, \quad \text{normal order,} && (1.85)\\ \hat{D}(\alpha) &= e^{-\alpha^*\hat{a}}e^{\alpha\hat{a}^\dagger}e^{|\alpha|^2/2}, \quad \text{anti-normal order.} && (1.86) \end{aligned}$$

  Note: they are exactly the same operators, only the order of creation and annihilation operators is different!

- We now use the displacement operator to transform both the ladder operators and the Fock states as

$$\begin{aligned} \hat{a}' &= \hat{D}(\alpha)\,\hat{a}\,\hat{D}^\dagger(\alpha), && (1.87)\\ |n'\rangle &= \hat{D}(\alpha)\,|n\rangle. && (1.88) \end{aligned}$$

- For the transformation of the operators, we use the representations (1.85) and (1.86), and write

$$\begin{aligned} \hat{a}' = \hat{D}(\alpha)\,\hat{a}\,\hat{D}^\dagger(\alpha) &= \underbrace{e^{\alpha\hat{a}^\dagger}e^{-\alpha^*\hat{a}}e^{-|\alpha|^2/2}}_{\text{normal order}}\,\hat{a}\,\underbrace{e^{\alpha^*\hat{a}}e^{-\alpha^*\hat{a}^\dagger}e^{|\alpha|^2/2}}_{\text{anti-normal order}}\\ &= e^{\alpha\hat{a}^\dagger}\hat{a}e^{-\alpha^*\hat{a}^\dagger}\\ &= \left(1+\alpha\hat{a}^\dagger+\frac{1}{2!}\alpha^2(\hat{a}^\dagger)^2+\cdots\right)\hat{a}\left(1-\alpha^*\hat{a}^\dagger+\frac{1}{2!}(\alpha^*)^2(\hat{a}^\dagger)^2+\cdots\right)\\ &= \hat{a}-\alpha. && (1.89) \end{aligned}$$

- Applied to the transformed ground state $|0'\rangle$, we have

$$\hat{a}'|0'\rangle \equiv 0 = (\hat{a}-\alpha)\,\hat{D}(\alpha)\,|0\rangle. \tag{1.90}$$

  We now call this transformed ground state

$$|0'\rangle = \hat{D}(\alpha)\,|0\rangle = |\alpha\rangle,$$

  since it depends on the complex number α.

- From Eq.(1.90), we see that the coherent states $|\alpha\rangle$ are right-hand eigenstates of the annihilation operator $\hat{a}$, i.e.

$$\boxed{\hat{a}|\alpha\rangle = \alpha\,|\alpha\rangle.} \tag{1.91}$$

- Analogously, there are, of course, also left-hand eigenstates of $\hat{a}^\dagger$, namely

$$\langle\alpha|\hat{a}^\dagger = \langle\alpha|\alpha^*.$$

- The coherent states are normalized, $\langle\alpha|\alpha\rangle = 1$, and the amplitude α determines, in the complex phase space, the point corresponding to the coherent amplitude of the harmonic oscillator. Since they are eigenstates of a non-Hermitian operator, they are not orthogonal to one another and therefore do not satisfy an orthogonality relation. However, we can use the completeness of the Fock states (1.67) to expand the coherent states in terms of them,

$$\begin{aligned}
|\alpha\rangle &= \sum_{n=0}^{\infty} |n\rangle\langle n|\alpha\rangle \\
&= \sum_{n=0}^{\infty} \langle n|\hat{D}(\alpha)|0\rangle|n\rangle \\
&= \sum_{n=0}^{\infty} \langle n|\mathrm{e}^{\alpha\hat{a}^\dagger}\mathrm{e}^{-\alpha^*\hat{a}}\mathrm{e}^{-|\alpha|^2/2}|0\rangle|n\rangle \\
&= \sum_{n=0}^{\infty} \mathrm{e}^{-|\alpha|^2/2}\langle n|\mathrm{e}^{\alpha\hat{a}^\dagger}|0\rangle|n\rangle \\
&= \sum_{n=0}^{\infty} \frac{\alpha^n}{\sqrt{n!}}\mathrm{e}^{-|\alpha|^2/2}|n\rangle.
\end{aligned} \tag{1.92}$$

- The photon number states in a coherent state are Poissonian-distributed, $|\langle n|\alpha\rangle|^2 = |\alpha|^{2n}\mathrm{e}^{-|\alpha|^2}/n!$, with a mean value $\langle\alpha|\hat{n}|\alpha\rangle = |\alpha|^2$. It can be shown that the coherent states are overcomplete and satisfy the relation

$$\frac{1}{\pi}\int \mathrm{d}^2\alpha\,|\alpha\rangle\langle\alpha| = \mathbb{1}. \tag{1.93}$$

1.2.2.1 Photon number statistics of coherent states

- With these definitions, the statistical properties of the coherent states follow immediately. As required at the beginning, the expectation value of the k-th component of the electric field is indeed

$$\langle\alpha|\hat{E}_k(\mathbf{r})|\alpha\rangle = \mathrm{i}\omega\left[A_k(\mathbf{r})\alpha - A_k^*(\mathbf{r})\alpha^*\right]. \tag{1.94}$$

- The variance of the electric field is, however,

$$\langle\alpha|[\Delta\hat{E}_k(\mathbf{r})]^2|\alpha\rangle = \omega^2|A_k(\mathbf{r})|^2, \tag{1.95}$$

  that is, independent of the coherent amplitude. The electric field variance in a coherent state always has the same value as in the ground state.

- This means that the relative noise of the electric field

$$\sqrt{\frac{\langle\alpha|[\Delta\hat{E}_k(\mathbf{r})]^2|\alpha\rangle}{[\langle\alpha|\hat{E}_k(\mathbf{r})|\alpha\rangle]^2}} = \frac{1}{2|\alpha|\,|\sin\varphi(A_k,\alpha)|} \geq \frac{1}{2\sqrt{\bar{n}}}, \tag{1.96}$$

  decreases with the square root of the mean photon number $|\alpha| = \sqrt{\langle\alpha|\hat{n}|\alpha\rangle} = \sqrt{\bar{n}}$. This behavior resembles classical noise, i.e. classical statistical concept of independent measurements. Therefore, coherent states are very close to classical states.

1.2.2.2 States of minimal uncertainty

- To obtain a better picture of coherent states in phase space, we introduce the *quadrature operators*

$$\hat{x}(\phi) = \hat{a}\mathrm{e}^{\mathrm{i}\phi} + \hat{a}^\dagger\mathrm{e}^{-\mathrm{i}\phi}, \tag{1.97}$$

  which depend on a phase φ. We can express the operator of the electric field by means of the quadrature operator as $\hat{E}_k(\mathbf{r}) = \omega|A_k(\mathbf{r})|\hat{x}(\phi)$ with $\phi = \arg A_k(\mathbf{r}) + \pi/2$. The quadrature operators for two different angles ϕ and ϕ' satisfy the commutation relation

$$[\hat{x}(\phi), \hat{x}(\phi')] = 2\mathrm{i}\sin(\phi - \phi'). \tag{1.98}$$

- This means that two quadrature operators with orthogonal phases $\phi' = \phi + \pi/2$ can be regarded as position and momentum operators in phase space, since $[\hat{x}(\phi), \hat{x}(\phi + \pi/2)] = 2\mathrm{i}$.

- The general HEISENBERG uncertainty relation[1] for these operators thus reads

$$\Delta\hat{x}(\phi)\,\Delta\hat{x}(\phi+\pi/2) \geq 1. \tag{1.99}$$

The electric field variance (1.95) in a coherent state can now be rewritten using the quadrature operators, yielding the result

$$\langle\alpha|[\Delta\hat{x}(\phi)]^2|\alpha\rangle = 1 \tag{1.100}$$

for all angles ϕ. This means that the coherent states are *minimum-uncertainty states*, i.e., they are those states for which the uncertainty relation (1.99) exactly attains its lower bound.

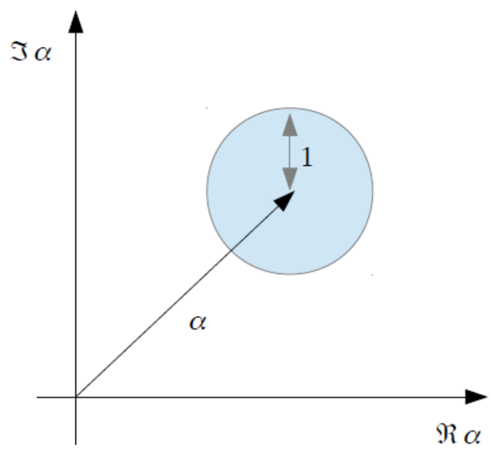

1.2.3 Squeezed states

- HEISENBERG's uncertainty relation only limits the area of uncertainty in phase space that the variances of the quadrature operators must occupy, but not the shape of this area.

- It is possible to reduce the quadrature noise in one direction in phase space on the expense of the quadrature orthogonal to it ("squeezing"). Such quantum states actually exist and are called *squeezed states*.

- The squeezed states are generated, like the coherent states, by a unitary operator, which in this case is given by

$$\hat{U} = \hat{S}(\xi) = \exp\left[\frac{1}{2}\left(\xi^*\hat{a}^2 - \xi(\hat{a}^\dagger)^2\right)\right], \tag{1.101}$$

[1] $\Delta\hat{A}\Delta\hat{B} \geq \frac{1}{2}\langle[\hat{A},\hat{B}]\rangle$

and depends on the (complex) squeezing parameter ξ.

- We will see later that such operators can be realized with nonlinear optics.
- The squeezing operator $\hat{S}(\xi)$ transforms the ladder operators as

$$\hat{a}' = \hat{S}(\xi)\hat{a}\hat{S}^\dagger(\xi) = \mu\hat{a} + \nu\hat{a}^\dagger, \tag{1.102}$$

$$(\hat{a}^\dagger)' = \hat{S}(\xi)\hat{a}^\dagger\hat{S}^\dagger(\xi) = \nu^*\hat{a} + \mu\hat{a}^\dagger, \tag{1.103}$$

where $\mu = \cosh|\xi|$ and $\nu = e^{i\phi_\xi}\sinh|\xi|$.

- These relations can be derived either by direct Taylor expansion or by using the Baker–Hausdorff lemma

$$e^{z\hat{A}}\hat{B}e^{-z\hat{A}} = \sum_{n=0}^{\infty}\frac{z^n}{n!}[\hat{A},\hat{B}]_n \tag{1.104}$$

$$= \hat{B} + z[\hat{A},\hat{B}] + \frac{z^2}{2!}[\hat{A},[\hat{A},\hat{B}]] + \ldots, \tag{1.105}$$

with $\hat{B} = \hat{a}$ (or $\hat{B} = \hat{a}^\dagger$), and $[\hat{A},\hat{B}]_n = [\hat{A},[\hat{A},\hat{B}]_{n-1}], \quad [\hat{A},\hat{B}]_0 = \hat{B}$.
Take $z\hat{A} = \frac{1}{2}\left(\xi^*\hat{a}^2 - \xi\hat{a}^{+2}\right) \quad \Rightarrow \quad z[\hat{A},\hat{a}] = \xi\hat{a}^\dagger, \qquad z[\hat{A},\hat{a}^+] = \xi^*\hat{a}$.

- Equations (1.102) and (1.103) are unitary transformation mixing creation and annihilation operators ("Bogoljubov transformation").

1.2.3.1 Photon number statistics of the squeezed vacuum

- *Definition*: The squeezed vacuum is defined as

$$|\xi\rangle = \hat{S}(\xi)|0\rangle. \tag{1.106}$$

- Operator disentangling theorem (without proof):

$$\hat{S}(\xi) = \exp\left(-\frac{\nu}{2\mu}\hat{a}^{\dagger 2}\right)\left(\frac{1}{\mu}\right)^{\hat{n}+1/2}\exp\left(\frac{\nu^*}{2\mu}\hat{a}^2\right).$$

Hence

$$|\xi\rangle = \frac{1}{\sqrt{\mu}}\exp\left(-\frac{\nu}{2\mu}\hat{a}^{\dagger 2}\right)|0\rangle,$$

$$= \frac{1}{\sqrt{\mu}}\sum_{n=0}^{\infty}\frac{1}{n!}\left(-\frac{\nu}{2\mu}\right)^n(\hat{a}^\dagger)^{2n}|0\rangle,$$

$$= \frac{1}{\sqrt{\mu}}\sum_{n=0}^{\infty}\left(-\frac{\nu}{2\mu}\right)^n\frac{\sqrt{(2n)!}}{n!}|2n\rangle. \tag{1.107}$$

The squeezed vacuum state contains only even photon numbers!

- The mean photon number reads

$$\begin{aligned}
\langle\xi|\hat{n}|\xi\rangle &= \langle 0|\hat{S}^\dagger(\xi)\hat{n}\hat{S}(\xi)|0\rangle \\
&= \langle 0|\big[\hat{S}^\dagger(\xi)\hat{a}^\dagger\hat{S}(\xi)\big]\big[\hat{S}^\dagger(\xi)\hat{a}\hat{S}(\xi)\big]|0\rangle \\
&= \langle 0|\big[\hat{S}(-\xi)\hat{a}^\dagger\hat{S}^\dagger(-\xi)\big]\big[\hat{S}(-\xi)\hat{a}\hat{S}^\dagger(-\xi)\big]|0\rangle \\
&= \langle 0|\big[-\nu^*\hat{a}+\mu\hat{a}^\dagger\big]\big[\mu\hat{a}-\nu\hat{a}^\dagger\big]|0\rangle \\
&= |\nu|^2 \\
&= \sinh^2|\xi|.
\end{aligned} \tag{1.108}$$

- The mean electric field is calculated as

$$\langle\xi|\hat{E}_k(\mathbf{r})|\xi\rangle = \omega|A_k(\mathbf{r})|\langle\xi|\hat{x}(\phi)|\xi\rangle, \tag{1.109}$$

where

$$\begin{aligned}
\langle\xi|\hat{x}(\phi)|\xi\rangle &= \langle 0|\hat{S}^\dagger(\xi)\,\hat{x}(\phi)\,\hat{S}(\xi)|0\rangle \\
&= \langle 0|\big(\mu\hat{a}-\nu\hat{a}^\dagger\big)\mathrm{e}^{\mathrm{i}\phi}+\big(-\nu^*\hat{a}+\mu\hat{a}^\dagger\big)\mathrm{e}^{-\mathrm{i}\phi}|0\rangle \\
&= 0,
\end{aligned} \tag{1.110}$$

hence

$$\langle\xi|\hat{E}_k(\mathbf{r})|\xi\rangle = 0. \tag{1.111}$$

- Analogously, one finds for the electric field variance

$$\langle\xi|[\Delta\hat{E}_k(\mathbf{r})]^2|\xi\rangle = \omega^2|A_k(\mathbf{r})|^2\langle\xi|\hat{x}^2(\phi)|\xi\rangle, \tag{1.112}$$

where the quadrature variance

$$\begin{aligned}
\langle\xi|[\Delta\hat{x}(\phi)]^2|\xi\rangle &= \langle\xi|\hat{x}^2(\phi)|\xi\rangle - \underbrace{\big(\langle\xi|\hat{x}(\phi)|\xi\rangle\big)^2}_{=0} \\
&= \langle\xi|\hat{x}^2(\phi)|\xi\rangle \\
&= \langle 0|\hat{S}(-\xi)\big(\hat{a}\mathrm{e}^{\mathrm{i}\phi}+\hat{a}^\dagger\mathrm{e}^{-\mathrm{i}\phi}\big)^2\hat{S}^\dagger(-\xi)|0\rangle \\
&= \langle 0|\Big[\big(\mu\mathrm{e}^{\mathrm{i}\phi}-\nu^*\mathrm{e}^{-\mathrm{i}\phi}\big)\hat{a}+\big(\mu\mathrm{e}^{-\mathrm{i}\phi}-\nu\mathrm{e}^{\mathrm{i}\phi}\big)\hat{a}^\dagger\Big]^2|0\rangle \\
&= |\mu\mathrm{e}^{\mathrm{i}\phi}-\nu^*\mathrm{e}^{-\mathrm{i}\phi}|^2 \\
&= |\mu-|\nu|\mathrm{e}^{-\mathrm{i}(2\phi+\phi_\xi)}|^2,
\end{aligned} \tag{1.113}$$

which is minimal for $\mathrm{e}^{-\mathrm{i}(2\phi+\phi_\xi)}=1$: $\langle\xi|\hat{x}^2(\phi_{\min})|\xi\rangle = \big|\mu-|\nu|\big|^2 = \mathrm{e}^{-2|\xi|}$, and maximal for $\mathrm{e}^{-\mathrm{i}(2\phi+\phi_\xi)}=-1$: $\langle\xi|\hat{x}^2(\phi_{\max})|\xi\rangle = \big|\mu+|\nu|\big|^2 = \mathrm{e}^{2|\xi|}$.

- The noise is reduced below vacuum noise by $e^{-2|\xi|}$ in one quadrature, and increased by $e^{2|\xi|}$ in the orthogonal quadrature:

$$\begin{aligned} 2\phi + \phi_\xi &= 0 \quad \curvearrowright \quad \frac{\langle \xi|[\Delta \hat{E}_k(\mathbf{r})]^2|\xi\rangle}{\langle 0|[\Delta \hat{E}_k(\mathbf{r})]^2|0\rangle} = e^{-2|\xi|}, \\ 2\phi + \phi_\xi &= \frac{\pi}{2} \quad \curvearrowright \quad \frac{\langle \xi|[\Delta \hat{E}_k(\mathbf{r})]^2|\xi\rangle}{\langle 0|[\Delta \hat{E}_k(\mathbf{r})]^2|0\rangle} = e^{2|\xi|}. \end{aligned} \tag{1.114}$$

- The product of the variances in the two orthogonal directions shows, however, that the squeezed state is still a state of minimal uncertainty, so that HEISENBERG's uncertainty relation is not violated. Squeezed states therefore cause a phase-sensitive suppression of quantum noise.

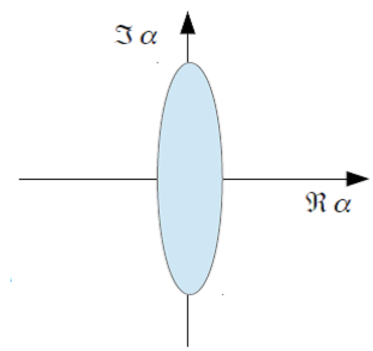

1.2.3.2 Two-mode squeezed vacuum

- The non-degenerate version of the single-mode squeeze operator is

$$\hat{S}(\xi) = \exp\left(\xi^* \hat{a}_1\hat{a}_2 - \xi\hat{a}_1^\dagger\hat{a}_2^\dagger\right) = \exp\left(-\frac{\nu}{\mu}\hat{a}_1^\dagger\hat{a}_2^\dagger\right)\left(\frac{1}{\mu}\right)^{\hat{n}_1+\hat{n}_2+1}\exp\left(\frac{\nu^*}{\mu}\hat{a}_1\hat{a}_2\right).$$

- The operators can be transformed as

$$\hat{S}^\dagger(\xi)\,\hat{a}_1\,\hat{S}(\xi) = \mu\hat{a}_1 - \nu\hat{a}_2^\dagger, \qquad \hat{S}^\dagger(\xi)\,\hat{a}_2\,\hat{S}(\xi) = \mu\hat{a}_2 - \nu\hat{a}_1^\dagger.$$

- The two-mode squeezed vacuum reads

$$
\begin{aligned}
|\mathrm{TMSV}\rangle &= \hat{S}(\xi)|0,0\rangle \\
&= \frac{1}{\mu}\exp\left(-\frac{\nu}{\mu}\hat{a}_1^\dagger\hat{a}_2^\dagger\right)|0,0\rangle \\
&= \frac{1}{\mu}\sum_{n=0}^{\infty}\left(-\frac{\nu}{\mu}\right)^n|n,n\rangle.
\end{aligned} \tag{1.115}
$$

- This is a quantum state with correlated photon numbers in both modes $\Rightarrow$ entangled state.

- For weak squeezing:

$$
|\xi| \ll 1 \qquad \Rightarrow \qquad |\mathrm{TMSV}\rangle \simeq |0,0\rangle - |\xi|\,|1,1\rangle + \dots \tag{1.116}
$$

1.2.4 Nonclassical light

- We already said that, e.g., FOCK states are strongly nonclassical states, but what does *'nonclassical'* really mean?

- We look for criteria based on statistical properties of classical and quantum physics

- The general nonclassicality criteria have to be based on the theory of quantum statistical distributions, e.g., in phase space (see later).

- Meanwhile, one can look for certain pragmatic criteria (which might not be mutually exclusive).

- A quantum state of the electromagnetic field is called *nonclassical* if its photon statistics cannot be simulated by any classical light source.

- The term "statistics" implies that we must take a closer look at the properties of certain correlation functions.

1.2.4.1 Nonclassicality criterion: squeezing

- Recall field fluctuations in vacuum state

$$
\langle 0|[\Delta\hat{E}_k(\mathbf{r})]^2|0\rangle = \omega^2|\mathbf{A}_k(\mathbf{r})|^2. \tag{1.117}
$$

- A quantum state shows squeezing if, for some direction in phase space,

$$\langle [\Delta \hat{E}_k(\mathbf{r})]^2 \rangle < \langle 0 | [\Delta \hat{E}_k(\mathbf{r})]^2 | 0 \rangle. \tag{1.118}$$

- Rewrite criterion as

$$\begin{aligned} \langle (\Delta \hat{E}_k)^2 \rangle &= \langle \hat{E}_k^2 \rangle - \langle \hat{E}_k \rangle^2 \\ &= \langle (\hat{E}_k^{(+)} + \hat{E}_k^{(-)})^2 \rangle - \langle \hat{E}_k \rangle^2 \\ &= \langle : (\Delta \hat{E}_k)^2 : \rangle + \langle [\hat{E}^{(+)}, \hat{E}^{(-)}]_k \rangle, \end{aligned} \tag{1.119}$$

with the normal-ordering symbol $:\hat{O}:$ as the normally ordered version of the operator $\hat{O}$ *without* use of the commutation relation $[\hat{a}, \hat{a}^\dagger] = 1$ (for example: $: \hat{a}\hat{a}^\dagger := \hat{a}^\dagger \hat{a}$).

- Note that

$$\langle [\hat{E}_k^{(+)}, \hat{E}_k^{(-)}] \rangle = \omega^2 |\mathbf{A}_k|^2 \langle [\hat{a}, \hat{a}^\dagger] \rangle = \omega^2 |\mathbf{A}_k|^2. \tag{1.120}$$

- The quantum state is squeezed if

$$\boxed{\langle : (\Delta \hat{E}_k)^2 : \rangle < 0.} \tag{1.121}$$

- Why is that nonclassical?

- The classical expectation value of a quantity O reads

$$\langle O \rangle = \int \mathrm{d}^2\alpha O(\alpha, \alpha^*) P_{\mathrm{cl}}(\alpha), \qquad P_{\mathrm{cl}}(\alpha) \geq 0. \tag{1.122}$$

Here

$$O(\alpha, \alpha^*) = \left[\Delta E_k(\mathbf{r}, \alpha, \alpha^*) \right]^2 \geq 0 \quad \Rightarrow \quad \langle O \rangle = \left\langle \left[\Delta E_k(\mathbf{r}, \alpha, \alpha^*) \right]^2 \right\rangle \geq 0, \tag{1.123}$$

i.e., a quantum state with $\langle : (\Delta \hat{E}_k)^2 : \rangle < 0$ does not have a classical counterpart.

1.2.4.2 Nonclassicality criterion: anti-bunching

- Define the normally ordered and time-ordered intensity correlation function (measurable in a Hanbury Brown–Twiss interferometer) as

$$\begin{aligned} G^{(2)}(\mathbf{r}_1, t+\tau; \mathbf{r}_2, t) &= \langle : \hat{I}(\mathbf{r}_1, t+\tau) \hat{I}(\mathbf{r}_2, t) : \rangle \\ &= \langle \hat{E}_i^{(-)}(\mathbf{r}_2, t) \hat{E}_j^{(-)}(\mathbf{r}_1, t+\tau) \hat{E}_j^{(+)}(\mathbf{r}_1, t+\tau) \hat{E}_i^{(+)}(\mathbf{r}_2, t) \rangle \end{aligned}$$

with classical analogue

$$\begin{aligned} G_{\mathrm{cl}}^{(2)}(\mathbf{r}_1, t+\tau; \mathbf{r}_2, t) &= \langle I(\mathbf{r}_1, t+\tau) I(\mathbf{r}_2, t) \rangle \rangle \\ &= \int \mathrm{d}I \mathrm{d}I' P_{\mathrm{cl}}(I, t+\tau, I', t) I(\mathbf{r}_1) I'(\mathbf{r}_2). \end{aligned} \tag{1.124}$$

- The Cauchy–Schwarz inequality

$$G_{\mathrm{cl}}^{(2)}(\mathbf{r}_1, t+\tau; \mathbf{r}_2, t) \leq \left[\langle I^2(\mathbf{r}_1, t+\tau) \rangle \right]^{1/2} \left[\langle I^2(\mathbf{r}_2, t) \rangle \right]^{1/2} \tag{1.125}$$

implies

$$G_{\mathrm{cl}}^{(2)}(\mathbf{r}_1, t+\tau; \mathbf{r}_2, t) \leq \left[\int \mathrm{d}I \, P_{\mathrm{cl}}(I, t+\tau) \, [I(\mathbf{r}_1)]^2 \right]^{1/2} \left[\int \mathrm{d}I' \, P_{\mathrm{cl}}(I', t) \, [I'(\mathbf{r}_2)]^2 \right]^{1/2} \tag{1.126}$$

with marginal distributions

$$P_{\mathrm{cl}}(I, t) = \int \mathrm{d}I' P_{\mathrm{cl}}(I, t; I', t). \tag{1.127}$$

- In the stationary limit $t \to \infty$, define

$$G^{(2)}(\tau) = \lim_{t\to\infty} G_{\mathrm{cl}}^{(2)}(\mathbf{r}_1, t+\tau; \mathbf{r}_2, t) \quad \Rightarrow \quad G^{(2)}(\tau) \leq G^{(2)}(0). \tag{1.128}$$

i.e., classical statistics predict larger intensity correlations for short delay times (bunching).

- The quantum states with

$$\boxed{G^{(2)}(\tau) > G^{(2)}(0)} \tag{1.129}$$

cannot be modeled by a classical probability distribution (photon anti-bunching).

- The normalized second-order intensity correlation function reads

$$g^{(2)}(\tau) = \lim_{t\to\infty} \frac{\langle : \hat{I}(\mathbf{r}_1, t+\tau) \hat{I}(\mathbf{r}_2, t) : \rangle}{\langle \hat{I}(\mathbf{r}_1, t+\tau) \rangle \langle \hat{I}(\mathbf{r}_2, t) \rangle}. \tag{1.130}$$

- **Example:** for coherent state

$$\hat{\mathbf{E}}^{(+)}(\mathbf{r}_i) \, |\alpha\rangle = \mathrm{i}\omega \, \mathbf{A}(\mathbf{r}_i) \, \alpha |\alpha\rangle, \tag{1.131}$$

$$\Rightarrow \langle \alpha | \, : \hat{I}(\mathbf{r}_1) \, \hat{I}(\mathbf{r}_2) : \, |\alpha\rangle = \langle \alpha | \hat{I}(\mathbf{r}_1) | \alpha \rangle \langle \alpha | \hat{I}(\mathbf{r}_2) | \alpha \rangle, \tag{1.132}$$

$$\Rightarrow g^{(2)}(\tau) = 1. \tag{1.133}$$

- **Example:** for a Fock state $|1\rangle$

$$\hat{\mathbf{E}}^{(+)}(\mathbf{r}_i) \, |1\rangle = \mathrm{i}\omega \, \mathbf{A}(\mathbf{r}_i) \, |0\rangle, \tag{1.134}$$

$$\Rightarrow g^{(2)}(\tau) = 0. \tag{1.135}$$

1.3 Qunatum optics in phase-space

- The statistical properties of quantum states should be reflected by distribution functions.
- The classical average in phase space reads

$$\langle X\rangle_{\rm cl} = \int d^2\alpha\, P_{\rm cl}(\alpha)\, X(\alpha), \tag{1.136}$$

with classical probability distribution $P_\alpha(\alpha) \geq 0$ and $\int d^2\alpha\, P_\alpha = 1$.

- The quantum average of operator $\hat{O}$ is

$$\langle\hat{O}\rangle_\rho = \mathrm{Tr}[\hat{\rho}\,\hat{O}]. \tag{1.137}$$

Q Can one define a similar expression in phase space?

A Take operator $\hat{O}$ to be a functional of amplitude operators $\hat{a}, \hat{a}^\dagger$

$$\hat{O} \Rightarrow \hat{O}(\hat{a}, \hat{a}^\dagger)$$

$\Rightarrow$ classical analogue by formally replacing

$$\hat{a} \rightarrow \alpha, \qquad \hat{a}^\dagger \rightarrow \alpha^*.$$

- But: watch out for operator ordering, e.g.,

$$\begin{aligned}
\hat{x}^2(\phi) &= \hat{a}^2 e^{2i\phi} + (\hat{a}^\dagger)^2 e^{-2i\phi} + \left(\hat{a}\hat{a}^\dagger + \hat{a}^\dagger\hat{a}\right) && \text{symmetric order} && (1.138)\\
&= \hat{a}^2 e^{2i\phi} + (\hat{a}^\dagger)^2 e^{-2i\phi} + \left(2\hat{a}^\dagger\hat{a} + 1\right) && \text{normal order} && (1.139)\\
&= \hat{a}^2 e^{2i\phi} + (\hat{a}^\dagger)^2 e^{-2i\phi} + \left(2\hat{a}^\dagger\hat{a} - 1\right) && \text{anti-normal order.} && (1.140)
\end{aligned}$$

- For now we use symmetric order. Rewrite classical function $O(\alpha, \alpha^*)$ identically

$$O(\alpha, \alpha^*) = \int d^2\beta\delta(\alpha - \beta)O(\beta, \beta^*), \tag{1.141}$$

with 2D-delta function of complex variable $\alpha = \alpha' + i\alpha''$

$$\begin{aligned}
\delta(\alpha) &= \delta(\alpha')\delta(\alpha'')\\
&= \frac{1}{(2\pi)^2}\iint dx dy e^{i(\alpha' x + \alpha'' y)}\\
&\overset{\gamma=\frac{i}{2}(x+iy)}{=} \frac{1}{\pi^2}\int d^2\gamma e^{\alpha\gamma^* - \alpha^*\gamma}\\
&= \frac{1}{\pi^2}\int d^2\gamma e^{\alpha^*\gamma - \alpha\gamma^*},
\end{aligned} \tag{1.142}$$

so that

$$O(\alpha,\alpha^*) = \frac{1}{\pi^2}\iint \mathrm{d}^2\beta\mathrm{d}^2\gamma \mathrm{e}^{(\alpha^*-\beta^*)\gamma-(\alpha-\beta)\gamma^*}O(\beta,\beta^*) \tag{1.143}$$

- Formally replace again $\alpha \to \hat{a}$, $\alpha^* \to \hat{a}^\dagger$

$$\hat{O}(\hat{a},\hat{a}^\dagger) = \frac{1}{\pi^2}\iint \mathrm{d}^2\beta\mathrm{d}^2\gamma \mathrm{e}^{(\hat{a}^\dagger-\beta^*)\gamma-(\hat{a}-\beta)\gamma^*}O(\beta,\beta^*) \tag{1.144}$$

with operator-valued delta function in symmetric order

$$\hat{\delta}(\hat{a}-\beta) = \frac{1}{\pi^2}\int \mathrm{d}^2\gamma \mathrm{e}^{(\hat{a}^\dagger-\beta^*)\gamma-(\hat{a}-\beta)\gamma^*} = \frac{1}{\pi^2}\int \mathrm{d}^2\gamma \mathrm{e}^{\gamma^*\beta-\gamma\beta^*}\hat{D}(\gamma) \tag{1.145}$$

given as a 2D-Fourier transform of displacement operator $\hat{D}(\gamma)$.

1.3.1 Wigner function

- Formal expansion of operator

$$\hat{O}(\hat{a},\hat{a}^\dagger) = \int \mathrm{d}^2\beta\hat{\delta}(\hat{a}-\beta)O(\beta,\beta^*) \tag{1.146}$$

and its expectation value yields

$$\langle\hat{O}(\hat{a},\hat{a}^\dagger)\rangle = \int \mathrm{d}^2\beta\, W(\beta)\, O(\beta,\beta^*), \tag{1.147}$$

where

$$\boxed{W(\beta) = \langle\hat{\delta}(\hat{a}-\beta)\rangle = \mathrm{Tr}\left[\hat{\rho}\hat{\delta}(\hat{a}-\beta)\right]} \tag{1.148}$$

is the Wigner function.

- Expression for quantum average looks *formally* the same as classical average.
- Wigner function replaces classical probability distribution.
- But: Wigner function is *not* positive semi-definite, thus not a classical probability distribution (quasi-probability distribution).

1.3.1.1 Operator expansion in phase space

- So far: only formal relation for operators in phase space as we have no precise way yet of computing the classical correspondence:

$$O(\alpha,\alpha^*) \;\to\; \text{compute from } \hat{O}(\hat{a},\hat{a}^\dagger) \text{ by inversion.}$$

- Using

$$\mathrm{Tr}\big[\hat{\delta}(\hat{a}-\beta)\,\hat{\delta}(\hat{a}-\gamma)\big] = \frac{1}{\pi^4}\iint \mathrm{d}^2\alpha_1 \mathrm{d}^2\alpha_2 \mathrm{e}^{\alpha_1^*\beta-\alpha_1\beta^*}\,\mathrm{e}^{\alpha_2^*\gamma-\alpha_2\gamma^*}\,\mathrm{Tr}\big[\hat{D}(\alpha_1)\,\hat{D}(\alpha_2)\big] \tag{1.149}$$

with

$$\begin{aligned}
\mathrm{Tr}\left[\underbrace{\hat{D}(\alpha_1)}_{\text{normal}}\ \underbrace{\hat{D}(\alpha_2)}_{\text{anti-normal}}\right] &= \mathrm{Tr}\left[\mathrm{e}^{\alpha_1\hat{a}^\dagger}\mathrm{e}^{-\alpha_1^*\hat{a}}\,\mathrm{e}^{-\alpha_2^*\hat{a}}\mathrm{e}^{\alpha_2\hat{a}^\dagger}\right]\mathrm{e}^{(|\alpha_2|^2-|\alpha_1|^2)/2} \\
&= \mathrm{Tr}\left[\mathrm{e}^{(\alpha_1+\alpha_2)\hat{a}^\dagger}\mathrm{e}^{-(\alpha_2^*+\alpha_1^*)\hat{a}}\right]\mathrm{e}^{(|\alpha_2|^2-|\alpha_1|^2)/2} \\
&= \frac{1}{\pi}\int \mathrm{d}^2\alpha\,\langle\alpha|\mathrm{e}^{(\alpha_1+\alpha_2)\hat{a}^\dagger}\mathrm{e}^{-(\alpha_1^*+\alpha_2^*)\hat{a}}|\alpha\rangle\mathrm{e}^{(|\alpha_2|^2-|\alpha_1|^2)/2} \\
&= \frac{1}{\pi}\int \mathrm{d}^2\alpha\,\mathrm{e}^{(\alpha_1+\alpha_2)\alpha^*-(\alpha_1^*+\alpha_2^*)\alpha}\mathrm{e}^{(|\alpha_2|^2-|\alpha_1|^2)/2} \\
&= \pi\,\delta(\alpha_1+\alpha_2).
\end{aligned} \tag{1.150}$$

Hence,

$$\begin{aligned}
\mathrm{Tr}\big[\hat{\delta}(\hat{a}-\beta)\hat{\delta}(\hat{a}-\gamma)\big] &= \frac{1}{\pi^3}\int \mathrm{d}^2\alpha_1 \mathrm{e}^{\alpha_1\beta^*-\alpha_1^*\beta}\,\mathrm{e}^{-\alpha_1\gamma^*+\alpha_1^*\gamma} \\
&= \frac{1}{\pi^3}\int \mathrm{d}^2\alpha_1 \mathrm{e}^{\alpha_1(\beta^*-\gamma^*)-\alpha_1^*(\beta-\gamma)} \\
&= \frac{1}{\pi^3}\big[\pi^2\delta(\beta-\gamma)\big] \\
&= \frac{1}{\pi}\delta(\beta-\gamma).
\end{aligned} \tag{1.151}$$

- Multiplying Eq. (1.146) from the right by $\hat{\delta}(\hat{a}-\gamma)$ yields

$$\hat{O}(\hat{a},\hat{a}^\dagger)\hat{\delta}(\hat{a}-\gamma) = \int \mathrm{d}^2\beta\hat{\delta}(\hat{a}-\beta)\hat{\delta}(\hat{a}-\gamma)O(\beta,\beta^*). \tag{1.152}$$

Taking the trace of both sides and using the identity (1.151) we find

$$O(\beta,\beta^*) = \pi\,\mathrm{Tr}\left[\hat{O}(\hat{a},\hat{a}^\dagger)\,\hat{\delta}(\hat{a}-\beta)\right]. \tag{1.153}$$

- Plugging Eq.(1.153) into Eq.(1.146) we obtain the formal operator expansion

$$\hat{O}(\hat{a},\hat{a}^\dagger) = \pi\int \mathrm{d}^2\alpha\mathrm{Tr}\left[\hat{O}(\hat{a},\hat{a}^\dagger)\hat{\delta}(\hat{a}-\alpha)\right]\hat{\delta}(\hat{a}-\alpha) \tag{1.154}$$

that works for all operators $\hat{O}$, in particular the density operator $\hat{\rho}$, for which

$$\mathrm{Tr}\big[\hat{\rho}\,\hat{\delta}(\hat{a}-\alpha)\big] = W(\alpha) \tag{1.155}$$

- Expansion of density operator in symmetric order

$$\hat{\rho} = \pi \int \mathrm{d}^2\alpha W(\alpha)\, \hat{\delta}(\hat{a} - \alpha). \tag{1.156}$$

- Finally we confirmed that there is one-to-one relation

$$\boxed{\hat{\rho} \iff W(\alpha)} \tag{1.157}$$

1.3.1.2 Examples of Wigner functions

- **Example 1:** Coherent state $\hat{\rho} = |\alpha_0\rangle\langle\alpha_0|$

$$\begin{aligned} W(\alpha) &= \langle\alpha_0|\hat{\delta}(\hat{a} - \alpha)|\alpha_0\rangle & (1.158)\\ &= \frac{1}{\pi^2}\int \mathrm{d}^2\beta \mathrm{e}^{\alpha\beta^* - \alpha^*\beta}\langle\alpha_0|\hat{D}(\beta)|\alpha_0\rangle & (1.159)\\ &= \frac{1}{\pi^2}\int \mathrm{d}^2\beta\, \mathrm{e}^{(\alpha-\alpha_0)\beta^* - (\alpha^* - \alpha_0^*)\beta - |\beta|^2/2} & (1.160)\\ &= \frac{2}{\pi}\mathrm{e}^{-2|\alpha-\alpha_0|^2} & (1.161) \end{aligned}$$

- Wigner function is positive, bounded by $2/\pi$, FWHM = unit disk which corresponds to uncertainty area in "naive" phase-space picture. For $\alpha_0 = 1 + \mathrm{i}$, the corresponding Wigner function is depicted below

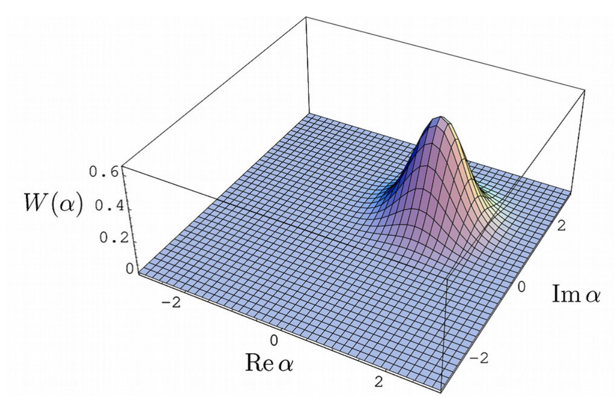

- **Example 2:** Squeezed vacuum state $\hat{\rho} = |\xi\rangle\langle\xi|$

- Starting from the relation

$$\langle\xi|\hat{D}(\beta)|\xi\rangle = \langle 0|\hat{S}^{\dagger}(\xi)\, \hat{D}(\beta)\, \hat{S}(\xi)|0\rangle, \tag{1.162}$$

expand displacement operator in TAYLOR series

$$\hat{S}^\dagger(\xi)\,\hat{D}(\beta)\,\hat{S}(\xi) = \hat{D}(\beta\mu + \beta^*\nu). \tag{1.163}$$

- The WIGNER function reads

$$\begin{aligned} W(\alpha) &= \frac{1}{\pi^2}\int \mathrm{d}^2\beta\, \mathrm{e}^{\alpha\beta^* - \alpha^*\beta}\, \mathrm{e}^{-|\beta\mu+\beta^*\nu|^2/2} \\ &= \frac{2}{\pi}\exp\left[-2\left(\frac{\alpha'^2}{\mathrm{e}^{-2\xi}} + \frac{\alpha''^2}{\mathrm{e}^{2\xi}}\right)\right] \end{aligned} \tag{1.164}$$

- WIGNER function is positive, bounded by $2/\pi$, FWHM = squeeze ellipse, i.e. corresponds to the uncertainty ellipse in phase-space.

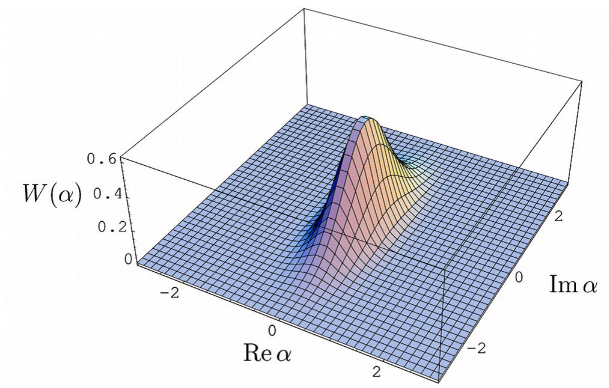

- **Example 3:** FOCK state $\hat{\rho} = |n\rangle\langle n|$, we have

$$\begin{aligned} \langle n|\hat{D}(\beta)|n\rangle &= \mathrm{e}^{-|\beta|^2/2}\langle n|e^{\beta\hat{a}^\dagger}\mathrm{e}^{-\beta^*\hat{a}}|n\rangle \\ &= \mathrm{e}^{-|\beta|^2/2}\sum_{m=0}^{n}\frac{(-|\beta|^2)^m}{(m!)^2}\langle n|(\hat{a}^\dagger)^m\hat{a}^m|n\rangle \\ &= \mathrm{e}^{-|\beta|^2/2}\sum_{m=0}^{n}\frac{(-1)^m}{m!}\binom{n}{m}|\beta|^{2m} \\ &= \mathrm{e}^{-|\beta|^2/2}L_n(|\beta|^2). \end{aligned} \tag{1.165}$$

- FOURIER transform of LAGUERRE polynomial is again a LAGUERRE polynomial

$$W(\alpha) = \frac{2}{\pi}(-1)^n\mathrm{e}^{-2|\alpha|^2}L_n\left(4|\alpha|^2\right). \tag{1.166}$$

- WIGNER function no longer positive semi-definite $-\frac{2}{\pi} \leq W(\alpha) \leq \frac{2}{\pi}$, cannot be interpreted as a classical probability distribution. Oscillatory behaviour in radial direction, no phase information.

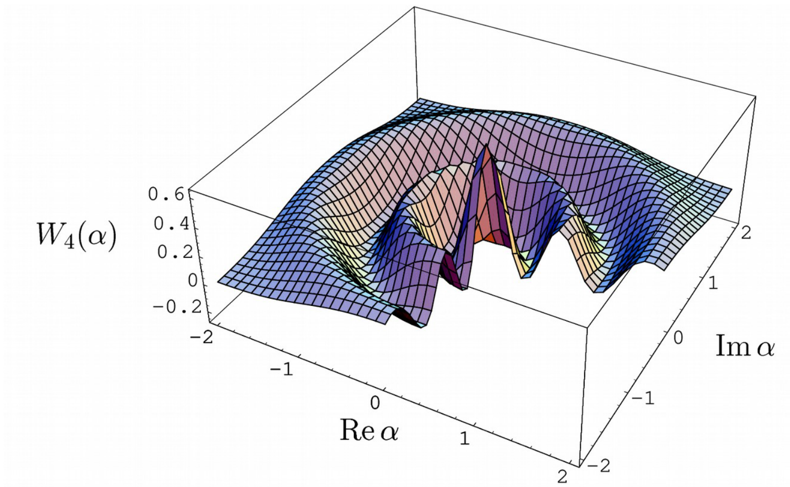

1.3.2 Normal and anti-normal operator order

- Wigner function is strictly associated with symmetrically ordered operator products.
- Sometimes it is important (or necessary) to obtain expectation values of (anti-) normally ordered operator products.
- Wigner function of squeezed states is positive: is the squeezed vacuum classical?
- In normal ordering all creation operators to the left of all annihilation operators using commutator $[\hat{a}, \hat{a}^\dagger] = 1$, e.g.,

$$\hat{x}^2(\phi) = \hat{a}^2 \mathrm{e}^{2i\phi} + (\hat{a}^\dagger)^2 \mathrm{e}^{-2i\phi} + (2\hat{a}^\dagger\hat{a} + 1), \qquad \hat{D}(\alpha) = \mathrm{e}^{\alpha\hat{a}^\dagger} \mathrm{e}^{-\alpha^*\hat{a}} \mathrm{e}^{-|\alpha|^2/2} \tag{1.167}$$

- Recall

$$\langle \hat{O}(\hat{a}, \hat{a}^\dagger) \rangle = \int \mathrm{d}^2\alpha \, W(\alpha) \, O(\alpha, \alpha^*) \tag{1.168}$$

  for symmetrically ordered operators $\hat{O}(\hat{a}, \hat{a}^\dagger)$ with associated classical function $O(\alpha, \alpha^*)$.

- For normally ordered operator $\hat{O}^{(\mathrm{N})}(\hat{a}, \hat{a}^\dagger)$ with classical function $O^{(\mathrm{N})}(\alpha, \alpha^*)$, define

$$\langle \hat{O}(\hat{a}, \hat{a}^\dagger) \rangle = \int \mathrm{d}^2\alpha \, P(\alpha) \, O^{(\mathrm{N})}(\alpha, \alpha^*) \tag{1.169}$$

  with Glauber–Sudarshan P function $P(\alpha)$.

- Because of normal ordering we write

$$
\begin{aligned}
O^{(\mathrm{N})}(\alpha, \alpha^*) &= \langle\alpha|\hat{O}(\hat{a}, \hat{a}^\dagger)|\alpha\rangle \\
&= \mathrm{Tr}\Big[|\alpha\rangle\langle\alpha|\hat{O}(\hat{a}, \hat{a}^\dagger)\Big]. \qquad (1.170)
\end{aligned}
$$

Plugging into Eq. (2.67) yields

$$
\begin{aligned}
\langle\hat{O}(\hat{a}, \hat{a}^\dagger)\rangle &= \mathrm{Tr}\Big[\hat{\rho}\,\hat{O}(\hat{a}, \hat{a}^\dagger)\Big] \\
&= \int \mathrm{d}^2\alpha\, P(\alpha)\,\mathrm{Tr}\Big[|\alpha\rangle\langle\alpha|\hat{O}(\hat{a}, \hat{a}^\dagger)\Big]. \qquad (1.171)
\end{aligned}
$$

Thus

$$
\boxed{\hat{\rho} = \int \mathrm{d}^2\alpha\, P(\alpha)\,|\alpha\rangle\langle\alpha|.} \qquad (1.172)
$$

- Looks formally like a statistical average over phase space of coherent states.
- $P(\alpha)$ can be highly singular and negative, hence not a classical probability distribution.
- **Example:** For a coherent state we have

$$
\hat{\rho} = |\alpha_0\rangle\langle\alpha_0| \quad \Rightarrow \quad P(\alpha) = \delta(\alpha - \alpha_0) \qquad (1.173)
$$

Q How to compute the Glauber–Sudarshan P function, and what is its relation to the Wigner function W?

A Starting from the fact that

$$
\begin{aligned}
O(\alpha, \alpha^*) &= \frac{1}{\pi^2}\iint \mathrm{d}^2\beta\mathrm{d}^2\gamma \mathrm{e}^{(\alpha^*-\beta^*)\gamma-(\alpha-\beta)\gamma^*} O(\beta, \beta^*) \\
&= \frac{1}{\pi^2}\iint \mathrm{d}^2\beta\mathrm{d}^2\gamma \mathrm{e}^{(\alpha^*-\beta^*)\gamma}\mathrm{e}^{-(\alpha-\beta)\gamma^*} O^{(N)}(\beta, \beta^*). \qquad (1.174)
\end{aligned}
$$

Therefore

$$
\begin{aligned}
\hat{O}(\hat{a}, \hat{a}^\dagger) &= \frac{1}{\pi^2}\iint \mathrm{d}^2\beta\mathrm{d}^2\gamma \mathrm{e}^{(\hat{a}^\dagger-\beta^*)\gamma}\mathrm{e}^{-(\hat{a}-\beta)\gamma^*} O^{(N)}(\beta, \beta^*) \\
&= \int \mathrm{d}^2\beta \left[\frac{1}{\pi^2}\int \mathrm{d}^2\gamma \mathrm{e}^{\gamma^*\beta-\gamma\beta^*}\hat{D}(\gamma)\mathrm{e}^{\frac{1}{2}|\gamma|^2}\right] O^{(N)}(\beta, \beta^*). \\
&= \int \mathrm{d}^2\beta \left[\frac{1}{\pi^2}\int \mathrm{d}^2\gamma \mathrm{e}^{\gamma^*\beta-\gamma\beta^*} :\hat{D}(\gamma):\right] O^{(N)}(\beta, \beta^*). \qquad (1.175)
\end{aligned}
$$

Recall that $:\hat{O}:$ is the *normal-ordering symbol* that brings the operator $\hat{O}$ into normal order without using the commutation relation $[\hat{a}, \hat{a}^\dagger] = 1$. Finally we obtain that

$$
\boxed{P(\beta) = \langle:\hat{\delta}(\hat{a} - \beta):\rangle} \qquad (1.176)
$$

- Since $\hat{D}(\alpha) = :\hat{D}(\alpha):\, \mathrm{e}^{-|\alpha|^2/2}$ we write

$$\begin{aligned}
\hat{\delta}(\hat{a}-\alpha) &= \mathrm{FT}\left[\hat{D}(\alpha)\right] \\
&= \mathrm{FT}\left[:\hat{D}(\alpha):\, \mathrm{e}^{-|\alpha|^2/2}\right] \\
&= :\hat{\delta}(\hat{a}-\alpha): * \mathrm{FT}\left[\mathrm{e}^{-|\alpha|^2/2}\right] \\
&= \frac{2}{\pi}\int \mathrm{d}^2\gamma\, \mathrm{e}^{-2|\alpha-\gamma|^2}\, :\hat{\delta}(\hat{a}-\gamma):
\end{aligned} \tag{1.177}$$

$$W(\alpha) = P(\alpha) * \mathrm{FT}\left[\mathrm{e}^{-|\alpha|^2/2}\right] = \frac{2}{\pi}\int \mathrm{d}^2\gamma\, P(\gamma)\, \mathrm{e}^{-2|\alpha-\gamma|^2}, \tag{1.178}$$

i.e., Wigner function is the convolution of the P function with a Gaussian.

- In the case of anti-normal ordering we have

$$\begin{aligned}
\hat{D}(\alpha) &= \mathrm{e}^{-\alpha^*\hat{a}}\mathrm{e}^{\alpha\hat{a}^\dagger}\mathrm{e}^{|\alpha|^2/2} \\
&= \ddagger\hat{D}(\alpha)\ddagger\, \mathrm{e}^{|\alpha|^2/2}.
\end{aligned} \tag{1.179}$$

- Husimi Q function is defined as

$$\boxed{Q(\beta) = \langle\beta|\ddagger\,\hat{\delta}(\hat{a}-\beta)\ddagger|\beta\rangle.} \tag{1.180}$$

- *Smoothing relation:*

$$\boxed{P(\alpha) * \mathrm{e}^{-|\alpha|^2/2} \;\Rightarrow\; W(\alpha) * \mathrm{e}^{-|\alpha|^2/2} \;\Rightarrow\; Q(\alpha).}$$

- As an example for the smoothing relation between phase-space functions, consider a coherent state $\hat{\rho} = |\alpha_0\rangle\langle\alpha_0|$:

- Normal order:

$$\hat{\rho} = \int \mathrm{d}^2\alpha\, P(\alpha)\, |\alpha\rangle\langle\alpha| \quad \Rightarrow \quad P(\alpha) = \delta(\alpha-\alpha_0) \tag{1.181}$$

$$W(\alpha) = \frac{2}{\pi}\int \mathrm{d}^2\gamma\, P(\alpha)\mathrm{e}^{-2|\alpha-\gamma|^2} = \frac{2}{\pi}\mathrm{e}^{-2|\alpha-\alpha_0|^2} \tag{1.182}$$

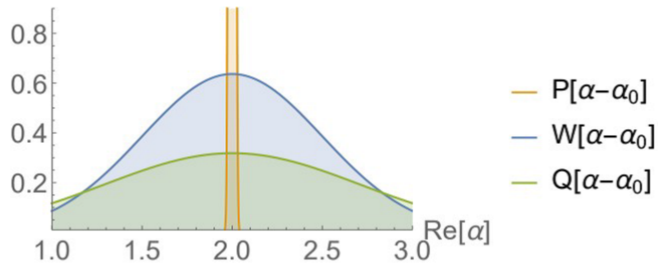

- Anti-normal order: convolution with Gaussian

$$Q(\alpha) = \frac{2}{\pi}\int d^2\gamma W(\alpha)e^{-2|\alpha-\gamma|^2} = \frac{1}{\pi}e^{-|\alpha-\alpha_0|^2} = \langle\alpha|\alpha_0\rangle. \tag{1.183}$$

- There is a one-to-one correspondence between density operator and phase-space distributions $\Rightarrow$ use phase-space distributions to compute expectation values of operators.

- **Recipe:**

  1. Bring operator $\hat{O}(\hat{a},\hat{a}^\dagger)$ into suitable operator order (normal, symmetric, anti-normal).
  2. Construct classical function $O(\alpha,\alpha^*)$ by replacing amplitude operators by complex amplitudes.
  3. Use appropriate phase-space function (P, W, Q) to compute expectation value $\langle\hat{O}(\hat{a},\hat{a}^\dagger)\rangle$.

- **Example** : mean photon number $\langle\hat{n}\rangle$

  1. Normal order:

$$\hat{n} = \hat{a}^\dagger\hat{a} \quad \Rightarrow \quad n(\alpha,\alpha^*) = |\alpha|^2 \quad \Rightarrow \quad \langle\hat{n}\rangle = \int d^2\alpha\,|\alpha|^2 P(\alpha). \tag{1.184}$$

  2. Symmetric order:

$$\hat{n} = \tfrac{1}{2}(\hat{a}^\dagger\hat{a}+\hat{a}\hat{a}^\dagger-1) \quad \Rightarrow \quad n(\alpha,\alpha^*) = |\alpha|^2-\tfrac{1}{2} \quad \Rightarrow \quad \langle\hat{n}\rangle = \int d^2\alpha\left(|\alpha|^2-\tfrac{1}{2}\right)W(\alpha). \tag{1.185}$$

  3. Anti-normal order:

$$\hat{n} = \hat{a}\hat{a}^+ - 1 \quad \Rightarrow \quad n(\alpha,\alpha^*) = |\alpha|^2-1 \quad \Rightarrow \quad \langle\hat{n}\rangle = \int d^2\alpha\left(|\alpha|^2-1\right)Q(\alpha). \tag{1.186}$$

1.4 Manipulation of quantum states of light by linear optical elements

- Quantum light can be manipulated by optical elements similar to classical light $\longrightarrow$ manipulation of spatial mode functions.
- Linear optical elements: devices consist of (dielectric) materials with *linear* response to electromagnetic fields $\longrightarrow$ no mixing of frequencies, e.g.
  1. Mirrors: reflection of light beams at material interfaces.
  2. Phase shifters: retardation of light by propagation through material.
  3. Beam splitters: reflected and transmitted beams at material interface.

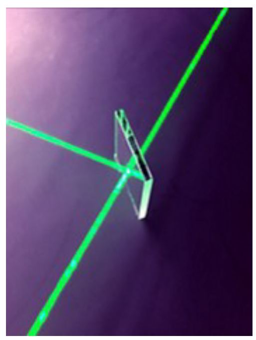

1.4.1 Quantum theory of phase shifters

- Look for (unitary) operator that rotates coherent states in phase space

$$|\alpha\rangle = \sum_{n=0}^{\infty} \frac{\alpha^n}{\sqrt{n!}} \mathrm{e}^{-|\alpha|^2/2} |n\rangle.$$

Thus

$$\begin{aligned} |\alpha\,\mathrm{e}^{\mathrm{i}\phi}\rangle &= \sum_{n=0}^{\infty} \frac{\left(\alpha\,\mathrm{e}^{\mathrm{i}\phi}\right)^n}{\sqrt{n!}} \mathrm{e}^{-|\alpha|^2/2} |n\rangle \\ &= \mathrm{e}^{\mathrm{i}\phi\,\hat{n}} \sum_{n=0}^{\infty} \frac{\alpha^n}{\sqrt{n!}} \mathrm{e}^{-|\alpha|^2/2} |n\rangle \\ &= \mathrm{e}^{\mathrm{i}\phi\,\hat{n}} |\alpha\rangle. \end{aligned} \tag{1.187}$$

Finally we obtain the corresponding unitary operator

$$\hat{U}_{\mathrm{ph}}(\phi) = \mathrm{e}^{\mathrm{i}\phi\,\hat{n}}. \tag{1.188}$$

1.4.2 Quantum theory of lossless beam splitters

- Construct quantum-optical input output relations at a dielectric plate (effective one-dimensional propagation). Consider dielectric plate of thickness d, restrict to one particular linear polarization and propagation along x-direction.

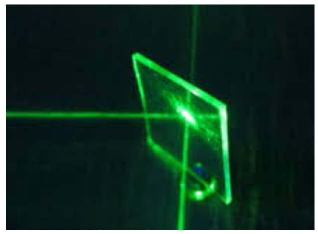

- For a lossless beam splitter, the input/output photonic operators are depicted

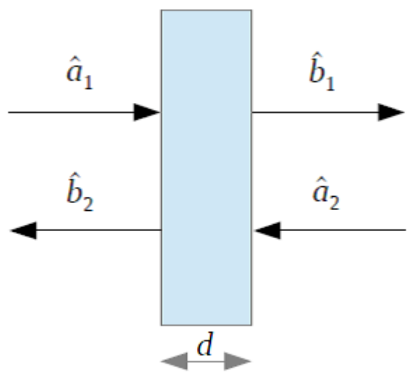

Fig. 1.2: Representation of the input/output photonic operators

- The scalar electric field operator reads

$$\hat{E}(x) = \mathrm{i} \int \mathrm{d}k\, c\, |k|\, A(x,k)\, \hat{a}(k) - \mathrm{i} \int \mathrm{d}k\, c\, |k|\, A^*(x,k)\, \hat{a}^\dagger(k). \tag{1.189}$$

- The scalar mode functions $A^*(x,k)$ fulfill HELMHOLTZ equation

$$\frac{\partial^2}{\partial x^2} A(x,k) + n^2(x,k)\, k^2\, A(x,k) = 0. \tag{1.190}$$

- Assume a refractive index profile as

$$n(x) = \begin{cases} n, & -\frac{d}{2} \le x \le \frac{d}{2}, \\ 1, & |x| > \frac{d}{2}. \end{cases} \tag{1.191}$$

- The solution to HELMHOLTZ equation is similar to the solution of the SCHRÖDINGER equation at a potential wall.

- An incoming plane wave $\mathrm{e}^{\mathrm{i}kx}$ from the left ($k > 0$) splits into a reflected part $R(\omega)\,\mathrm{e}^{-\mathrm{i}kx}$ and a transmitted part $T(\omega)\,\mathrm{e}^{\mathrm{i}kx}$.

- An incoming plane wave $\mathrm{e}^{\mathrm{i}kx}$ from the right ($k < 0$) splits into a reflected part $R'(\omega)\,\mathrm{e}^{-\mathrm{i}kx}$ and a transmitted part $T'(\omega)\,\mathrm{e}^{\mathrm{i}kx}$.

- Mode functions: For $k > 0$,

$$A(x,k) = \sqrt{\frac{\hbar}{4\pi\varepsilon_0\,\omega\,A}} \begin{cases} \mathrm{e}^{\mathrm{i}kx} + R(\omega)\,\mathrm{e}^{-\mathrm{i}kx}, & x < -\dfrac{d}{2}, \\ T(\omega)\,\mathrm{e}^{\mathrm{i}kx}, & x > \dfrac{d}{2}. \end{cases} \tag{1.192}$$

- For $k < 0$,

$$A(x,k) = \sqrt{\frac{\hbar}{4\pi\varepsilon_0\,\omega\,A}} \begin{cases} T'(\omega)\,\mathrm{e}^{\mathrm{i}kx}, & x < -\dfrac{d}{2}, \\ \mathrm{e}^{\mathrm{i}kx} + R'(\omega)\,\mathrm{e}^{-\mathrm{i}kx}, & x > \dfrac{d}{2}. \end{cases} \tag{1.193}$$

- Reflection and transmission coefficients depend on the details of the beam splitter.

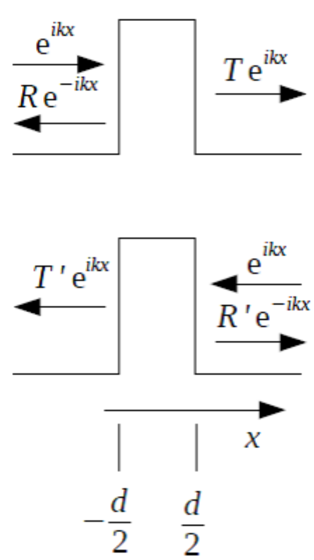

1.4.2.1 Input-output relations

- So far, we have decomposed the spatial mode functions into incoming and outgoing waves. Now, we decompose the electric field itself into incoming and outgoing fields as

  1. Incoming field

$$\hat{E}_{\text{in}}(x) = \mathrm{i}\int_0^\infty \mathrm{d}\omega \sqrt{\frac{\hbar}{4\pi\varepsilon_0\omega A}} \left[\mathrm{e}^{\mathrm{i}\omega x/c}\, \hat{a}_1(\omega) + \mathrm{e}^{-\mathrm{i}\omega x/c}\, \hat{a}_2(\omega)\right] + \text{h.c.} \tag{1.194}$$

  2. Outgoing field

$$\hat{E}_{\text{out}}(x) = \mathrm{i}\int_0^\infty \mathrm{d}\omega \sqrt{\frac{\hbar}{4\pi\varepsilon_0\omega A}} \left[\mathrm{e}^{\mathrm{i}\omega x/c}\, \hat{b}_1(\omega) + \mathrm{e}^{-\mathrm{i}\omega x/c}\, \hat{b}_2(\omega)\right] + \text{h.c.} \tag{1.195}$$

- According to Fig. (1.2), the beam splitter input-output relations are

$$\begin{aligned} \hat{b}_1(\omega) &= T(\omega)\,\hat{a}_1(\omega) + R'(\omega)\,\hat{a}_2(\omega), \\ \hat{b}_2(\omega) &= R(\omega)\,\hat{a}_1(\omega) + T'(\omega)\,\hat{a}_2(\omega). \end{aligned}$$

  or

$$\boxed{\hat{\mathbf{b}}(\omega) = \mathbf{T}(\omega)\cdot\hat{\mathbf{a}}(\omega)} \tag{1.196}$$

  where

$$\hat{\mathbf{b}}(\omega) = \begin{pmatrix} \hat{b}_1(\omega) \\ \hat{b}_2(\omega) \end{pmatrix}, \quad \hat{\mathbf{a}}(\omega) = \begin{pmatrix} \hat{a}_1(\omega) \\ \hat{a}_2(\omega) \end{pmatrix}, \text{ and } \quad \mathbf{T}(\omega) = \begin{pmatrix} T(\omega) & R'(\omega) \\ R(\omega) & T'(\omega) \end{pmatrix}. \tag{1.197}$$

- From the commutation relations for incoming fields

$$\left[\hat{a}_i(\omega), \hat{a}_j^\dagger(\omega)\right] = \delta_{ij}, \tag{1.198}$$

  where

$$\left[\hat{a}_1(\omega), \hat{a}_1^\dagger(\omega)\right] = 1, \quad \left[\hat{a}_2(\omega), \hat{a}_2^\dagger(\omega)\right] = 1, \quad \left[\hat{a}_1(\omega), \hat{a}_2^\dagger(\omega)\right] = 0, \tag{1.199}$$

  we find from the commutation relations for outgoing fields

$$\left[\hat{b}_i(\omega), \hat{b}_j^\dagger(\omega)\right] = \delta_{ij}, \tag{1.200}$$

  that

$$\left[\hat{b}_1(\omega), \hat{b}_1^\dagger(\omega)\right] = 1 = |T(\omega)|^2 + |R'(\omega)|^2, \tag{1.201}$$

  and

$$\left[\hat{b}_2(\omega), \hat{b}_2^\dagger(\omega)\right] = 1 = |R(\omega)|^2 + |T'(\omega)|^2. \tag{1.202}$$

- Equations (1.201) and (1.202) ensure photon-number (energy) conservation.
- The commutation relation
$$\left[\hat{b}_2(\omega), \hat{b}_1^\dagger(\omega)\right] = 0 = T^*(\omega)R(\omega) + R'^*(\omega)T'(\omega) \tag{1.203}$$
yields *phase* relation between transmission and reflection coefficients from both sides where
$$|T(\omega)| = |T'(\omega)|, \quad |R(\omega)| = |R'(\omega)| \tag{1.204}$$
which says that the modulus of the transmission (reflection) coefficient from one side to the beam splitter is the same as from the other side "Onsager-Lorentz reciprocity theorem". We choose the following phase relation:
$$T'(\omega) = T^*(\omega), \quad R'(\omega) = -R^*(\omega). \tag{1.205}$$
Hence reflection and transmission coefficients are not independent. Thus, the beam-splitter matrix $\mathbf{T}$ is unitary.
$$\mathbf{T}(\omega) = \begin{pmatrix} T(\omega) & -R^*(\omega) \\ R(\omega) & T^*(\omega) \end{pmatrix} \in \mathrm{SU}(2)^2. \tag{1.206}$$

1.4.2.2 Quantum-state transformation at lossless beam splitters

- Regard density operator as functional of amplitude operators (drop frequency index) $\hat{\rho}_{\text{in}} \equiv \hat{\rho}_{\text{in}}\left[\hat{\mathbf{a}}, \hat{\mathbf{a}}^\dagger\right]$.
- Given that the density operator is expressed as functional of the amplitude operators of the incoming fields, one has to replace those with the amplitude operators of the outgoing fields to obtain transformed density operator
$$\boxed{\hat{\rho}_{\text{out}}\left[\hat{\mathbf{a}}, \hat{\mathbf{a}}^\dagger\right] = \hat{\rho}_{\text{in}}\left[T^\dagger\!\cdot\hat{\mathbf{a}},\ T^T\!\cdot\hat{\mathbf{a}}^\dagger\right],} \tag{1.207}$$
i.e., the transformation of quantum states (i.e. density operators) is inverse of the transformation of photonic amplitude operators. This can be understood from the discrete time evolution in Schrödinger picture vs. Heisenberg picture
$$\begin{aligned} \langle\hat{O}\rangle = \mathrm{Tr}\left[\hat{\rho}\hat{O}(t)\right] &= \mathrm{Tr}\left[\hat{\rho}\hat{U}^\dagger(t)\hat{O}\hat{U}(t)\right] \quad \text{"Heisenberg"} && (1.208)\\ &= \mathrm{Tr}\left[\underbrace{\hat{U}(t)\hat{\rho}\hat{U}^\dagger(t)}_{\hat{\rho}(t)}\hat{O}\right] \quad \text{"Schrödinger"} && (1.209)\\ &= \mathrm{Tr}\left[\hat{\rho}(t)\hat{O}\right], && (1.210)\end{aligned}$$
where $\hat{U}(t)\hat{\rho}\hat{U}^\dagger(t)$ is the inverse time-evolution of the quantum state $\hat{\rho}(t)$.

[2]Special unitray 2×2 matrix with determinat equals $+1$.

- **Example:** Two-single photons

$$|\psi_{\rm in}\rangle = |1,1\rangle = \hat{a}_1^\dagger \hat{a}_2^\dagger |0,0\rangle. \tag{1.211}$$

Thus

$$\begin{aligned} |\psi_{\rm out}\rangle &= \left(T\hat{b}_1^\dagger + R\hat{b}_2^\dagger\right)\left(T^*\hat{b}_2^\dagger - R^*\hat{b}_1^\dagger\right)|0,0\rangle \\ &= \left(T^*R(\hat{b}_2^\dagger)^2 - TR^*(\hat{b}_1^\dagger)^2 + (|T|^2-|R|^2)\hat{b}_1^\dagger\hat{b}_2^\dagger\right)|0,0\rangle \\ &= \sqrt{2}T\,R^*|0_1,2_2\rangle - \sqrt{2}T\,R^*|2_1,0_2\rangle + (|T|^2-|R|^2)|1_1,1_2.\rangle \end{aligned}$$

- In the case of balanced beam splitter (50/50) with $R = T = 1/\sqrt{2}$

$$|\psi_{\rm out}\rangle = \frac{1}{\sqrt{2}}\left(|0,2\rangle - |2,0\rangle\right). \tag{1.212}$$

- This is due to *quantum interference* between amplitudes of both photons being either reflected or being transmitted (Hong-Ou-Mandel effect).

$\boxed{\textbf{Q}}$ Why the two probability amplitudes (3) and (4) vanish?

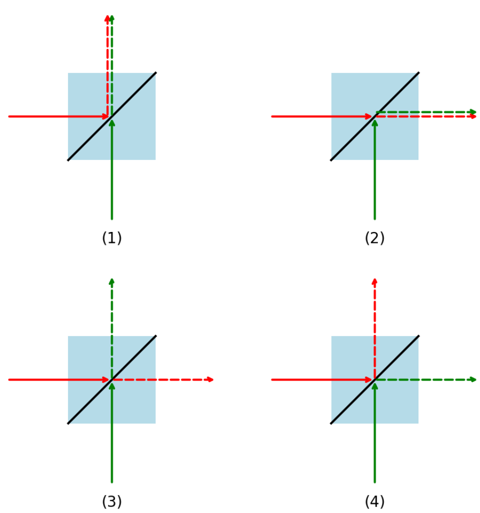

$\boxed{\textbf{A}}$ In quantum mechanics, the probability amplitudes add up *before* squaring. We know from classical electromagnetism, a phase shift occurs upon reflection. The probability amplitude (4) has a phase shift of π due to two reflections, hence the same magnitude as (3) but opposite sign. These two paths vanish in the sum.

Chapter 2

Lasers

2.1 A brief history of lasers

- LASER acronym for Light Amplification by Stimulated Emission of Radiation.The lasing process is based on *stimulated emission* which has to compete with the inverse process of *absorption*. The laser consists of a gain (amplifying) medium where the stimulated emission process occurs, a resonator made of fully and partial reflecting mirrors, and a pumping process, as seen in Fig. (2.1).

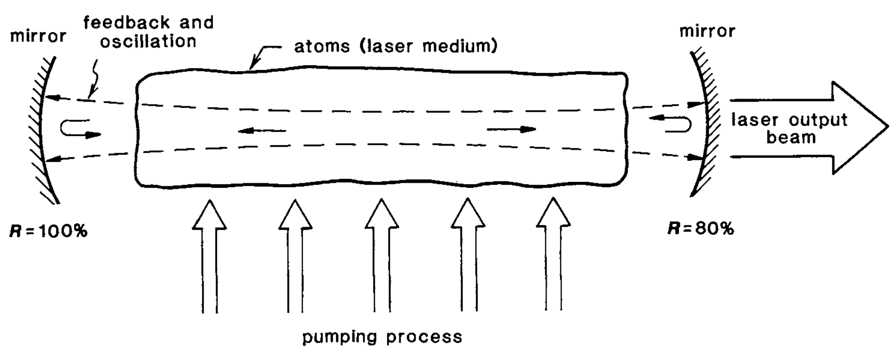

Fig. 2.1: Elements of a typical laser.

- 1917 Einstein used stimulated emission do derive Planck's equation for radiation.

- 1928 Ladenburg measured stimulated emission.

- 1954 Townes used stimulated emission for the amplification of radiation. He build a MASER (with microwaves).

- 1954 Basov and Prokhorov calculated MASERS.
- 1958 Schawlow and Townes build a resonator.
- 1959 Gould find a patent about lasers.
- 1960 Maiman build the first laser (ruby laser at 694 nm).
- 1961 Javan made the first He-Ne gas laser at 633 nm.
- 1964 Townes, Basov and Prokhorov received the Nobel Prize in physics for ”fundamental work in the field of quantum electronics, which has led to the construction of oscillators and amplifiers based on the maser–laser principle”.
- It’s fascinating that only a few years after the first laser was developed, by the mid-1960s, laser activity had been observed in all types of media, including gases, liquids, semiconductors, and crystalline solids. However, the titanium sapphire laser, which holds significant economic importance, is a notable exception, as it wasn’t developed until 1984.
- The range of laser types, technologies, and applications after forty years of research and development is so vast that a comprehensive list is nearly impossible. Applications span from the treatment of retina to laser-induced nuclear fusion, and from beam steering in tunnel construction to the study of ultrafast chemical processes with sub-10-fs pulses and quantum information transfer.

Materials	**Technologies**
1960 Maiman: Ruby laser (694 nm). 1961 Javan: He-Ne laser (1150 nm, 633 nm). 1961 Snitzer: Nd^{3+} glass laser (1064 nm). various: GaAS diode laser (840 nm). 1964 Patel: CO_2 laser, Geusic: Nd:YAG laser. 1965 Kasper and Pimentel: chemical HCl laser. 1966 Sorokin and Lankard: dye laser. 1971 Basov: Excimer laser. 1985 Moulton: Ti-Sa laser (800 nm, pulsed).	1961 Collins: Q-switch. 1965 Mocker and Collins: passive mode locking (ps pulses). 1968 Bradley and Durrant: synchroneous pumping. 1971 Kogelnik and Shank: distributed feedback laser. 1985 Strickland and Mourou: chirped pulse amplification. 1991 Spence: Kerr lens mode locking.

Table 2.1: Laser materials and technologies

2.2 Properties of laser radiation

- An ideal monochromatic source emits electromagnetic radiation at a single frequency as plane wave homogeneous electric field

$$\begin{aligned} \mathbf{E}(t) &= \mathbf{E}_0 \cos(\mathbf{k}\cdot\mathbf{r} - \omega t) && (2.1)\\ &= \mathbf{E}_0 \mathrm{Re}\{\mathrm{e}^{\mathrm{i}\phi}\},\ \phi = \mathbf{k}\cdot\mathbf{r} - \omega t && (2.2)\\ &= \mathbf{E}_0 \frac{\mathrm{e}^{\mathrm{i}\phi} + \mathrm{e}^{-\mathrm{i}\phi}}{2}. && (2.3) \end{aligned}$$

Definitions:

i) $\phi = \mathbf{k}\cdot\mathbf{r} - \omega t$ is the phase.

ii) $k = 2\pi/\lambda$ is the wave vector.

iii) $\omega = 2\pi\nu$ is the angular frequency.

- The electric field $\mathbf{E}$ is determined by the amplitude E_0 and the phase ϕ.

- The speed of light is $c = \lambda\nu = 299792458\,\mathrm{m/s}$.

- The photon energy is given by $E = h\nu = mc^2 = pc$, with the momentum $p = mc$, such that $p = h/\lambda$ is the momentum of light where $h = 6.626 \times 10^{-34}$J.s is Planck's constant.

- The intensity of the field reads

$$I(t) = \epsilon_0 c |\mathbf{E}(t)|^2, \qquad (2.4)$$

where $\epsilon_0 = 8.8 \times 10^{-12}\,\mathrm{A\,s/V\,m}$ is the dielectric constant. Since the photodetectors are too slow to measure $I(t)$ instantaneously, averaging over time yields

$$I = \frac{1}{2}\epsilon_0 c E_0^2. \qquad (2.5)$$

2.3 Important laser parameters

- Parameters needed to describe a laser beam are:

a) Spectral or temporal intensity distribution.

b) Spatial intensity distribution.

c) **Temporal and spatial coherence.**

d) **Polarization.**

a) FOURIER transform connects spectrum to temporal behavior

$$\tilde{I}(\omega) = \int_{-\infty}^{+\infty} I(t)\mathrm{e}^{-\mathrm{i}\omega t}\mathrm{d}t, \tag{2.6}$$

time-limited pulses have always a broad spectrum.

b) If a laser beam is not ideally symmetric as a Gaussian beam, one uses for identifying the beam radius W the definition of the second moment (which is measurable quantity)

$$W^2(z) := \frac{\int\int r^2 I(r,\phi,z) r\mathrm{d}r\mathrm{d}\phi}{\int\int I(r,\phi,z) r\mathrm{d}r\mathrm{d}\phi} \tag{2.7}$$

The divergence angle is defined as

$$\theta := \frac{W_2 - W_1}{z_2 - z_1}. \tag{2.8}$$

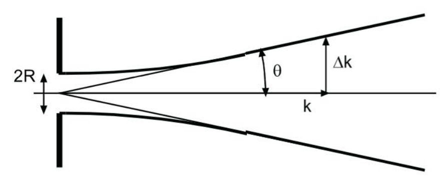

Fig. 2.2: The divergence of a collimated laser beam at an aperture.

- An intuitive connection between $W(z=0)$ and θ can be explained using particle-wave duality:

  1. **The particle character**: the photon is a particle that can transfer energy, angular momentum, or parity during an interaction.
  2. **The wave character**: the light is a wave when discussing interference, diffraction, beam propagation, etc.

- The *interference* phenomena that occurs for waves behind a double slit works as well for photons. The non-local character of a wave does not arise from the overlapping of many photons. The ability to interfere is not an ensemble property; indeed, the interference pattern of the double-slit setup arises even when the photon flux is too low that at any given time, no more than one photon is detected.

- The following example aims to illustrate particle-wave duality: One could detect an interference pattern behind a double slit, for instance, by using an arrangement of photomultipliers. Each photomultiplier is localized with an extent Δx in the plane perpendicular to the direction of photon propagation, and individual photons are detected by triggering an electron avalanche.

- The quantum nature of photons implies an uncertainty in momentum $\Delta x \Delta p \geq h/\pi$[1]. The distribution of photons is similar to the wave character. The uncertainty relation is also valid for particular propagation. For example an aperture with radius $R = \Delta x$ causes a *divergence* angle

$$R = \Delta x, \quad \Delta p = \hbar \Delta k \Longrightarrow \theta = \frac{\Delta k}{k} \geq \frac{\lambda}{R\pi}. \tag{2.9}$$

- This phenomenon is called *diffraction*. Due to diffraction, there cannot be a collimated laser beam over arbitrary distances. The finite diameter of the laser beam inevitably leads to divergence. Following the beam path in the opposite direction, one realizes that a corresponding laser beam cannot be focused into an infinitesimal point but only into a finite, diffraction-limited spot. In fact, this spot is at least 1.4 times larger than given in Eq. (2.9). This is related to the definition of beam width Δx, for which, conventionally, the $1/e^2$ width of the intensity distribution, equivalent to the $1/e$ width of the amplitude distribution, has been taken here. The laser beam is diffraction-limited

$$\boxed{\theta \geq \frac{\lambda}{R\pi}.} \tag{2.10}$$

- Moreover the product of the divergence angle and the beam waist fulfills

$$\boxed{\theta W_0 \geq \frac{\lambda}{\pi},} \tag{2.11}$$

where $W_0 = W(z = 0)$.

- For ideal Gaussian beams $\theta W_0 = \frac{\lambda}{\pi}$, and for real beams $\theta \overline{W}_0 > \frac{\lambda}{\pi}$. Let us define factor $Q = M^2$, called the beam propagation factor (M^2 factor), which indicates the beam quality of a real beam. One forms the quotient of the real beam radius $\overline{W}_0$ with the ideal beam radius

$$Q = M^2 = \frac{\overline{W}_0}{W_0} = \overline{W}_0 \frac{\pi\theta}{\lambda}. \tag{2.12}$$

[1] The exact form depends somewhat on the choice of wave functions and the precise definition of Δx and Δp.

- This value indicates by how much the beam diameter is larger compared to the ideal (Gaussian) beam, while maintaining the same divergence angle. Therefore, it is a measure of the beam's ability to focus.

- Similarly, it indicates by how much the divergence angle Θ of a real beam is larger than the divergence angle θ of the ideal beam, given the same radius of the beam waist:
$$\Theta = M^2\theta. \tag{2.13}$$
The term "beam quality factor" illustrates that divergence is a consequence of diffraction.

- For certain applications, such as material processing, the definition of *brightness* is meaningful. It is essentially the quotient of power and beam quality:
$$L = \frac{P}{(\Theta W_0)^2}. \tag{2.14}$$

- Finally, the *brilliance* takes into account the spectral distribution of the radiation and is defined as:
$$B(\lambda) = L\frac{\lambda/1000}{\Delta\lambda}. \tag{2.15}$$

c) Coherence

- The measurement of the phase of a wave emitted from a light source $E(\mathbf{r}, t)$ at two distinct points in space $(\mathbf{r}_1, \mathbf{r}_2)$ and time (t_1, t_2) reveals the coherence properties (temporal and spatial) of the light source.

- Suppose we measure this field at some point $\mathbf{r}_1$ and different times t_1, t_2. For stationary light source we define the first-order temporal correlation function
$$\begin{aligned}\Gamma^{(1)}(\mathbf{r}_1, t_1; \mathbf{r}_1, t_2) &= \Gamma^{(1)}(\mathbf{r}_1, \mathbf{r}_1, \tau) \\ &= \langle E^*(\mathbf{r}_1, t+\tau)E(\mathbf{r}_1, t)\rangle_{\text{ens}} \end{aligned} \tag{2.16}$$
where $\langle\cdots\rangle_{\text{ens}}$ states for an ensemble average and $\tau = t_1 - t_2$ is some time delay.

- Assuming *ergodicity*, i.e., the ensemble average is equivalent to time average. Therefore
$$\Gamma^{(1)}(\mathbf{r}_1, \mathbf{r}_1, \tau) \equiv \Gamma^{(1)}(\tau) = \lim_{T\longrightarrow\infty}\frac{1}{T}\int_0^T E^*(\mathbf{r}_1, t+\tau)E(\mathbf{r}_1, t)\mathrm{d}t. \tag{2.17}$$

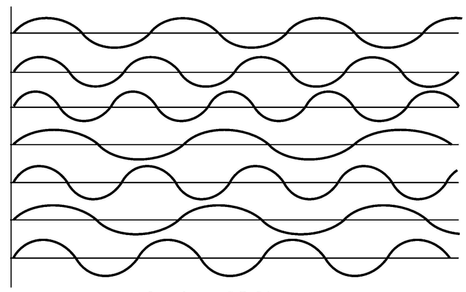

(a)

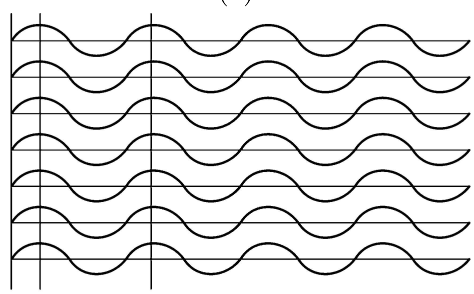

(b)

Fig. 2.3: Coherence.

- Moreover, the normalized coherence function can be written as

$$\begin{aligned} g^{(1)}(\tau) &= \frac{\langle E^*(\mathbf{r}_1, t+\tau)E(\mathbf{r}_1, t)\rangle}{\langle E^*(\mathbf{r}_1, t+\tau)E(\mathbf{r}_1, t+\tau)\rangle^{1/2}\langle E^*(\mathbf{r}_1, t)E(\mathbf{r}_1, t)\rangle^{1/2}} \\ &= \frac{\langle E^*(\mathbf{r}_1, t+\tau)E(\mathbf{r}_1, t)\rangle}{\langle I(\mathbf{r}_1, t)\rangle}. \end{aligned} \tag{2.18}$$

- $g^{(1)}(\tau)$ is the complex degree of temporal coherence, and its modulus $|g^{(1)}(\tau)|$ is the degree of temporal coherence.
- Properties of $g^{(1)}(\tau)$:
  1. $g^{(1)}(0) = 1$.
  2. $g^{(1)}(-\tau) = g^{(1)^*}(\tau)$.
  3. $|g^{(1)}(\tau)| \leq 1$.
- If $|g^{(1)}(\tau)| = 1, \forall\tau$, the beam is perfectly *coherent*.
- If $|g^{(1)}(\tau)| = 0, \forall\tau > 0$, the beam is completely *incoherent*.

- In the case of monochromatic wave $E(\mathbf{r},t) = E_0(\mathbf{r})\mathrm{e}^{-\mathrm{i}\omega t}$

$$\begin{aligned}\Gamma^{(1)}(\mathbf{r}_1,\mathbf{r}_1,\tau) &= \lim_{T\longrightarrow\infty}\frac{1}{T}\int_0^T |E(\mathbf{r}_1)|^2\mathrm{e}^{\mathrm{i}\omega(t+\tau)}\mathrm{e}^{-\mathrm{i}\omega t}\mathrm{d}t \\ &= |E(\mathbf{r}_1)|^2\mathrm{e}^{\mathrm{i}\omega\tau} \\ &= I(\mathbf{r}_1)\mathrm{e}^{\mathrm{i}\omega\tau},\end{aligned} \tag{2.19}$$

so that

$$|g^{(1)}(\tau)| = 1, \quad \forall\tau, \tag{2.20}$$

i.e., perfect coherence.

- Since $|g^{(1)}(\tau)|$ is symmetric in τ, the coherence time τ_{coh} is defined as

$$\tau_{\mathrm{coh}} = \int_{-\infty}^{+\infty} |g^{(1)}(\tau)|^2\mathrm{d}\tau, \tag{2.21}$$

where $\tau_{\mathrm{coh}} \longrightarrow \infty$ in the case of *perfect coherence* and $\tau_{\mathrm{coh}} \longrightarrow 0$ for *complete incoherence*.

- The coherence length reads

$$L_{\mathrm{coh}} = c\tau_{\mathrm{coh}}. \tag{2.22}$$

- Michelson interferometer measures the degree of coherence of light waves. A light source impinges on $50:50$ beam splitter, one part $E_1(t)$ propagates upward and reflected by a mirror and the other part $E_2(t)$ is transmitted by the beam splitter and reflected back by a movable mirror. The light field $E_2(t)$ is equivalent to $E_1(t+\tau)$ because it travels an excess amount of time $\tau = 2d/c$ whenever recombines to the beam splitter. Finally, the detector measures simultaneously the electric field at different times.

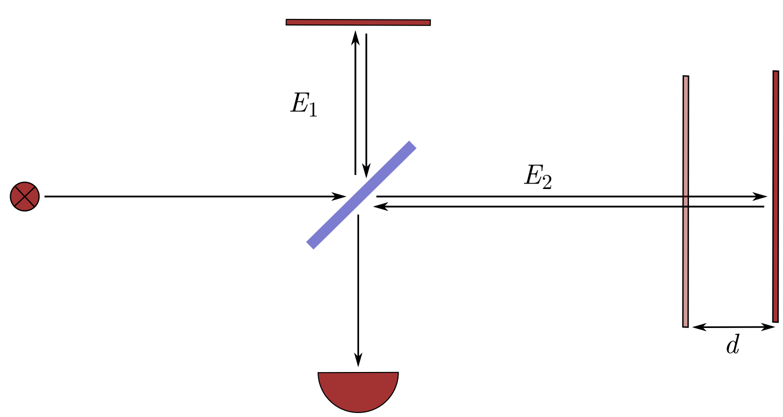

Fig. 2.4: Michelson interferometer.

- The electric field at the detector is

$$\begin{aligned} E(t) &= E_1(t) + E_2(t) \\ &= E_1(t) + E_1(t+\tau), \end{aligned} \tag{2.23}$$

hence the intensity would be

$$\begin{aligned} I(\tau) &= \Big\langle \big(E_1(t) + E_2(t)\big)^* \big(E_1(t) + E_2(t)\big) \Big\rangle \\ &= \langle E_1^*(t) E_1(t) \rangle + \langle E_2^*(t) E_2(t) \rangle + \langle E_1^*(t) E_2(t) \rangle + \langle E_2^*(t) E_1(t) \rangle \\ &= 2I_1 + 2\mathrm{Re}\, \langle E_1^*(t) E_2(t) \rangle \\ &= 2I_1 + 2\mathrm{Re}\, \Gamma^{(1)}(\mathbf{r}, \mathbf{r}, \tau). \end{aligned} \tag{2.24}$$

- For a monochromatic wave $E_1(t) = E_0 \mathrm{e}^{-\mathrm{i}\omega t}$

$$\begin{aligned} I(\tau) &= 2I_1 + 2I_1 \mathrm{Re}\, \mathrm{e}^{\mathrm{i}\omega\tau} \\ &= 2I_1(1 + \cos\omega\tau) \\ &= 2I_1(1 + \mathrm{Re}\, g^{(1)}(\tau)). \end{aligned} \tag{2.25}$$

- For monochromatic light wave entering the interferometer, the intensity at the detector oscillates with frequency ω and period τ. Additionally, the amplitude of the intensity varies between 0 and $4I_1$.

- According to Eq. (2.24), the intensity amplitude is maximum/minimum at maximum/minimum $\mathrm{Re}\, \Gamma^{(1)}(\tau)$. The figure (2.5) shows the intensity at the detector for different light waves.

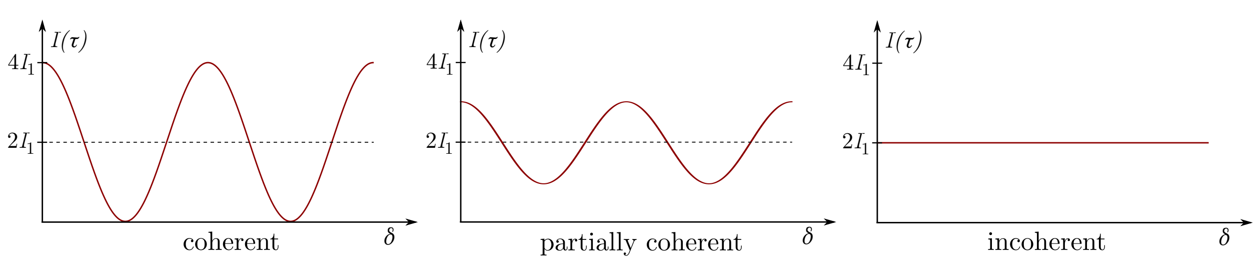

Fig. 2.5: Intensity of the signal for different light sources.

- The coherence order can also be quantified via the *fringe visibility*

$$V = \frac{I_{\mathrm{max}}(\tau_1) - I_{\mathrm{min}}(\tau_2)}{I_{\mathrm{max}}(\tau_1) + I_{\mathrm{min}}(\tau_2)}. \tag{2.26}$$

- Assuming that $\mathrm{Re}\,\Gamma^{(1)}(\tau_1) \approx -\mathrm{Re}\,\Gamma^{(1)}(\tau_2) \approx |\Gamma^{(1)}(\tau)|$, we find from (2.24) that

$$\begin{aligned} I_{\max}(\tau_1) &= 2I_1 + 2|\Gamma^{(1)}(\tau)| && (2.27) \\ I_{\min}(\tau_2) &= 2I_1 - 2|\Gamma^{(1)}(\tau)|, && (2.28) \end{aligned}$$

  which implies that

$$\boxed{V(\tau) = |g^{(1)}(\tau)|.} \tag{2.29}$$

  Thus measuring the fringe visibility provides a direct access to the degree of temporal coherence.

- The spectrum of a stochastic light source is given by Fourier transform

$$\tilde{E}(\mathbf{r},\omega) = \int_{-\infty}^{+\infty} E(\mathbf{r},t)\mathrm{e}^{-\mathrm{i}\omega t}\mathrm{d}t, \quad \text{and} \quad \tilde{E}(\mathbf{r},\omega) = 0 \quad \text{for} \quad \omega < 0. \tag{2.30}$$

- The quantity $\left\langle |\tilde{E}(\mathbf{r},\omega)|^2 \right\rangle$ is called the *spectral energy density*.

- The expression (2.30) is not well-defined for monochromatic waves, hence cut-off at finite time T is needed for stationary light fields

$$\tilde{E}_T(\mathbf{r},\omega) = \int_{-T/2}^{+T/2} E(\mathbf{r},t)\mathrm{e}^{-\mathrm{i}\omega t}\mathrm{d}t, \tag{2.31}$$

  and the *spectral power density* reads

$$S(\omega) = \lim_{T\to\infty} \frac{1}{T} \left\langle \left|\tilde{E}_T(\mathbf{r},\omega)\right|^2 \right\rangle \quad \text{and} \quad S(\omega) = 0 \quad \text{for} \quad \omega < 0. \tag{2.32}$$

- The *average total intensity* is therefore

$$I(\omega) = \int_0^{\infty} S(\omega)\mathrm{d}\omega. \tag{2.33}$$

- The integral (2.32) is a *convolution* of electric fields and can be written as

$$\boxed{S(\omega) = \int_{-\infty}^{+\infty} \Gamma^{(1)}(\mathbf{r},\mathbf{r},\tau)\mathrm{e}^{-\mathrm{i}\omega\tau}\mathrm{d}\tau,} \tag{2.34}$$

  which is known as *Wiener-Khinchin theorem*.

Proof. We insert Eq. (2.30) into Eq. (2.32):

$$\begin{aligned}
S(\omega) &= \lim_{T\to\infty}\frac{1}{T}\left\langle \tilde{E}_T^*(\mathbf{r},\omega)\tilde{E}_T(\mathbf{r},\omega)\right\rangle \\
&= \lim_{T\to\infty}\frac{1}{T}\left\langle \int_{-T/2}^{+T/2} E^*(\mathbf{r},t_2)\mathrm{e}^{\mathrm{i}\omega t_2}\mathrm{d}t_2 \int_{-T/2}^{+T/2} E(\mathbf{r},t_1)\mathrm{e}^{-\mathrm{i}\omega t_1}\mathrm{d}t_1 \right\rangle \\
&= \lim_{T\to\infty}\frac{1}{T}\int_{-T/2}^{+T/2}\int_{-T/2}^{+T/2} \mathrm{e}^{-\mathrm{i}\omega(t_1-t_2)}\left\langle E^*(\mathbf{r},t_2)E(\mathbf{r},t_1)\right\rangle \mathrm{d}t_1\mathrm{d}t_2 \\
&= \lim_{T\to\infty}\frac{1}{T}\int_{-T/2}^{+T/2}\int_{-T/2}^{+T/2} \mathrm{e}^{-\mathrm{i}\omega(t_1-t_2)}\Gamma^{(1)}(\mathbf{r},t_1;\mathbf{r},t_2)\mathrm{d}t_1\mathrm{d}t_2 \\
&= \lim_{T\to\infty}\frac{1}{T}\int_{-T/2}^{+T/2}\int_{-T/2-t_1}^{+T/2+t_1} \mathrm{e}^{-\mathrm{i}\omega\tau}\Gamma^{(1)}(\mathbf{r},\mathbf{r},\tau)\mathrm{d}\tau\mathrm{d}t_1 \\
&= \lim_{T\to\infty}\frac{1}{T}\int_{-T/2}^{+T/2} \tilde{\Gamma}^{(1)}(\mathbf{r},\mathbf{r},\omega)\mathrm{d}t_1 = \tilde{\Gamma}^{(1)}(\mathbf{r},\mathbf{r},\omega). \qquad (2.35)
\end{aligned}$$

- The spectral width (line width) is the width of the spectral density function $S(\omega)$ because $S(\omega)$ and $\Gamma^{(1)}(\tau)$ are FOURIER-transform pairs.

- The widths of $S(\omega)$ and $\Gamma^{(1)}(\tau)$ are inversely proportional to one another

$$\Delta\omega_{\mathrm{coh}} = \frac{\left(\int_0^\infty S(\omega)\mathrm{d}\omega\right)^2}{\int_0^\infty S^2(\omega)\mathrm{d}\omega} \propto \frac{1}{\tau_{\mathrm{coh}}}. \qquad (2.36)$$

Source	$\Delta\nu_{\mathrm{coh}}$	$\tau_{\mathrm{coh}} = 1/\Delta\nu_{\mathrm{coh}}$	$L_{\mathrm{coh}} = c\tau_{\mathrm{coh}}$
Sunlight $400-800$ nm	3.74×10^{14} Hz	2.67 fs	800 nm
LED $\lambda_0 = 1\,\mu$m	1.5×10^{13} Hz	67 fs	20 µm
Single-mode laser $\lambda_0 = 632$ nm	1×10^{6} MHz	1 µs	300 m

Table 2.2: Coherence properties for different light sources

- Nowadays, there exist lasers having sub-hertz linewidths, and hundreds of kilometers coherence lengths.

d) Polarization

- Since the wave equation is a linear differential equation, the supperposition principle holds. Consider a plane wave propagating in z-direction, then the cartesian components of the electric field are

$$
\begin{aligned}
E_x(z,t) &= |E_x|\cos(kz-\omega t+\varphi_x) && (2.37)\\
E_y(z,t) &= |E_y|\cos(kz-\omega t+\varphi_y) && (2.38)\\
E_z(z,t) &= 0. && (2.39)
\end{aligned}
$$

- If $\varphi_x \neq \varphi_y$, the polarization is called *elliptic* and the field vector $\mathrm{Re}\,\mathbf{E}(\mathbf{r},t)$ rotates at $\mathbf{r}$ on an ellipse spanned by the unit vectors $\mathbf{e}_x$ and $\mathbf{e}_y$.

- If $\varphi_x = \varphi_y \pm \pi/2$ and $|E_x| = |E_y|$, the polarization is called *circular*.

- If $\varphi_x = \varphi_y + n\pi$ and $|E_x| = 0$ or $|E_y| = 0$, the polarization is called *linear*.

- At $z = 0$ the electric field components becomes

$$
\begin{aligned}
E_x(t) &= |E_x|\cos(-\omega t+\varphi_x) && (2.40)\\
E_y(t) &= |E_y|\cos(-\omega t+\varphi_y). && (2.41)
\end{aligned}
$$

Therefore, an equation of ellipse derived from Eq.(2.40) and Eq.(2.41) reads

$$
\left(\frac{E_x}{|E_x|}\right)^2 + \left(\frac{E_x}{|E_x|}\right)^2 - \frac{2E_xE_y}{|E_x||E_y|}\cos(\varphi_x-\varphi_y) = \sin^2(\varphi_x-\varphi_y). \qquad (2.42)
$$

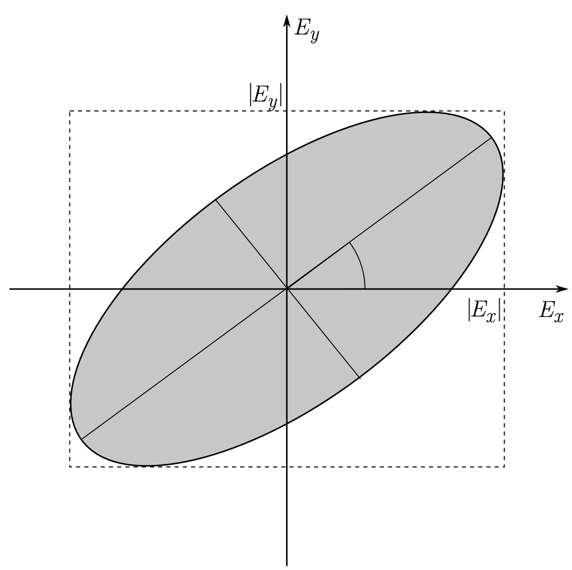

Fig. 2.6: Elliptic polarization

2.4 Einstein coefficients and the Planck's law of radiation

- Assume an idealized material with two nondegenerate energy levels, 1 and 2, having populations N_1 and N_2, respectively. Moreover, let us consider that the total number of atoms in these two levels is constant

$$N_1 + N_2 = N. \tag{2.43}$$

- We can distinguish three forms of interaction between light and atoms (introduced in 1917 by A. Einstein):

  a) **Spontaneous emission**
  An excited atom emits a photon spontaneously (or induced via vacuum fluctuations) when the electron in the upper energy level E_2 jumps to the lower energy level E_1. The rate $\mathrm{d}N_2^{\mathrm{sp}}/\mathrm{d}t$ describing the depopulation of E_2 reads

$$\frac{\mathrm{d}N_2^{\mathrm{sp}}}{\mathrm{d}t} = -A_{21}N_2, \quad A_{21} = \frac{1}{\tau_{\mathrm{sp}}} \tag{2.44}$$

  where A_{21} is Einstein coefficient for spontaneous emission and τ_{sp} being the lifetime for spontaneous radiation in the upper energy level. The emitted photons are not coherent and the radiation is isotropic.

  b) **Stimulated emission**
  An incoming photon induces an excited atom to emit another one. The radiation is not isotropic (the emitted photons have the same direction and with the same phase). The corresponding rate equation reads

$$\frac{\mathrm{d}N_2^{\mathrm{st}}}{\mathrm{d}t} = -B_{21}N_2\rho(\nu), \tag{2.45}$$

  where B_{21} is Einstein coefficient for the stimulated emission and $\rho(\nu)$ is the spectral energy density.

  c) **Induced absorption**
  An incoming photon is absorbed by an electron in the lower energy level E_1, and subsequently the electron jumps into the upper energy level E_2:

$$\frac{\mathrm{d}N_1^{\mathrm{abs}}}{\mathrm{d}t} = -B_{12}N_1\rho(\nu), \tag{2.46}$$

  where B_{12} is Einstein coefficient for absorption.

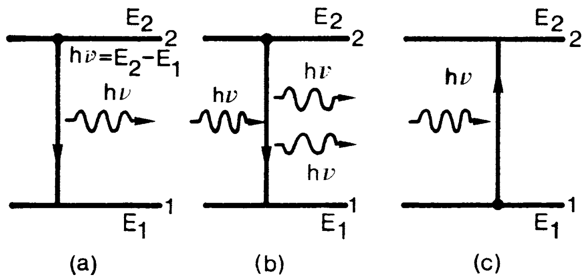

Fig. 2.7: Schematic illustration of the three processes: (a) spontaneous emission; (b) stimulated emission; (c) absorption.

- With A_{21}, B_{21} and B_{12} EINSTEIN was able to derive PLANCK's law for black-body radiation.

- Combining the three processes, the change of upper- and lower-level populations can be written as

$$\frac{\mathrm{d}N_1}{\mathrm{d}t} = -\frac{\mathrm{d}N_2}{\mathrm{d}t} = B_{21}N_2\rho(\nu) - B_{12}N_1\rho(\nu) + A_{21}N_2. \tag{2.47}$$

- The relation

$$\frac{\mathrm{d}N_2}{\mathrm{d}t} = -\frac{\mathrm{d}N_1}{\mathrm{d}t} \tag{2.48}$$

can be easily derived from Eq.(2.43).

- Assumption: atoms are in thermal equilibrium with a reservoir of temperature T require equal numbers of "upward" and "downward" transitions such that

$$\frac{\mathrm{d}N_2}{\mathrm{d}t} = \frac{\mathrm{d}N_1}{\mathrm{d}t} = 0, \tag{2.49}$$

and the population N_1 and N_2 are given by the BOLTZMANN distribution $N_1 \sim \mathrm{e}^{-E_1/k_\mathrm{B}T}$, $N_2 \sim \mathrm{e}^{-E_2/k_\mathrm{B}T}$ where $k_\mathrm{B} = 1.38 \times 10^{-23}\mathrm{J.K}^{-1}$ is the BOLTZMANN constant. Hence

$$\frac{N_2}{N_1} = \mathrm{e}^{-\frac{(E_2-E_1)}{k_\mathrm{B}T}} = \mathrm{e}^{-\frac{h\nu}{k_\mathrm{B}T}} \tag{2.50}$$

where $E_2 - E_1 = h\nu$ is the photon energy.

- Equation (2.50) implies that $N_1 > N_2$, thus more absorption than stimulated emission.

- For high intense light, the spontaneous emission is negligible and, therefore, both levels are equally populated, i.e., $N_1 \approx N_2$.

- Equation (2.49) yields

$$B_{21}N_2\rho(\nu) - B_{12}N_1\rho(\nu) + A_{21}N_2 = 0,$$

so that

$$\frac{N_2}{N_1} = \frac{B_{12}\rho(\nu)}{B_{21}\rho(\nu) + A_{21}}. \tag{2.51}$$

Comparison of Eq. (2.51) and (2.50) gives

$$\rho(\nu) = \frac{A_{21}}{B_{21}} \frac{1}{\left(\frac{B_{12}}{B_{21}} \mathrm{e}^{\frac{h\nu}{k_\mathrm{B}T}} - 1\right)} \tag{2.52}$$

Q What is the relation between coefficients A_{21}, B_{21} and B_{12}?

A Following EINSTEIN approach for $T \longrightarrow \infty \curvearrowright \rho(\nu) \longrightarrow \infty$:
Since $A_{21} < \infty$,

$$\begin{aligned}
\lim_{T\longrightarrow\infty} \rho(\nu) &= \lim_{T\longrightarrow\infty} \frac{A_{21}}{B_{12}\mathrm{e}^{\frac{h\nu}{k_\mathrm{B}T}} - B_{21}} = \infty \\
&\Rightarrow \lim_{T\longrightarrow\infty} (B_{12}\underbrace{\mathrm{e}^{\frac{h\nu}{k_\mathrm{B}T}}}_{=1} - B_{21}) = 0 \\
&\Rightarrow \boxed{B_{12} = B_{21}.}
\end{aligned} \tag{2.53}$$

Hence

$$\rho(\nu) = \frac{A_{21}}{B_{21}(\mathrm{e}^{\frac{h\nu}{k_\mathrm{B}T}} - 1)} \tag{2.54}$$

- Now we compare with the experimental results of RAYLEIGH-JEANS at low frequencies ($\nu \longrightarrow 0$)

$$\rho^{\mathrm{RJ}}(\nu) = \frac{8\pi\nu^2}{c^3} k_\mathrm{B}T \tag{2.55}$$

Taylor expansion around $\nu \longrightarrow 0$:

$$\mathrm{e}^{\frac{h\nu}{k_\mathrm{B}T}} = \sum_{\nu=0}^{\infty} \left(\frac{h\nu}{k_\mathrm{B}T}\right)^{\nu} \frac{1}{\nu!} \approx 1 + \frac{h\nu}{k_\mathrm{B}T} \tag{2.56}$$

thus

$$\lim_{\nu\longrightarrow 0} \rho(\nu) = \frac{A_{21}}{B_{21}(1 + \frac{h\nu}{kT} - 1)} = \frac{A_{21}}{B_{21}\frac{h\nu}{kT}} = \frac{A_{21}}{B_{21}} \frac{k_\mathrm{B}T}{h\nu}. \tag{2.57}$$

Comparing Eq.(2.55) with (2.57) yields

$$\frac{A_{21}}{B_{21}}\frac{k_{\mathrm{B}}T}{h\nu} \stackrel{!}{=} \frac{8\pi\nu^2}{c^3}k_{\mathrm{B}}T$$

or

$$\boxed{\frac{A_{21}}{B_{21}} = \frac{8\pi h\nu^3}{c^3}.} \tag{2.58}$$

- Thus

$$\boxed{\rho(\nu) = \frac{8\pi h\nu^3}{c^3}\frac{1}{\mathrm{e}^{\frac{h\nu}{k_{\mathrm{B}}T}}-1}} \tag{2.59}$$

which is PLANCK's law of black-body radiation.

- **Note:** The speed of light c is here the value in the medium $c = c_0/n$, where c_0 is the speed of light in vacuum and n is the index of refraction.

- EINSTEIN derivation was a strong indication that the concept of quanta with $E = h\nu$ is correct.

- PLANCK's law is universal since it is independent of the atoms that take part and the particular energy levels. The only condition is that the body is able to absorb photons of all frequencies.

- **Example:** Consider black-body radiation for a sphere filled with gas, in thermal equilibrium $T = 1000\,^{\circ}\mathrm{C}$. The ratio of spontaneous to stimulated emission is

  1. For visible light, $\frac{A_{21}}{B_{21}} = 10^{10}$.
  2. For radio frequencies, $\frac{A_{21}}{B_{21}} = 10^{8}$.

2.5 Line shape and line broadening mechanisms

- So far we considered the laser field as a plane wave. In reality lasers are not monochromatic and have certain distribution of spectrum implying line shape.

- Lines are broadened via various mechanisms:

  - *Homogeneous broadening* is a particle property, the same for all atoms that take part.
  - *Inhomogeneous broadening* is an ensemble property, only a selection of atoms participate.

a) **Natural broadening**

- Is a consequence of HEISENBERG's uncertainty principle.
- The shape and width of a transition between two energy levels $\hbar\omega = E_2 - E_1$ depends on the decay time τ of the excited state.
- The line shape function

$$g(\omega) = \frac{1}{2\pi} \frac{\gamma}{(\omega - \omega_0)^2 + (\gamma/2)^2} \tag{2.60}$$

is Lorentzian "homegeneous mechanism".

- The full width at half maximum (FWHM): $\Delta\omega = \gamma = 1/\tau$ (inverse lifetime of the upper level), hence $\hbar\Delta\omega\tau = \Delta E\tau = \hbar$ is, indeed, an uncertainty relation.
- Defining of a quality factor "line fidelity" for characterizing the natural line width

$$Q = \frac{\omega_0}{\Delta\omega}. \tag{2.61}$$

- **Example:** For calcium, the lifetime of an upper level, τ, is about $4.6\,\mathrm{ns}$ for a transition wavelength $\lambda = 423\,\mathrm{nm}$. The corresponding frequency is $\nu = c/\lambda = 7 \times 10^{14}\,\mathrm{Hz}$. During τ, the electromagnetic wave oscillates $\nu\tau = 3 \times 10^6$ times until the intensity drops to $1/\mathrm{e}$, therefore

$$Q = \frac{\omega_0}{\Delta\omega} \approx 4.4 \times 10^{15}\mathrm{s}^{-1} \cdot 4.6 \times 10^{-9}\mathrm{s} \approx 2 \times 10^7.$$

b) **Doppler broadening**

- If the atom moves with a velocity v_z relative to the observer, then the resonance frequencies are shifted due to DOPPLER effect

$$\omega = \omega_0 + \mathbf{k} \cdot \mathbf{v} = \omega_0 \left(1 + \frac{1}{2\pi\nu} \frac{2\pi}{\lambda} v_z\right) = \omega_0 \left(1 + \frac{v_z}{c}\right) \tag{2.62}$$

where $\mathbf{k}$ is the wave vector.

- This is the case of an inhomogeneous broadening.
- If $\mathbf{k} \perp \mathbf{v} \Rightarrow \omega = \omega_0$.

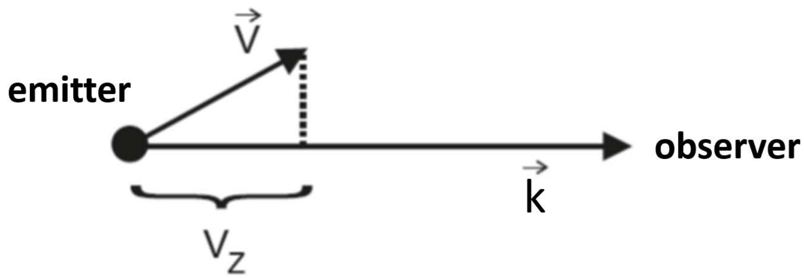

Fig. 2.8: Radiation emitter moves with a velocity component towards the observer.

- The angular frequency of the received radiation will be shifted (into the blue for positive v_z and into the red for negative v_z).
- A gas that absorb or emit light consists of atoms with mass M following, at thermal equilibrium, a statistical distribution that depends on T, namely MAXWELL-BOLTZMANN distribution of velocities.
- The number of atoms $\mathrm{d}N$ whose velocities between v_z and $v_z + \mathrm{d}v_z$ is given by MAXWELL's distribution
$$\mathrm{d}N = N\mathrm{e}^{-\frac{Mv_z^2(\omega)}{2k_\mathrm{B}T}}\mathrm{d}v_z. \tag{2.63}$$
Using
$$\frac{\mathrm{d}\omega}{\mathrm{d}v_z} = \frac{\omega_0}{c}, \quad v_z = \frac{c(\omega-\omega_0)}{\omega_0} \tag{2.64}$$
we obtain
$$\mathrm{d}N = N\mathrm{e}^{-\frac{Mc^2}{2k_\mathrm{B}T}\frac{(\omega-\omega_0)^2}{\omega_0^2}}\frac{c}{\omega_0}\mathrm{d}\omega. \tag{2.65}$$
- Given that the spectral intensity distribution $I(\omega)\mathrm{d}\omega \sim \mathrm{d}N$ and the intensity profile of the emitted line $I(\omega) = I(\omega_0)g(\omega)$, the line shape function $g(\omega)$ will follow as
$$g(\omega) = \frac{1}{\omega_0}\sqrt{\frac{Mc^2}{2\pi k_\mathrm{B}T}}\mathrm{e}^{-\frac{Mc^2}{2k_\mathrm{B}T}\frac{(\omega-\omega_0)^2}{\omega_0^2}}. \tag{2.66}$$
- The FWHM of this distribution is (left as an exercise)
$$\begin{aligned}\Delta\omega &= \frac{2\omega_0}{c}\sqrt{\frac{2k_\mathrm{B}T}{M}\ln 2}\\ &= 7.16\times10^{-7}\omega_0\sqrt{\frac{T}{M}}\end{aligned} \tag{2.67}$$
T the temperature of the emitters in K, and M the atomic weight in atomic mass units (amu).

- DOPPLER broadening depends on the frequency ω_0 itself and produces a Gaussian profile.
- DOPPLER broadening increases with temperature and with the frequency of the line, and decreases as the atomic mass increases.
- The comparison between Gaussian and Lorentzian profiles reveals that the Gaussian decays faster, the wings of the line profile are still determined by the Lorentzian.
- DOPPLER broadening is created by emission of many DOPPLER-shifted lines with a natural (Lorentzian) line width. The convolution of many Lorentzian distribution functions yields Gaussian distribution.

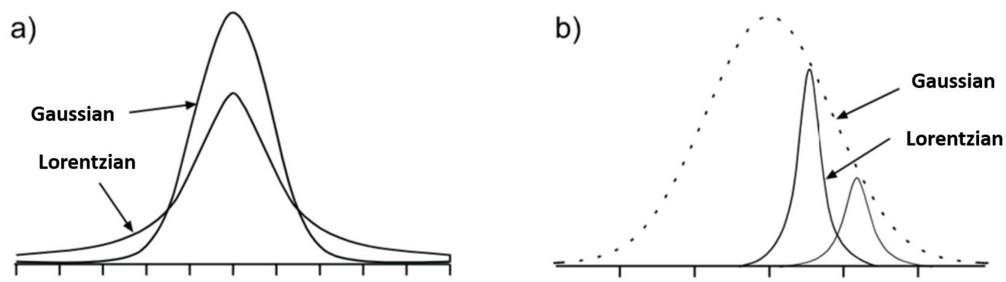

Fig. 2.9: a) Comparison between a Gaussian and a Lorentzian curve with the same half-width and area. b) DOPPLER broadening arises from the emission of many DOPPLER-shifted lines with natural line width.

c) **Saturation broadening**

- If the intensity of the laser increases, a considerable part of the atom ensemble is excited (spontaneous emission cannot depopulate the upper levels sufficiently quick, hence absorption reduced). This is called *saturation* of a transition.
- Using rate equations

$$\frac{\mathrm{d}N_2}{\mathrm{d}t} = \underbrace{B_{12}N_1\rho(\nu)}_{\text{induced absorption}} - \underbrace{B_{21}N_2\rho(\nu)}_{\text{stimulated emission}} - \underbrace{A_{21}N_2}_{\text{spontaneous emission}} = -\frac{\mathrm{d}N_1}{\mathrm{d}t} = 0. \tag{2.68}$$

Since $B_{21} = B_{12}$ we write

$$2B_{12}\rho(\nu)(N_2 - N_1) + 2A_{21}N_2 = 0$$

or

$$2B_{12}\rho(\nu)(N_2 - N_1) + A_{21}(N_2 + N_1) + A_{21}(N_2 - N_1) = 0. \tag{2.69}$$

Calling Eq. (2.43) gives

$$N_1 - N_2 = \frac{N}{1 + 2\frac{B_{12}\rho(\nu)}{A_{21}}} := \frac{N}{1 + \frac{I(\nu)}{I_s}} \tag{2.70}$$

with $I(\nu) = c\rho(\nu)$ and $I_s = cA_{21}/2B_{12}$ is the saturation intensity.

- With the difference in population numbers, the absorption coefficient α (i.e., the material dependent cross-section for absorption, independent of the line shape function) also becomes a function of intensity

$$\alpha = \frac{\alpha_0}{1 + \frac{I}{I_s}}. \tag{2.71}$$

- The impact on the line shapes depends on the type of broadening (homogeneous or inhomogeneous). Both cases are outlined in Figure (2.10).

- In the case of a homogeneous mechanism (if the Doppler shift is not considered). The Lorentzian line shape function is no longer normalized:

$$g(\omega) = \frac{C}{(\omega - \omega_0)^2 + (\gamma_s/2)^2} \tag{2.72}$$

with $\gamma_s = \gamma\sqrt{1 + \frac{I}{I_s}}$, thus $\gamma_s > \gamma$. This means that the line shape is maintained but the line gets wider as the absorption in the center of the line is more reduced than in the wings.

- At the saturation intensity $I = I_s$, according to Eq. (2.70), $N_2 = N/4$, meaning a quarter of all atoms are in the excited state, and the line width has increased by a factor of $\sqrt{2}$.

- In the case of inhomogeneous transitions, however, spectral selective saturation occurs. With sufficiently narrowband excitation, so-called *hole burning* occurs. For Doppler broadening, for example, each frequency component of the line profile can be assigned to a group of atoms with specific velocities. When light of a certain frequency is irradiated, interaction occurs only with atoms of matching velocity or frequency. The width of the resulting hole cannot be narrower than the natural line width.

- If Doppler effect is not removed, then the broadening is inhomogeneous (the effect is not the same for different velocities), hence selective spectral saturation or *spectral hole burning*.

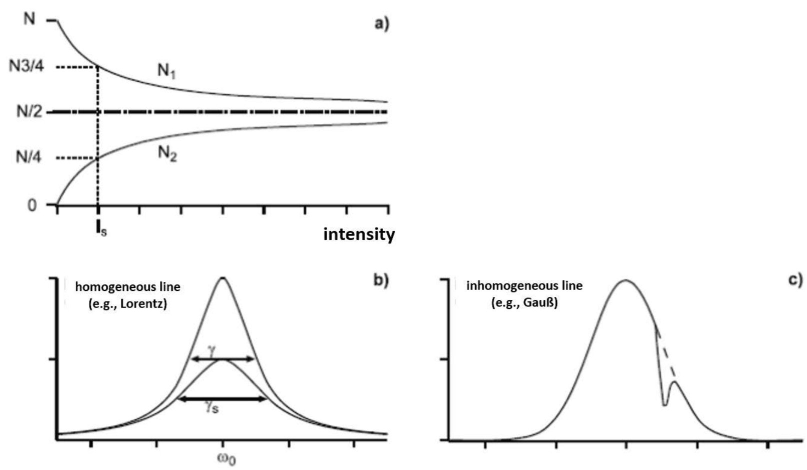

Fig. 2.10: a) Intensity dependence of the population numbers in the two-level atom. b) Saturation broadening of a homogeneous line. c) Spectral hole burning in an inhomogeneously broadened line profile.

d) **Pressure broadening**

- In the presence of collisions with other atoms the phase of the emitted photon is disturbed.
- The phase interrupts and thus shortens the emission process (increases energy uncertainty).
- The collisions can be interpreted as a decay taking into account that the rate has an additional decay channel.
- This leads to Lorentzian line profile (homogeneous broadening)

$$g(\omega) = \frac{1}{2\pi} \frac{\gamma_{\text{tot}}}{(\omega - \omega_0)^2 + (\gamma_{\text{tot}}/2)^2} \tag{2.73}$$

with the FWHM

$$\Delta\omega = \gamma + 2\gamma_{\text{coll}}, \tag{2.74}$$

where

$$\gamma_{\text{coll}} = \sigma \rho v_{\text{rel}} \tag{2.75}$$

is the collision rate which is proportional to the scattering cross section σ and ρv_{rel} is the flux of atoms, i.e., the density times the relative velocity. For a gas in thermal equilibrium we use the Maxwell-Boltzmann statistics to obtain $v_{\text{rel}} = 4\sqrt{k_B T/\pi M}$, and the ideal gas law yields $p = \rho k_B T$ for the pressure.

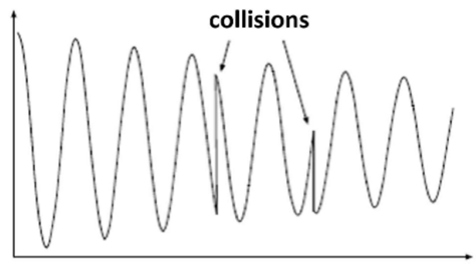

Fig. 2.11: Elastic collisions change the phase of the emitted wave of a damped harmonic oscillator.

- **Example:** For He-Ne laser, the half-width of collisional broadening at a pressure of $p = 0.5\,\mathrm{mbar}$ is $\Delta\omega = 100\,\mathrm{MHz}$.

e) **Time-of-flight broadening**

- This broadening mechanism results from the finite interaction time between the absorber material and the incident laser beam. This effect must be considered when the interaction time is short compared to the natural lifetime of the excited atom. In such cases, the line width of such a transition is not determined by the lifetime but by the flight time of an atom through a laser beam. The frequency profile of the radiation then depends on the intensity distribution of the laser beam and is typically an inhomogeneous mechanism as a result.

- **Example:** Calcium atoms from a $T = 1000\,°\mathrm{C}$ hot furnace have a root-mean-square velocity of $v_{\mathrm{rms}} = \sqrt{3k_{\mathrm{B}}T/M} = 790\,\mathrm{m\,s^{-1}}$. The lifetime of an upper level $\tau_{21}(\lambda = 657\,\mathrm{nm})$, is about $4.6\,\mathrm{ns}$. When focussing the laser beam down to $4\,\mu\mathrm{m}$, the time-of-flight broadening becomes relevant.

2.6 Important solutions to wave equation

- We provide here important (approximate) solutions for the wave equation

$$\left(\nabla^2 - \frac{1}{c^2}\frac{\partial^2}{\partial t^2}\right)\mathbf{E}(\mathbf{r}, t) = 0 \tag{2.76}$$

of the laser field in free space.
Consider a *monochromatic* wave

$$\mathbf{E}(\mathbf{r}, t) = \mathbf{E}(\mathbf{r})\mathrm{e}^{-\mathrm{i}\omega t}. \tag{2.77}$$

Plugging (2.77) into (2.76) yields

$$\boxed{(\Delta + k^2)\mathbf{E}(\mathbf{r}) = 0, \quad k = \frac{\omega}{c}} \tag{2.78}$$

which is called HELMHOLTZ *equation* for spatial modes.

- The solutions $\mathbf{E}(\mathbf{r}) \sim \mathbf{e}_\sigma \mathrm{e}^{\mathrm{i}\mathbf{k}\cdot\mathbf{r}}$ are special solutions to the equation (2.78). If we concentrate on one polarization, the scalar HELMHOLTZ equation for the field amplitude reads

$$(\Delta + k^2)E_0(\mathbf{r}) = 0. \tag{2.79}$$

a) **Plane waves**
Writing the Laplacian in Cartesian coordinates yields

$$\mathbf{E}(\mathbf{r}) = \mathbf{E}_0\mathrm{e}^{\mathrm{i}\mathbf{k}\cdot\mathbf{r}}. \tag{2.80}$$

b) **Spherical waves**

- In spherical coordinates the solution of Eq.(2.78) in one dimension reads

$$\mathbf{E}(\mathbf{r}) = A\frac{\mathrm{e}^{\mathrm{i}kr}}{r}. \tag{2.81}$$

with a constant A satisfying the scalar HELMHOLTZ equation in spherical coordinates. The wave fronts are spherical shells with a radial distance of $\lambda = 2\pi/k$, which propagate radially with the phase velocity c.

c) **Parabolic waves**

- The spherical waves can be simplified under certain circumstances. For example, we consider a spherical wave that propagates from the origin of coordinates at a location near the z-axis, so that the condition $\rho = \sqrt{x^2 + y^2} \ll z$ is fulfilled.

- Using the so-called FRESNEL *approximation*

$$r = \sqrt{\rho^2 + z^2} \approx z\left(1 + \frac{\rho^2}{2z^2}\right) = z + \frac{\rho^2}{2z} \tag{2.82}$$

and substituting in Eq (2.81) gives

$$\mathbf{E}(\mathbf{r}) = \frac{A}{z}\mathrm{e}^{\mathrm{i}kz}\mathrm{e}^{\mathrm{i}k\frac{\rho^2}{2z}}, \tag{2.83}$$

where we considered that $r \simeq z$ in the amplitude.

- The wave fronts are *paraboloids*. Moreover, if the distance z becomes much larger, the spherical wave turns into a plane wave.

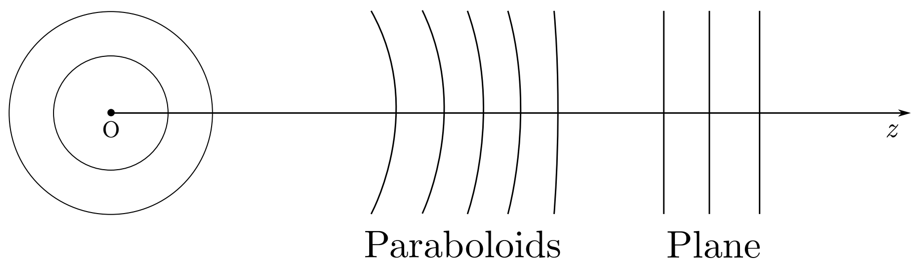

- Other way: approximate wave equation, then find exact solutions.

2.6.1 Paraxial Helmholtz equation

- If the wave fronts change only slightly along z-direction, we may in good approximation consider it as a plane wave. We therefore start from a plane wave

$$\mathbf{E}_0(\mathbf{r}) = A(\mathbf{r})\mathrm{e}^{\mathrm{i}kz} \tag{2.84}$$

with slowly varying amplitude $A(\mathbf{r})$ of the position.

- As a consequence the envelope $A(\mathbf{r})$ and its derivative with respect to z do not vary much within a wavelength $\lambda = 2\pi/k$ (this is the so-called *slowly varying envelope approximation*, or SVEA)

$$\frac{\partial A}{\partial z} \ll kA \quad \text{and} \quad \frac{\partial^2 A}{\partial z^2} \ll k^2 A. \tag{2.85}$$

- Inserting into HELMHOLTZ equation gives

$$\begin{aligned}\left(\nabla^2+k^2\right)A(\mathbf{r})\mathrm{e}^{\mathrm{i}kz} &= \nabla_{\mathrm{T}}^2A(\mathbf{r})\mathrm{e}^{\mathrm{i}kz}+\left(\frac{\partial^2}{\partial z^2}+k^2\right)A(\mathbf{r})\mathrm{e}^{\mathrm{i}kz}\\ &= \nabla_{\mathrm{T}}^2A(\mathbf{r})\mathrm{e}^{\mathrm{i}kz}+\left(\frac{\partial^2 A}{\partial z^2}-k^2A+2\mathrm{i}k\frac{\partial A}{\partial z}+k^2A\right)\mathrm{e}^{\mathrm{i}kz}\\ &\overset{\text{SVEA}}{\simeq} \nabla_{\mathrm{T}}^2A(\mathbf{r})\mathrm{e}^{\mathrm{i}kz}+2\mathrm{i}k\frac{\partial A}{\partial z}\mathrm{e}^{\mathrm{i}kz}.\end{aligned}$$

- Thus we obtain the *paraxial* HELMHOLTZ equation

$$\boxed{\left(\frac{\partial^2}{\partial x^2}+\frac{\partial^2}{\partial y^2}\right)A(\mathbf{r})+2\mathrm{i}k\frac{\partial}{\partial z}A(\mathbf{r})=0.} \tag{2.86}$$

- It also possible to verify that the parabolic waves (2.83) are even exact solutions of paraxial HELMHOLTZ equation (2.86).

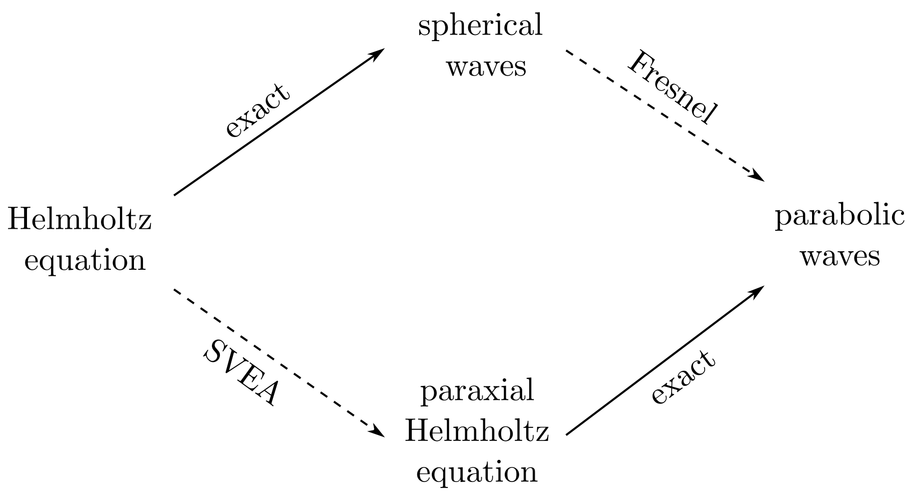

Fig. 2.12: Two different points of view for solving Helmholtz equation.

2.6.2 Gaussian beams

- Another class of solutions to the paraxial HELMHOLTZ equation is found by replacing $z \longrightarrow q(z) = z - \mathrm{i}z_{\mathrm{R}}$, with a constant z_{R}, in the parabolic wave

$$\mathbf{E}(\mathbf{r}) = \frac{A}{q(z)}\mathrm{e}^{\mathrm{i}kz}\mathrm{e}^{\mathrm{i}k\frac{\rho^2}{2q(z)}}. \tag{2.87}$$

- The function $1/q(z)$ can be divided into real and imaginary parts

$$\frac{1}{q(z)} = \frac{1}{R(z)} + \mathrm{i}\frac{\lambda}{\pi W^2(z)}, \tag{2.88}$$

where

$$W(z) = W_0\sqrt{1+\left(\frac{z}{z_\mathrm{R}}\right)^2}, \quad W_0^2 = \frac{\lambda z_\mathrm{R}}{\pi}, \quad R(z) = z\left[1+\left(\frac{z_\mathrm{R}}{z}\right)^2\right]. \tag{2.89}$$

- Redefining the constant $A \longmapsto A/(\mathrm{i}z_\mathrm{R})$ and the GOUY phase $\zeta(z) = -\arctan\left(\frac{z}{z_\mathrm{R}}\right)$, we then find for the complex amplitude

$$\mathbf{E}(\mathbf{r}) = \frac{AW_0}{W(z)}\exp\left(-\frac{\rho^2}{W^2(z)}\right)\exp\left[\mathrm{i}kz + \mathrm{i}k\frac{\rho^2}{2R(z)} + \mathrm{i}\zeta(z)\right], \tag{2.90}$$

so the intensity take the following form

$$I(\rho, z) = |A|^2\left(\frac{W_0}{W(z)}\right)^2\exp\left[-\frac{2\rho^2}{W^2(z)}\right] \tag{2.91}$$

which is Gaussian function of ρ for every z.

- The width of the beam is determined by $W(z)$, where at $z = 0$: $W(z=0) = W_0$ the beam is narrowest with waist radius W_0, or, the spot size of the beam is $2W_0$.

- The Gaussian beam diverges during the propagation, where z_R is the RAYLEIGH length which characterizes the defocusing. The focal length at which the beam waist increases by a factor of $\sqrt{2}$ is twice the RAYLEIGH length, i.e.,

$$2z_\mathrm{R} = \frac{2\pi W_0^2}{\lambda}. \tag{2.92}$$

- The wave fronts of the Gaussian beam are defined by the phase in (2.90), neglecting the z-dependence in $R(z)$ and $\zeta(z)$, then the wave fronts are given by the relation

$$z + \frac{\rho^2}{2R} \approx \text{const.} \tag{2.93}$$

This is an equation of a parabolic surface with radius of curvature R. The wave fronts are shown in Fig. 2.13.

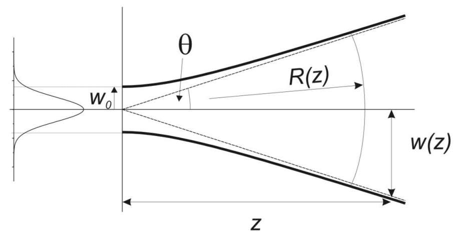

Fig. 2.13: Evolution of the beam radius of a Gaussian beam.

2.6.3 Hermite-Gauß modes

- The Gaussian beams are not the only modes that satisfy the paraxial HELMHOLTZ equation (2.86).

- An important and interesting class of modes arises when the complex envelope $E_G(\mathbf{r})$ of Gaussian beam is modified in such a way that

$$E(\mathbf{r}) = E_G(\mathbf{r}) f_x \left[\frac{\sqrt{2}x}{W(z)}\right] f_y \left[\frac{\sqrt{2}y}{W(z)}\right] \mathrm{e}^{\mathrm{i} f_z(z)} \tag{2.94}$$

  with real functions f_x,f_y and f_z.

- The phase of envelope given by $f_z(z)$ does not depend on x and y, and equals the phase of Gaussian beam. This means that the wave fronts coincide with those of the Gaussian beam. In particular, they have the same radius of curvature $R(z)$.

- These properties are ensured exactly when the envelope $E_0(\mathbf{r})$ (2.94) satisfies the paraxial HELMHOLTZ equation.

- Defining $u = \sqrt{2}x/W(z)$ and $v = \sqrt{2}y/W(z)$, we write

$$\frac{\partial f_x}{\partial x} = \frac{\sqrt{2}}{W(z)} \frac{\partial f_x}{\partial u}, \quad \frac{\partial f_x}{\partial z} = -\frac{u}{W(z)} \frac{\partial W(z)}{\partial z} \frac{\partial f_x}{\partial u} \tag{2.95}$$

  and

$$\frac{\partial}{\partial x} E_G(\mathbf{r}) = \mathrm{i}k \frac{x}{q(z)} E_G(\mathbf{r}) \tag{2.96}$$

$$\frac{1}{W(z)} \frac{\partial W(z)}{\partial z} = \frac{z W_0^2}{z_\mathrm{R}^2 W^2(z)} = \frac{1}{R(z)}. \tag{2.97}$$

- If we now use the relation $1/q(z) - 1/R(z) = 2\mathrm{i}/(kW^2(z))$, and since the Gaussian envelope $E_G(\mathbf{r})$ satisfies the paraxial HELMHOLTZ equation, one obtains the differential equation

$$\frac{1}{f_x}\left(\frac{\partial^2 f_x}{\partial u^2} - 2u\frac{\partial f_x}{\partial u}\right) + \frac{1}{f_y}\left(\frac{\partial^2 f_y}{\partial v^2} - 2v\frac{\partial f_y}{\partial v}\right) - kW^2(z)\frac{\partial f_z}{\partial z} = 0 \tag{2.98}$$

- This equation consists of the sum of three terms, each depends only on one of the variables (u, v, z). We therefore solve this equation by separating the variables with two separation constants $-2m$ and $-2n$, so that

$$-\frac{1}{2}\frac{\partial^2 f_x}{\partial u^2} + u\frac{\partial f_x}{\partial u} = m f_x \tag{2.99}$$

$$-\frac{1}{2}\frac{\partial^2 f_y}{\partial v^2} + v\frac{\partial f_y}{\partial v} = n f_y \tag{2.100}$$

$$z_\mathrm{R}\left[1 + \left(\frac{z}{z_\mathrm{R}}\right)^2\right]\frac{\partial f_z}{\partial z} = -(m+n). \tag{2.101}$$

- The first two equations are eigenvalue equations for the differential operators on the left side with the eigenvalues m and n. Moreover, the eigenfunctions are precisely the HERMITE polynomials $H_m(u)$ and $H_n(v)$, thus

$$f_x(u) = H_m(u), \quad f_y(v) = H_n(v). \tag{2.102}$$

Integrating the remaining equation yields

$$f_z(z) = -(m+n)\arctan\frac{z}{z_\mathrm{R}} = (m+n)\zeta(z). \tag{2.103}$$

- The complex amplitude thus becomes

$$\boxed{E_{m,n}(\mathbf{r}) = A_{m,n}\frac{W_0}{W(z)}h_m\left(\frac{\sqrt{2}x}{W(z)}\right)h_n\left(\frac{\sqrt{2}y}{W(z)}\right)\exp\left[\mathrm{i}kz + \mathrm{i}k\frac{\rho^2}{2R(z)} + \mathrm{i}(m+n+1)\zeta(z)\right]}, \tag{2.104}$$

where $h_l(u) = H_l(u)\mathrm{e}^{-u^2}$ represents the so-called HERMITE function.

- If $m = n = 0$, the amplitude is reduced to the usual Gaussian beam.

- The intensity distributions of the lowest HERMITE-GAUSS modes are shown in Fig.(2.14).

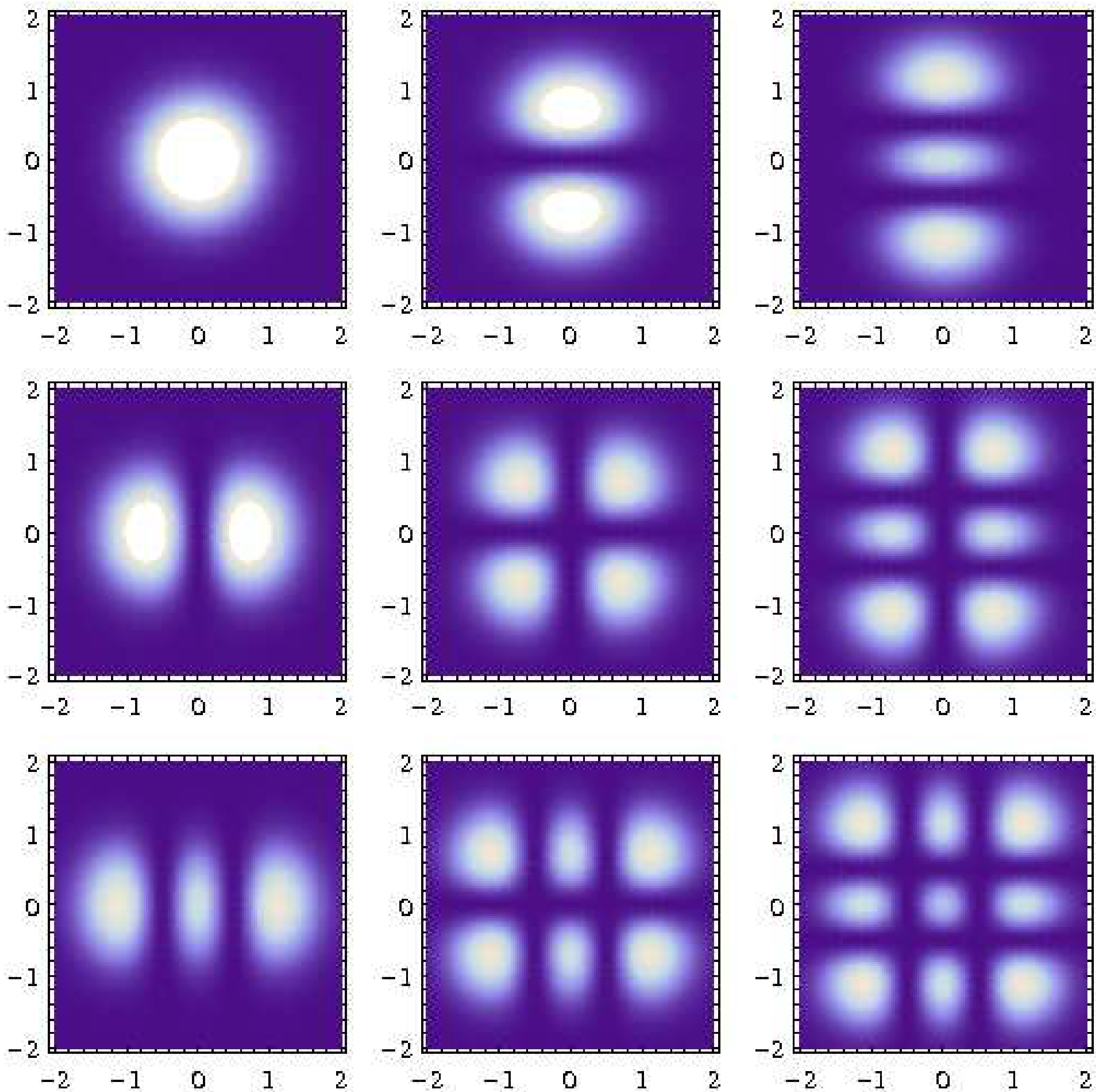

Fig. 2.14: Intensity distribution of the lowest Hermite–Gauß modes for $(m,n) = (0,1,2)$.

- These Hermite-Gauss modes are eigenmodes of confocal resonator that would fit exactly with these parabolic wave fronts. These modes are labeled as TEM_{mn}.

2.7 Pumping processes

a) **Optical Pumping**

- Shining a laser medium (solid or liquid) with a short-pulse flash lamp yields a fairly short pulses. Flash lamp pulses as short as ~ 1 μs exist.
- Unfortunately, this yields a pulse as long as the *excited-state lifetime* of the laser medium, which can be considerably longer than the pump pulse.
- Since solid-state laser media have lifetimes in the microsecond scale, it produces pulses *microseconds* to *milliseconds* long.

b) **Electrical Pumping**

- In gas lasers, the population inversion is achieved by using *avalanche electrons* in a high voltage discharge.
- As the electrons move in the discharge, they speed up and thus gain kinetic energy. The inelastic collision of an electron with an atom in the ground state leads to an energy transfer of a part this kinetic energy. As a result, the atom is excited and the electron moves with lower kinetic energy.

c) **Chemical Pumping**

- In some chemical reactions, the product is formed in an excited state, hence the condition of population inversion is established via creation of excited molecules.
- In reality, rare halide molecules exist solely in an excited state, therefore, population inversion is achievable. Lasers operating on such principle are known as *excimer laser*.

2.8 Phonomenological laser model

- To model a laser, one needs to consider
  - An active medium to amplify light.
  - A pumping mechanism to create population inversion.
  - A part of the amplified light has to be coupled back into the medium with the correct phase.

We aim to describe the functioning of a laser using a very simplified model, as depicted in Figure 2.15, in a phenomenological manner. The active medium has a gain coefficient γ and length L_{m}. Feedback occurs through reflection from two mirrors with reflectivity coefficients R_1 and R_2, with no additional losses beyond that.

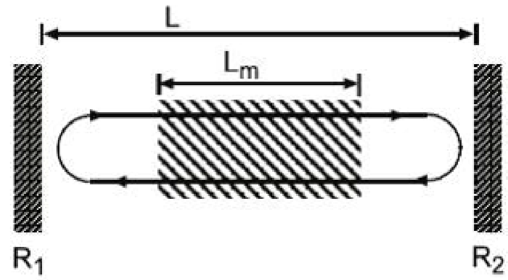

Fig. 2.15: Laser model. A gain medium of length L_m is situated within a resonator of length L, formed by mirrors with reflectivities R_1 and R_2.

- To keep the laser working, the amplitude of the electromagnetic wave needs to be stationary (temporally constant).
- The losses by mirrors (the out-coupled light) has to be compensated by the amplification caused by the pumping.
- The part of the wave that is reflected (not coupled out) has to be coupled back with the same phase.
- In each plane perpendicular to the laser axis the field $\mathbf{E}$ at time t has to exactly match the field $\mathbf{E}$ at time $t+\tau$ with τ is the round-trip time

$$\mathbf{E}(t) \stackrel{!}{=} \mathbf{E}(t+\tau). \tag{2.105}$$

- A continuous wave (cw) laser has a pulse length longer than the round-trip time.
- During propagation through the medium the field gets amplified with the factor $\mathrm{e}^{\gamma L_\mathrm{m}/2}$ and it gets damped to the mirrors with factors $\sqrt{R_1}$ and $\sqrt{R_2}$, respectively. Thus

$$\begin{aligned} \mathbf{E}(t) &= E_0 \mathrm{e}^{\mathrm{i}(kz-\omega t)} \\ &\stackrel{!}{=} E_0 \mathrm{e}^{\mathrm{i}(kz-\omega(t+\tau))} \mathrm{e}^{\gamma L_\mathrm{m}} \sqrt{R_1}\sqrt{R_2} \end{aligned}$$

- It follows that

$$\sqrt{R_1 R_2}\,\mathrm{e}^{-\mathrm{i}\omega\tau} \mathrm{e}^{\gamma L_\mathrm{m}} \stackrel{!}{=} 1 \tag{2.106}$$

which is the heuristic laser model.

- Introducing the refractive index n the round-trip time τ reads
$$\tau = 2\frac{nL_{\mathrm{m}}}{c} + 2\frac{L - L_{\mathrm{m}}}{c} = 2\frac{L'}{c}, \tag{2.107}$$
where $L' = L + L_{\mathrm{m}}(n-1)$ is the optical length.

- In order to fulfill the condition (2.105), the amplitude as well as the phase in Eq. (2.106) have to equal 1 independently, i.e.,
$$\boxed{\mathrm{e}^{-\mathrm{i}2\omega L'/c} = 1.} \quad \text{"phase condition"} \tag{2.108}$$
Hence
$$\frac{2\omega L'}{c} \overset{!}{=} 2q\pi, \quad q \in \mathbb{N}, \tag{2.109}$$
i.e., discrete values for the frequencies of the amplified and emitted light
$$\boxed{\omega_q = q\frac{\pi c}{L'}} \quad \text{or} \quad \boxed{\nu_q = q\frac{c}{2L'}.} \tag{2.110}$$
The arrangement of the two mirrors forms a *resonator* or *oscillator* with discrete resonance frequencies ν_q. The corresponding fields are called *longitudinal* modes of the resonator, and the frequency spacing is known as the *free spectral range* (FSR).

- **Example:** Typical length of a resonator for He-Ne laser is $L' = 50\,\mathrm{cm}$ at $\lambda = 633\,\mathrm{nm}$, thus the $q = 2.6 \times 10^6$-th longitudinal mode is excited, meaning that the corresponding standing wave has the same number of antinodes.

- The amplitude condition yields
$$\sqrt{R_1 R_2}\mathrm{e}^{\gamma L_{\mathrm{m}}} = 1, \tag{2.111}$$
which reads in logarithmic form as
$$\gamma = \frac{1}{L_{\mathrm{m}}} \ln\left(\frac{1}{\sqrt{R_1 R_2}}\right). \tag{2.112}$$

- The relationship between the required gain γL_{m} and the coupling losses due to the incomplete reflectivity $R_1 R_2 \leq 1$ of the two mirrors gives the conditions in the laser, ensured by saturation of the gain (see equation (**??**))
$$\mathrm{e}^{\gamma L_{\mathrm{m}}} = \frac{1}{\sqrt{R_1 R_2}} = \mathrm{e}^{\frac{\gamma_0 L_{\mathrm{m}}}{1 + I/I_{\mathrm{s}}}}, \tag{2.113}$$
we obtain
$$1 + \frac{I}{I_{\mathrm{s}}} = \frac{\gamma_0 L_{\mathrm{m}}}{\ln\left(\frac{1}{\sqrt{R_1 R_2}}\right)}. \tag{2.114}$$

- In the limit $I \longrightarrow 0$ ($I \ll I_s$), and using $\ln\left(\frac{1}{\sqrt{R_1R_2}}\right) \approx 1-\sqrt{R_1R_2}$ yields *the threshold for lasing*

$$\boxed{\gamma_0 L_m = 1-\sqrt{R_1R_2},} \quad \text{or} \quad \boxed{\sqrt{R_1R_2} = 1-\gamma_0 L_m}. \tag{2.115}$$

Hence, for a given reflectivity $R = \sqrt{R_1R_2}$, the gain $\gamma_0 L_m$ has to exceed a certain value (depending on the gain coefficient and the length of the gain medium) for the lasing process to start. Vice versa, for a given gain $\gamma_0 L_m$, the reflectivity $R = \sqrt{R_1R_2}$ has a lower bound for laser operation. The gain coefficient is spectrally limited. In only a few cases is its spectral width smaller than the free spectral range of the resonator, so that normally multiple modes are amplified. However, the number of active modes, as described the threshold condition, is also a function of the resonator losses, as only the modes for which the gain compensates for the coupling losses can oscillate. This is illustrated in Figure 2.16.

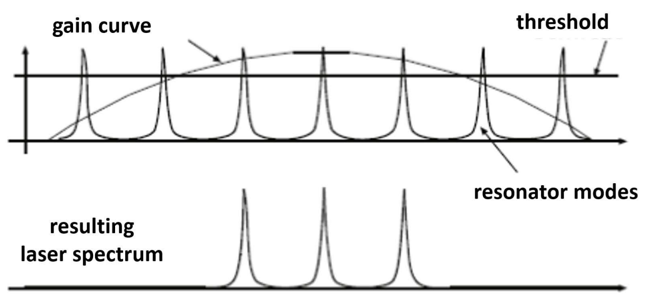

Fig. 2.16: Gain curve, lasing threshold, resonator modes, and the resulting active modes of a laser.

Alternative derivation using rate equations

- Let us consider N_2 the population of the upper level and $N_2 \gg N_1$

$$\frac{\mathrm{d}N_2}{\mathrm{d}t} = P_2 - \frac{N_2}{\tau_2} - \frac{\sigma}{h\nu} I N_2 \tag{2.116}$$

- Moreover, we define $\frac{I}{\tau_R}$ as losses due to finite lifetime of photon in resonator

$$\frac{1}{\tau_R} \approx (1-R)\frac{c}{L_m}, \tag{2.117}$$

where $R = \sqrt{R_1 R_2}$ and the above approximation holds if $R_1 \approx R_2 \approx 1$. The rate equation for the intensity I of light reads

$$\frac{\mathrm{d}I}{\mathrm{d}t} = c\sigma N_2 I - \frac{I}{\tau_\mathrm{R}}. \tag{2.118}$$

- In equilibrium ($\mathrm{d}I/dt = 0$), we obtain that

  $$c\sigma N_2 I - \frac{1}{\tau_\mathrm{R}} I = 0, \tag{2.119}$$

  hence

  $$N_2 = \frac{1}{c\sigma\tau_\mathrm{R}} \tag{2.120}$$

  which is independent on I.

- Assuming $I > 0$, the equilibrium condition ($\mathrm{d}N_2/dt = 0$) yields

  $$P_2 - \frac{N_2}{\tau_2} - \frac{\sigma}{h\nu} I N_2 = 0, \tag{2.121}$$

  therefore

  $$I = P_2 h\nu c\tau_\mathrm{R} - \frac{h\nu}{\sigma\tau_2}. \tag{2.122}$$

- At the threshold where $I \longrightarrow 0$, we find

  $$\begin{aligned} P_\mathrm{th} &= \frac{1}{c\sigma\tau_2\tau_\mathrm{R}} \\ &= \frac{1-R}{\sigma\tau_2 L_\mathrm{m}} \end{aligned} \tag{2.123}$$

  where we have used the relation (2.117).

- Thanks to the relation

  $$\gamma_0 = \sigma N_2 = \sigma P_2 \tau_2,$$

  we find the threshold condition for lasing

  $$\boxed{\gamma_0 L_\mathrm{m} = 1 - R.} \tag{2.124}$$

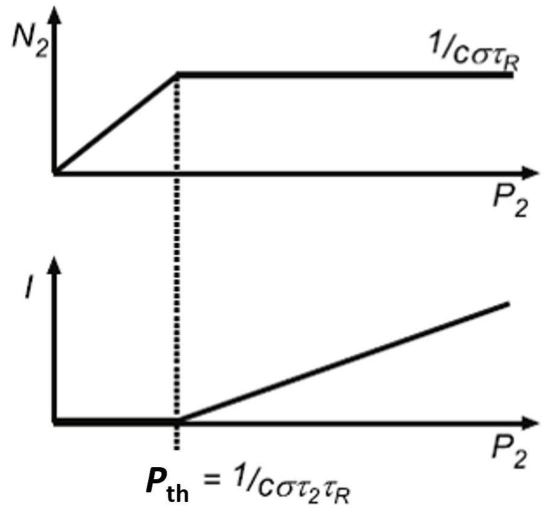

Fig. 2.17: The population of the upper laser level N_2 and the intensity I as a function of the pumping rate P_2.

2.9 Resoantors

- Optical resonators are devices in which the electromagnetic field is enclosed between highly reflective mirrors that define the mode structure.
- When deriving the mode of electromagnetic field in vacuum, we took advantage of the fact that we could use any complete set of orthonormal basis functions of the Helmholtz operator to represent the electromagnetic field.
- In particular, we did not care about the coordinate system used for derivation. In a resonator, it is the geometry of mirrors that determines a specific choice of modes. Therefore, it is immediately clear that optical resonators are suitable for selecting special modes.

2.9.1 Planar resonators

- We first consider two plane-parallel, infinitely extended plates, which are not completely reflecting, but rather have transmission coefficients T_1, T_2 and reflection coefficients R_1, R_2, respectively (Fig. 2.18). In this Fabry–Perot interferrometer (FPI) of length L, a monochromatic plane electromagnetic wave entering at an angle θ has the form

$$\mathbf{E}(z,t) = E_0 \mathbf{e}_\sigma \mathrm{e}^{\mathrm{i}(\mathbf{k}\cdot\mathbf{r}-\omega t)}. \tag{2.125}$$

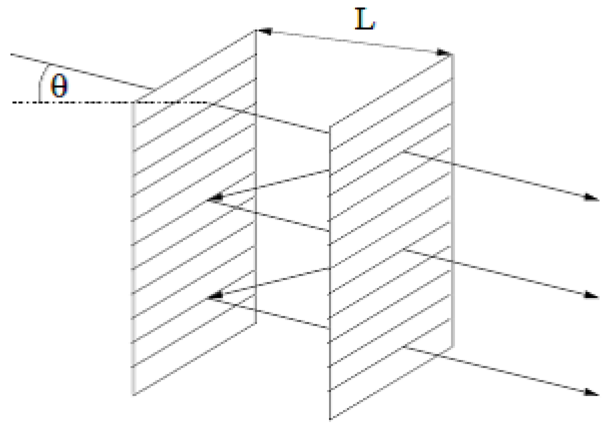

Fig. 2.18: FABRY–PEROT interferrometer consists of two plane-parallel mirrors with transmission coefficients T_1, T_2 and reflection coefficients R_1, R_2, respectively.

- The amplitude E_0' of the electromagnetic field behind the FABRY–PEROT resonator is then given as a superposition of all partial waves that are reflected many times inside the resonator.
- The reflection take place at inner sides of both mirrors, hence the phase jumps of π at the optically dense medium.
- The phase factor $\mathrm{e}^{\mathrm{i}(\mathbf{k}\cdot\mathbf{r}-\omega t)}$ is chosen such that is unity in the mirror plane.
- The transmitted complex amplitude reads

$$\begin{aligned} E_0' &= \sum_{i=1}^{\infty} E_{\mathrm{T}_i} \\ &= E_0 T_1 T_2 \underbrace{\mathrm{e}^{-\mathrm{i}\omega\frac{L}{c}\cos\theta}}_{(1)} + E_0 T_1 T_2 R_1 R_2 \underbrace{\mathrm{e}^{\mathrm{i}2\pi}}_{(2)} \underbrace{\mathrm{e}^{-\mathrm{i}\omega\frac{3L}{c}\cos\theta}}_{(3)} + E_0 T_1 T_2 R_1^2 R_2^2 \mathrm{e}^{\mathrm{i}4\pi}\mathrm{e}^{-\mathrm{i}\omega\frac{5L}{c}\cos\theta} + \cdots \\ &= E_0 T_1 T_2 \mathrm{e}^{-\mathrm{i}\omega\frac{L}{c}\cos\theta}\left(1 + R_1 R_2 \mathrm{e}^{-\mathrm{i}\omega\frac{2L}{c}\cos\theta} + R_1^2 R_2^2 \mathrm{e}^{-\mathrm{i}\omega\frac{4L}{c}\cos\theta} + \cdots\right) \end{aligned} \tag{2.126}$$

(1) : is the dynamic phase due to resonator length.
(2) : 2 times reflection at optically dense medium, i.e., $\left(\mathrm{e}^{\mathrm{i}\pi}\right)\left(\mathrm{e}^{\mathrm{i}\pi}\right) = \mathrm{e}^{2\mathrm{i}\pi}$.
(3) : is the dynamic phase due to 3 passes through the resonator.

$$\frac{E_0'}{E_0} = T\mathrm{e}^{-\mathrm{i}\frac{\delta}{2}}\left(1 + R\mathrm{e}^{-\mathrm{i}\delta} + R^2\mathrm{e}^{-2\mathrm{i}\delta} + \dots\right), \tag{2.127}$$

where we have assumed $T_1 = T_2 = \sqrt{T}$, $R_2 = R_1 = \sqrt{R}$ and defined the phase shift

$$\delta = \frac{\omega}{c}(2L)cos\theta \tag{2.128}$$

arising from the difference in travel between two adjacent partial waves.

- The infinite geometric series is evaluated using $\sum_{n=0}^{\infty} q^n = \frac{1}{1-q}$ with $q = R\mathrm{e}^{-\mathrm{i}\delta}$:

$$\frac{E_0'}{E_0} = \frac{T\mathrm{e}^{-\mathrm{i}\frac{\delta}{2}}}{1 - R\mathrm{e}^{-\mathrm{i}\delta}}. \tag{2.129}$$

- The transmission function of the resonator can be expressed as

$$T_{\mathrm{FP}} = \left|\frac{E_0'}{E_0}\right|^2 = \frac{T^2}{1 - 2R\cos\delta + R^2}. \tag{2.130}$$

Using $\cos\delta = 1 - 2\sin^2(\delta/2)$, the denominator of this expression can be cast in the form

$$1 - 2R\cos\delta + R^2 = (1-R)^2\left[1 + \frac{4R}{(1-R)^2}\sin^2\frac{\delta}{2}\right], \tag{2.131}$$

so that we obtain

$$\boxed{T_{\mathrm{FP}} = \left|\frac{E_0'}{E_0}\right|^2 = \left(\frac{T}{1-R}\right)^2\left[1 + \frac{4R}{(1-R)^2}\sin^2\frac{\delta}{2}\right]^{-1}.} \tag{2.132}$$

Equation (2.132) is known as the AIRY function. It is depicted in in Fig. 2.19 as a function of the phase shift $\delta/2\pi$.

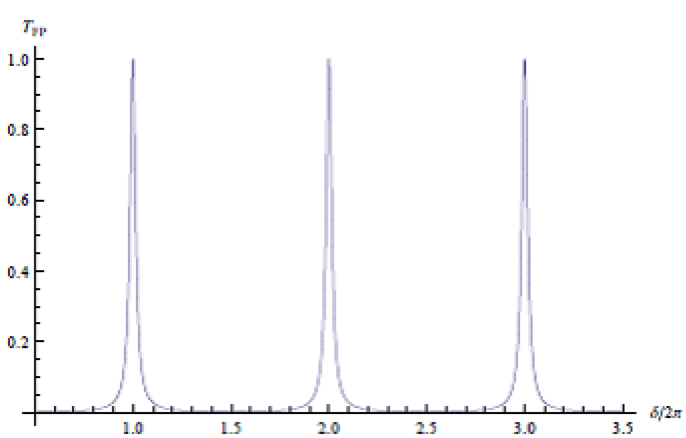

Fig. 2.19: Transmission of a FABRY–PEROT resonator.

- The maxima of the transmission function are reached at phase shifts $\delta = 2\pi m$ ($m \in \mathbb{N}_0$), i.e., with constructive interference of the partial waves. The maxima in the frequency space reads

$$\nu_m = \frac{\omega_m}{2\pi} = m\frac{c}{2L\cos\theta}, \tag{2.133}$$

hence the distance between two maxima

$$\delta\nu = \nu_{m+1} - \nu_m = \frac{c}{2L\cos\theta} \tag{2.134}$$

is called the dispersion region or the *free spectral range* (FSR).

- To compute the line width of the interference structure assume $\delta \ll 2\pi$ (very close to resonances), hence

$$T_{\mathrm{FP}} = \frac{T^2}{(1-R)^2 + 4R\sin^2(\frac{\omega}{c}L\cos\theta)} \simeq \frac{T^2}{(1-R)^2 + 4R\frac{\omega^2}{c^2}L^2\cos^2\theta} \tag{2.135}$$

which is a Lorentzian curve with a half-width $\omega_{1/2}$

$$\omega_{1/2}^2 = \frac{c^2(1-R)^2}{4RL^2\cos^2\theta} \tag{2.136}$$

corresponding to a linewidth (FWHM)

$$\Delta\nu = \frac{2\omega_{1/2}}{2\pi}, \tag{2.137}$$

or

$$\Delta\nu = \frac{c}{2L\cos\theta}\frac{1-R}{\pi\sqrt{R}}. \tag{2.138}$$

- The ratio of FSR to FWHM

$$\boxed{F = \frac{\delta\nu}{\Delta\nu} = \frac{\pi\sqrt{R}}{1-R}} \tag{2.139}$$

defines the *finesse* of the resonator.

- **Example:** A Fabry-Perot interferometer (FPI) with a length of $L = 30\,\mathrm{cm}$ and a mirror reflectivity $R = 99\%$. The finesse is $F = \pi\sqrt{0.99}/0.01 \simeq 314$. For normal incidence, the free spectral range is calculated as $\delta\nu = c/2L \simeq 500\,\mathrm{MHz}$ and hence $\Delta\nu = \delta\nu/F \simeq 1.6\,\mathrm{MHz}$.

- An intuition behind the connection between the lifetime of photons in the resonator and the finesse is based on the following considerations:

  – The larger R, the more round trips the photons experience in the resonator, so a storage time τ has to be taken into account.

- If one would abruptly block the flow of photons into the resonator, the transmitted intensity decays exponentially.

- Therefore, the spectrum is a LORENTZ curve with line width $\Delta\nu = \frac{\Delta\omega}{2\pi} = \frac{1}{2\pi\tau}$ and the finesse reads

$$F = \frac{c}{2L\cos\theta}\frac{1}{\Delta\nu} = \frac{c}{2L\cos\theta}2\pi\tau = \frac{c\pi\tau}{L\cos\theta}. \tag{2.140}$$

Replacing τ by NT, where N is the average of round trips in the resonator and $T = 2L\cos\theta/c$ is the time for one round trip, yields

$$F = \frac{c}{2L\cos\theta}2\pi NT = \frac{c}{2L\cos\theta}2\pi N\frac{2L\cos\theta}{c} = 2\pi N. \tag{2.141}$$

Thus, the finesse roughly indicates the average number of round trips of the photon in the resonator.

2.9.2 Spherical resonators

- Planar resonators have a crucial disadvantage that they have to be adjusted extremely precisely so that an incident beam (typically with a finite transverse extent) is superimposed to the reflected partial waves. This is the reason behind the usefulness of spherical resonators in practical applications.

- The eigenmodes of spherical resonators are the Gaussian modes. The reason is that their wave fronts are curved and, therefore, adapted to the curvature of mirrors. A Gaussian beam impinging on a spherical mirror is reflected into itself if its curvature matches with the beam. So we get a spherical resonator if we place mirrors with appropriate curvatures in the right places on the Gaussian profile in Fig. (2.13).

- We have seen that HERMITE–GAUSS modes are also solutions for paraxial HELMHOLTZ equation having the same wave fronts as Gaussian beams. This implies that HERMITE-GAUSS modes are also eigenmodes for spherical resonators. The corresponding phase whose indices (m, n) on the beam axis at $\rho = 0$ reads

$$\varphi(0, z) = kz + (m + n + 1)\zeta(z) \tag{2.142}$$

- To observe constructive interference, the phase shift of the wave after a complete trip through the resonator of length L must be a multiple of 2π,

$$2kL\cos\theta + 2(m + n + 1)\Delta\zeta = 2\pi q, \quad q \in \mathbb{Z}, \tag{2.143}$$

where $\Delta\zeta = \zeta(z_2) - \zeta(z_1)$ represents the difference of the GOUY phases at the mirror positions. Setting $k = 2\pi\nu/c$ the resonance frequencies of these resonator modes are

$$\nu_{m,n,q} = q\delta\nu + (m+n+1)\frac{\Delta\zeta}{\pi}\delta\nu, \tag{2.144}$$

where $\delta\nu$ is the distance between two resonance frequencies

$$\delta\nu = \frac{c}{2L\cos\theta}. \tag{2.145}$$

The three indices (m,n,q) are explained as follows: modes with different q but the same (m,n) have the same transverse intensity distributions are called *longitudinal* modes. The indices (m,n) describe the different *transverse* modes.

- From (2.144) one can deduce that all transverse modes with the sum index $m+n$ have the same resonance frequency. Two transverse modes with the same longitudinal index q have the frequency separation

$$\nu_{m,n,q} - \nu_{m',n',q} = \left[(m+n) - (m'+n')\right]\frac{\Delta\zeta}{\pi}\delta\nu, \tag{2.146}$$

which characterizes the frequency shift between the groups of longitudinal modes.

2.9.3 Stability of resonators

- Instead of fitting the two mirrors to a given Gaussian beam, we look for a Gaussian beam that match both curved mirrors M_1 and M_2 with radii of curvature R_1 and R_2 and spacing L.

- The curvature at z_1 and z_2 should match mirrors, thus we obtain three equations

$$R(z_1) = z_1 + \frac{z_\mathrm{R}^2}{z_1} = -R_1 \tag{2.147}$$

$$R(z_2) = z_2 + \frac{z_\mathrm{R}^2}{z_2} = +R_2 \tag{2.148}$$

and

$$L = z_2 - z_1. \tag{2.149}$$

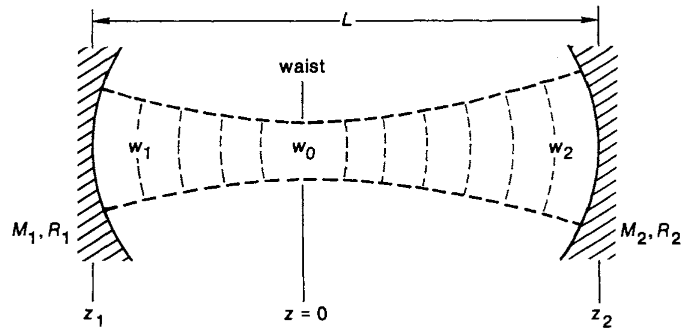

Fig. 2.20: Model for investigating stability analysis of the resonator.

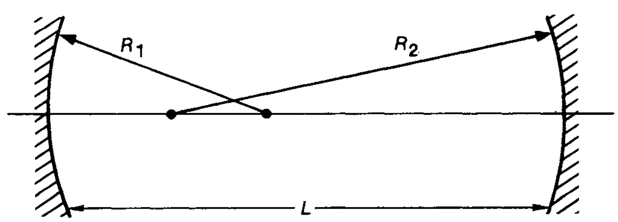

Fig. 2.21: The resonator g-factors.

- Let us define g-factors as

$$g_1 = 1 - \frac{L}{R_1} \quad \text{and} \quad g_2 = 1 - \frac{L}{R_2}. \tag{2.150}$$

- Therefore, the Rayleigh length of the mode is given by

$$z_{\mathrm{R}}^2 = \frac{g_1 g_2 (1 - g_1 g_2)}{(g_1 + g_2 - 2 g_1 g_2)^2} L^2, \tag{2.151}$$

  and the positions of the two mirrors with respect to beam waist are

$$z_1 = \frac{g_2 (1 - g_1)}{g_1 + g_2 - 2 g_1 g_2} L \quad \text{and} \quad z_2 = \frac{g_1 (1 - g_2)}{g_1 + g_2 - 2 g_1 g_2} L. \tag{2.152}$$

- Moreover, the mode sizes can be written as follows

  – Waist spot size:

$$W_0^2 = \frac{L\lambda}{\pi} \sqrt{\frac{g_1 g_2 (1 - g_1 g_2)}{(g_1 + g_2 - 2 g_1 g_2)^2}}. \tag{2.153}$$

- Spot size at first mirror:

$$W_1^2 = \frac{L\lambda}{\pi}\sqrt{\frac{g_2}{g_1(1-g_1g_2)}}. \tag{2.154}$$

- Spot size at second mirror:

$$W_2^2 = \frac{L\lambda}{\pi}\sqrt{\frac{g_1}{g_2(1-g_1g_2)}}. \tag{2.155}$$

- Real and finite solutions W_0, W_1 and W_2 can exist only if g-factors fulfills the stability condition for the resonator

$$\boxed{0 \leq g_1g_2 < 1.} \tag{2.156}$$

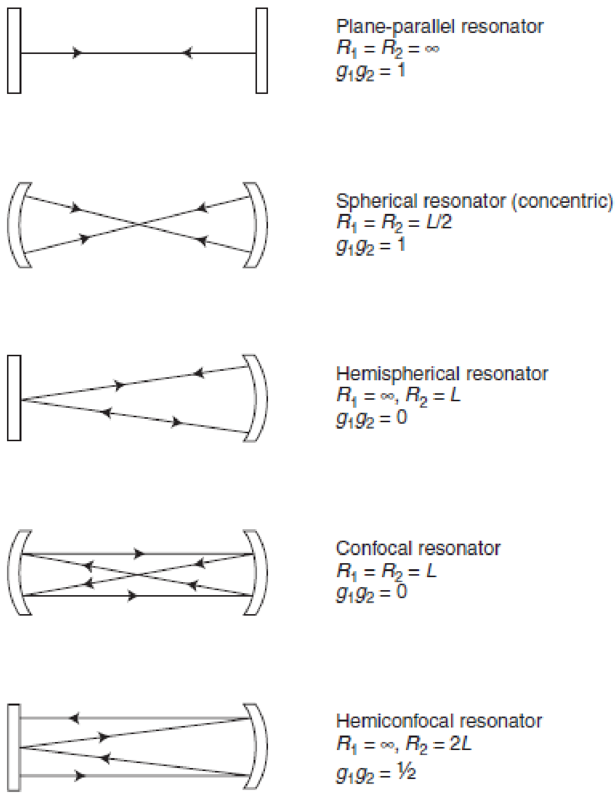

Fig. 2.22: Examples of stable resonators.

- Plane-parallel resonator: $g_1 = g_2 = 1$.
- Spherical (concentric) resonator: $g_1 = g_2 = -1$.
- Hemispherical resonator: $g_1 = 1$, $g_2 = 0$.

- Confocal resonator: $g_1 = g_2 = 0$.
- Hemiconfcal resonator: $g_1 = 1$, $g_2 = 1/2$.

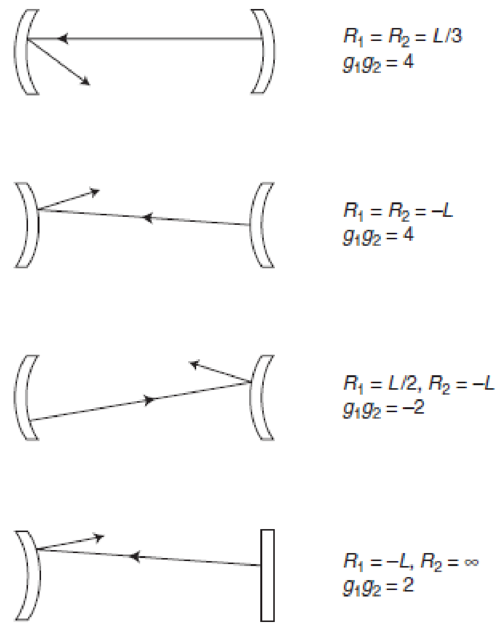

Fig. 2.23: Examples of unstable resonators.

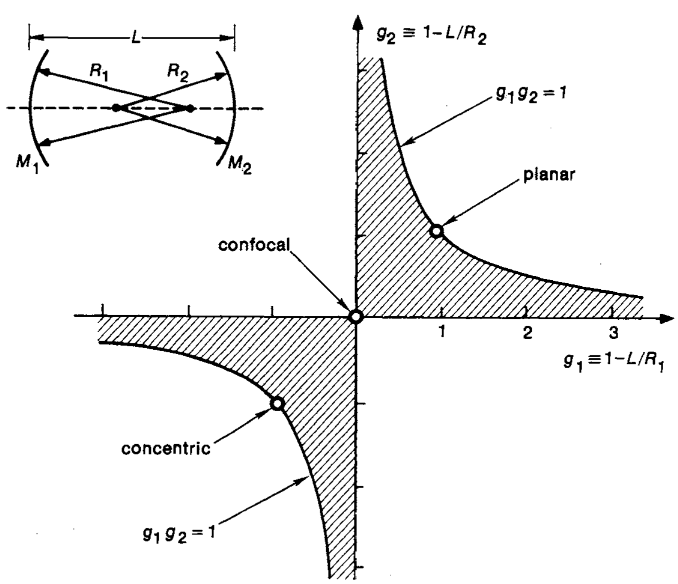

Fig. 2.24: Stability diagram for a two-mirror optical resonator.

- Semi-confocal is more stable because it is not on edge of stability region.

- The products of g-factors of the confocal, concentric, and hemispheric resonators reside exactly at the boundaries of stability region. Therefore, usually their parameters are slightly detuned to move inside the stability region.
- **Example:** Concentric resonator $L = 2R$, hence $g = -1$. Decreasing length by ΔL yields $L_{\text{new}} = 2R - \Delta L$, and $g_{\text{new}} = 1 - \frac{\Delta L}{R}$.
- Choosing a particular resonator due to certain requirements concerning mode volume, beam width, etc.
- Plane-parallel resonator has a large mode volume in its entire length, but very hard to adjust. Not often used in laser resonators.
- Confocal resonator has a very small mode volume, low diffraction losses, and easier to adjust.
- Hemispherical resonator is often used but has small beam waist. Having a good mode size at active medium, can change mode size by translating mirrors, and can change beam position by radially translating mirrors.
- Mode sizes for symmetric resonators ($g_1 = g_2 = g$)

$$W_0^2 = \frac{L\lambda}{\pi}\sqrt{\frac{1+g}{4(1-g)}}, \quad W_{1,2}^2 = \frac{L\lambda}{\pi}\sqrt{\frac{1}{1-g^2}}. \tag{2.157}$$

- All these resonators lie along the diagonal passing through the origin in the g-plane (see Fig. (2.24)).
- The curvature of mirrors can be steadily increased for a fixed spacing length L (see Fig. (2.25)).

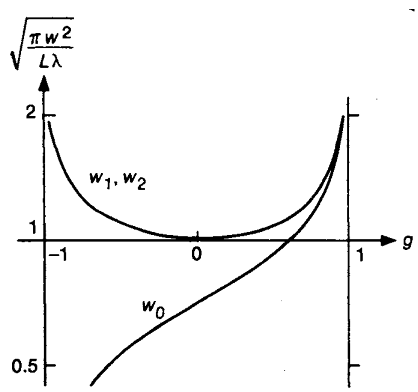

Fig. 2.25: Mode radii W_0 at the beam waist and $W_{1,2}$ at the mirrors of a symmetric resonator as a function of the g-parameter.

2.10 ABCD Formalism

- We want to describe the action of an optical element via matrix formalism. Consider a light ray in paraxial approximation travelling in z-direction at distance $y(z)$ from the optical axis till $y'(z)$, i.e., $y'(z) = \frac{\mathrm{d}y}{\mathrm{d}z} = \tan\Theta \simeq \Theta$.
- In geometrical optics, a ray is characterized by its distance from the axis and its slope.

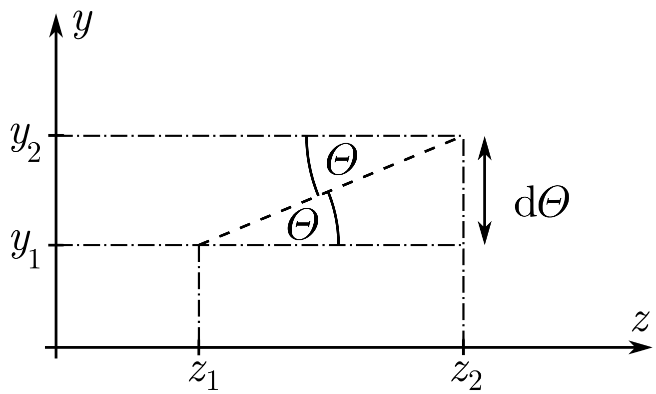

Fig. 2.26: The quantities y_1 and y_2 are distances of the ray from the optical axis before and after the optical element, Θ is the direction angle, and $z_2 - z_1 = \mathrm{d}$.

- For the translation from z_1 to z_2 in vacuum:

$$y(z_2) = y(z_1) + y'(z_1)(z_2 - z_1) \tag{2.158}$$
$$y'(z_2) = y'(z_1) \quad \text{(free space)} \tag{2.159}$$

Skipping the arguments, we rewrite both equations as

$$y_2 = y_1 + y_1'(z_2 - z_1) \tag{2.160}$$
$$y_2' = y_1' \tag{2.161}$$

- In matrix notation, the latter is equivalent to

$$\begin{pmatrix} y_2 \\ y_2' \end{pmatrix} = \begin{pmatrix} A & B \\ C & D \end{pmatrix} \begin{pmatrix} y_1 \\ y_1' \end{pmatrix} \Leftrightarrow \begin{array}{l} y_2 = Ay_1 + By_1' \\ y_2' = Cy_1 + Dy_1' \end{array} \tag{2.162}$$

- Free space

$$\begin{pmatrix} A & B \\ C & D \end{pmatrix} = \begin{pmatrix} 1 & z_2 - z_1 \\ 0 & 1 \end{pmatrix} \tag{2.163}$$

which is ABCD matrix for free space.

- Thin lens

$$\frac{1}{d_1} - \frac{1}{d_2} = \frac{1}{f} \quad \Rightarrow \frac{y_1}{d_1} - \frac{y_1}{d_2} = \frac{y_1}{f} \quad \Rightarrow y_2' = y_1' - \frac{y_1}{f} \quad \text{and} \quad y_2 = y_1. \tag{2.164}$$

  Thus

$$\begin{pmatrix} y_2 \\ y_2' \end{pmatrix} = \begin{pmatrix} 1 & 0 \\ -\frac{1}{f} & 1 \end{pmatrix} \begin{pmatrix} y_1 \\ y_1' \end{pmatrix} = \begin{pmatrix} y_1 \\ -\frac{y_1}{f} + y_1', \end{pmatrix} \tag{2.165}$$

  i.e. the lens changes the direction of the ray.

- In general, within ABCD formalism we can combine optical elements.

- **Example:** Ray passes through a lens with focal length f, then through free space d:

$$\begin{pmatrix} A & B \\ C & D \end{pmatrix} = \begin{pmatrix} 1 & d \\ 0 & 1 \end{pmatrix} \begin{pmatrix} 1 & 0 \\ -\frac{1}{f} & 1 \end{pmatrix} = \begin{pmatrix} 1 - \frac{d}{f} & d \\ -\frac{1}{f} & 1 \end{pmatrix}. \tag{2.166}$$

- **Summary of different ABCD matrices**

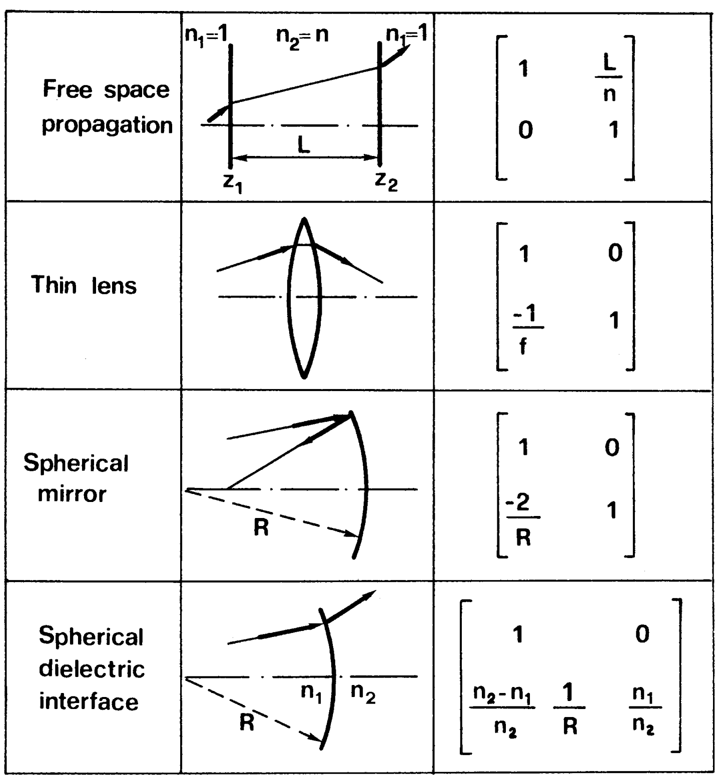

Fig. 2.27: ABCD matrices for some common cases.

- In the the case of gradient index lens or GRIN-lens of arbirary thickness L, where the refraction index profile reads

$$n(r) = n_0 - \frac{1}{2} n_2 r^2, \tag{2.167}$$

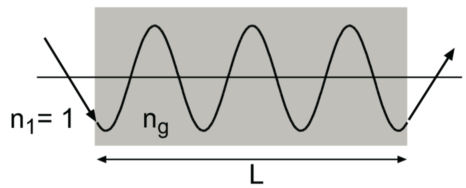

we have

$$\begin{pmatrix} A & B \\ C & D \end{pmatrix} = \begin{pmatrix} \cos\left(L\sqrt{\frac{n_2}{n_0}}\right) & \frac{1}{\sqrt{n_0 n_2}} \sin\left(L\sqrt{\frac{n_2}{n_0}}\right) \\ \sqrt{n_0 n_2} \sin\left(L\sqrt{\frac{n_2}{n_0}}\right) & \cos\left(L\sqrt{\frac{n_2}{n_0}}\right) \end{pmatrix} \tag{2.168}$$

- For a Gaussian aperture with the transmission profile

$$T(r) = T_0 \mathrm{e}^{-r^2/a^2} \tag{2.169}$$

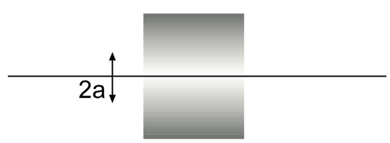

the ABCD matrix is

$$\begin{pmatrix} 1 & 0 \\ -\frac{\mathrm{i}\lambda}{\pi a} & 1 \end{pmatrix}, \tag{2.170}$$

where λ is the wavelength.